(12) INTERNATIONAL APPLICATION PUBLISHED UNDER THE PATENT COOPERATION TREATY (PCT)

(19) World Intellectual Property Organization
International Bureau

(43) International Publication Date
19 November 2020 (19.11.2020)

WIPO | PCT

(10) International Publication Number
WO 2020/231683 A1

(51) International Patent Classification:
G01N 3/20 (2006.01)

(21) International Application Number:
PCT/US2020/031553

(22) International Filing Date:
06 May 2020 (06.05.2020)

(25) Filing Language: English

(26) Publication Language: English

(30) Priority Data:

62/848,091	15 May 2019 (15.05.2019)	US
62/852,677	24 May 2019 (24.05.2019)	US
62/959,559	10 January 2020 (10.01.2020)	US

(71) Applicant: **CORNING INCORPORATED** [US/US]; 1 Riverfront Plaza, Corning, NY 14831 (US).

(72) Inventors: **AN, Chong, Pyung**; 18 Tall Meadow Court, Painted Post, NY 14870 (US). **AGNELLO, Gabriel, Pierce**; 19 Maynard St., Corning, NY 14830 (US). **HU, Zhenxing**; 8 Jacqueline Drive, Painted Post, NY 14870 (US). **JANG, Bosun**; 418 Lower Pace Road, A304, Corning, NY 14830 (US). **KNOWLES, Peter**; 857 Grove Street, Elmira, NY 14901 (US). **MEENAKSHI SUNDARAM, Balamurugan**; 3368 Conhocton Rd., Painted Post, NY 14870 (US). **NONI JR., Douglas, Miles**; 380 Hibbard Road, Horseheads, NY 14845 (US). **PRIESTLEY, Richard, Sean**; 125 Fieldview Drive, Painted Post, NY 14870 (US). **WESTBROOK, Jamie Todd**; 239 Oak Hill Drive, Sayre, PA 18840 (US).

(74) Agent: **HARDEE, Ryan, T.**; Corning Incorporated, Intellectual Property Department, SP-TI-03-1, Corning, NY 14831 (US).

(81) Designated States *(unless otherwise indicated, for every kind of national protection available)*: AE, AG, AL, AM, AO, AT, AU, AZ, BA, BB, BG, BH, BN, BR, BW, BY, BZ, CA, CH, CL, CN, CO, CR, CU, CZ, DE, DJ, DK, DM, DO, DZ, EC, EE, EG, ES, FI, GB, GD, GE, GH, GM, GT, HN, HR, HU, ID, IL, IN, IR, IS, JO, JP, KE, KG, KH, KN, KP, KR, KW, KZ, LA, LC, LK, LR, LS, LU, LY, MA, MD, ME, MG, MK, MN, MW, MX, MY, MZ, NA, NG, NI, NO, NZ, OM, PA, PE, PG, PH, PL, PT, QA, RO, RS, RU, RW, SA,

(54) Title: EDGE STRENGTH TESTING METHODS AND APPARATUS

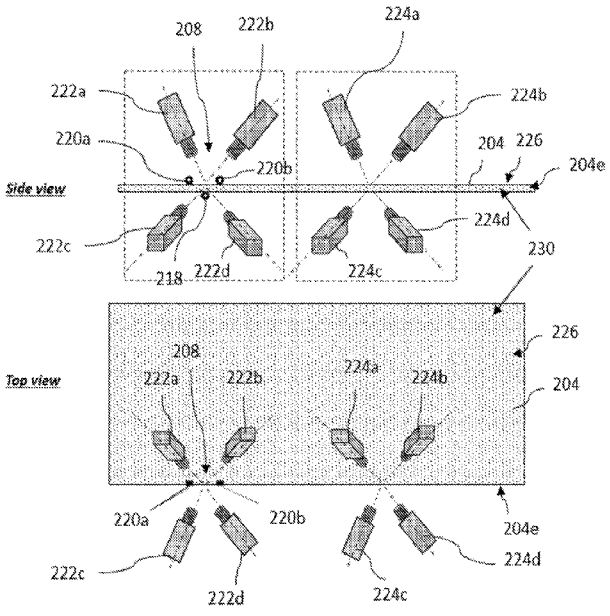


FIG. 14

(57) Abstract: An apparatus for testing a sheet of brittle material is disclosed. The apparatus can include a plurality of assemblies configured for selectively applying a 3-point bending load on an edge of the sheet of material in a test region of the apparatus, a detection mechanism that optically measures strain in the sheet of material in the region, and a processor that determines the stress in the sheet based on the measured strain by calculating the stress that would be required to produce the measured strain in the sheet of material.

WO 2020/231683 A1

[Continued on next page]

SC, SD, SE, SG, SK, SL, ST, SV, SY, TH, TJ, TM, TN, TR, TT, TZ, UA, UG, US, UZ, VC, VN, WS, ZA, ZM, ZW.

(84) **Designated States** *(unless otherwise indicated, for every kind of regional protection available)*: ARIPO (BW, GH, GM, KE, LR, LS, MW, MZ, NA, RW, SD, SL, ST, SZ, TZ, UG, ZM, ZW), Eurasian (AM, AZ, BY, KG, KZ, RU, TJ, TM), European (AL, AT, BE, BG, CH, CY, CZ, DE, DK, EE, ES, FI, FR, GB, GR, HR, HU, IE, IS, IT, LT, LU, LV, MC, MK, MT, NL, NO, PL, PT, RO, RS, SE, SI, SK, SM, TR), OAPI (BF, BJ, CF, CG, CI, CM, GA, GN, GQ, GW, KM, ML, MR, NE, SN, TD, TG).

Published:

— *with international search report (Art. 21(3))*

EDGE STRENGTH TESTING METHODS AND APPARATUS

CROSS-REFERENCE TO RELATED APPLICATIONS

[0001] This application claims the benefit of priority under 35 U.S.C. § 119 of U.S. Provisional Application Serial No. 62/848091 filed on May 15, 2019, U.S. Provisional Application Serial No. 62/852677 filed on May 24, 2019 and U.S. Provisional Application Serial No. 62/959559 filed on January 10, 2020, the contents of each of which are relied upon and incorporated herein by reference in their entireties.

FIELD OF THE DISCLOSURE

[0002] The present disclosure relates generally to apparatuses for testing glass and/or glass ceramics and methods of testing glass and/or glass ceramics.

BACKGROUND

[0003] High-performance display devices, such as liquid crystal displays (LCDs) and plasma displays, are commonly used in various electronics, such as cell phones, laptops, electronic tablets, televisions, and computer monitors. Currently marketed display devices can employ one or more high-precision glass sheets, for example, as substrates for electronic circuit components, or as color filters, to name a few applications. The leading technology for making such high-quality glass substrates is the fusion draw process, developed by Corning Incorporated, and described, e.g., in U.S. Patent Nos. 3,338,696 and 3,682,609, which are incorporated herein by reference in their entireties; however, embodiments described herein are applicable to any forming process including slot draw, redraw, float, and the like.

[0004] For each of these applications, a glass sheet is typically cut to size, and then resulting sharp edges of the glass sheet are beveled by grinding and/or polishing. Cutting, edge machining, grinding and other processing steps can introduce flaws, such as chips or cracks, at surfaces and edges of the glass sheet. These flaws can serve as fracture sources and thereby reduce the strength of the sheets, particularly if the glass is flexed such that the flaws experience tensile stress. Display devices experience some flexing, thus the existence of these flaws may be of concern. Flexible display devices by their very nature, may produce significant stress in the display substrate(s), either during the manufacturing process or in use. Thus, residual flaws that might be present in the glass sheets may result in

cracks in the glass sheet when the glass sheets experience sufficiently large stresses. Since typical display manufacturing involves cutting the glass to form individual displays, and cutting is known to create multiple flaws in the glass along the cut edge, glass substrate-based flexible display devices may have unacceptably high probability of fracture after the glass sheets are made into the final products.

[0005] Attempts to mitigate flaws at the edges of glass sheets have included laser cutting, grinding, polishing and so forth, all in the attempt to remove or minimize the flaws that are created when the glass sheet is cut to size. However, many of these approaches are unsatisfactory either because the technique is incapable of removing flaws down to the size needed for the expected stresses or because the technique is difficult to apply to such thin glass sheets (less than about 0.4 mm thick). Acid etching of glass edges may be used, but this may degrade the display device disposed on the substrate. Thus, some level of flaws will continue to exist in manufactured glass sheets, in particular at the edges of the sheet, and there is a need in the industry to accurately test the edge strength of such glass sheets, as well as panels or laminate structures using such glass sheets, in order to screen out glass sheets that have lower than desired edge strength.

[0006] Conventional inspection methods utilize over one hundred full time employees working exclusively on making V4PTB measurements on glass edge samples. Even with this large commitment of manpower, only a very small fraction of total production can be tested. This leads to quality leakage in the form of bad product reaching the customer stemming from the low frequency of testing. Also, because nearly all allocated resources are committed to keeping up pace with quality requirements, there is little or no opportunity for process optimization studies to help improve product quality. Conventional methods thus create a precarious situation where one may be making poor product but does not have the bandwidth to intercept this product before it leaves or to ascertain on how to fix the problem. Exemplary embodiments, however, lead to a drastic reduction in the amount of time devoted to edge quality control, a dramatic increase in total glass tested versus glass produced, a dramatic increase in the percentage of edge perimeter tested, and a means for simultaneous process feedback for use in pursuit of product improvement.

SUMMARY

[0007] Exemplary embodiments will be described directed to methods for the continuous measurement of the breaking strength of a glass edge by putting the edge under stress, such

that stresses away from the edge are significantly less than the breaking strength at their respective locations. Additionally, using exemplary embodiments both sides of an edge can be subject to substantially the same tensile stress during the measurement. Additionally, exemplary embodiments provide a continuous high speed nature which results in at least a 30x increase in processing speed, at least a 3x increase in the number of sample edges tested, and orders of magnitude of the size of the population of glass sheets that are covered by the sample of edges tested. This increase in statistical sampling can thus guarantee less leakage of defects to the customers and is amenable to online configurations.

[0008] In some embodiments, an apparatus for testing edge strength of a sheet of material is disclosed. The apparatus comprises a plurality of assemblies configured for selectively applying a 3-point bending load along an edge of the sheet of material in a test region of the apparatus, whereby the plurality of assemblies can establish a loaded condition on the sheet of material in the test region by applying the 3-point bending load and establish a no-load condition on the sheet of material in the test region by not applying the 3-point bending load. The apparatus also includes a detection mechanism configured for optically measuring strain in the sheet of material in the test region when the sheet of material is in the no-load condition and when the sheet of material is in the loaded condition. The loaded condition is produced by the 3-point bending load. The apparatus also includes a processor that is configured for determining stress in the sheet of material based on the measured strain.

[0009] In another embodiment of the apparatus for testing a sheet of material, the apparatus can include a plurality of assemblies configured for continuously advancing the sheet of material through a test region of the apparatus along an edge of the sheet. The plurality of assemblies are further configured for selectively applying a 3-point bending load on the edge of the sheet of material passing through the test region. The apparatus also includes a detection mechanism configured for optically measuring strain on a surface of the sheet passing through the test region, where the strain is produced by the applied load. The apparatus also includes a processor for determining stress in the sheet passing through the test region resulting from the applied load, where the stress is determined based on the measured strain. The applied load on the test region produces a strain on the surface of the test region because the load bends the test region of the sheet of material.

[0010] A method of testing edge strength of a sheet of material along an edge of the sheet is also disclosed. The method comprises: applying a surface pattern of visual markers on a surface of the sheet in a region of interest along the edge of the sheet; obtaining a first optical image of the surface of the sheet in the region of interest without any 3-point bending load applied to the region of interest; applying a 3-point bending load to the region of interest along the edge of the sheet; obtaining a second optical image of the surface of the sheet in the region of interest while the 3-point bending load is being applied to the region of interest; and determining stress on the surface of the region of interest along the edge of the sheet resulting from the application of the 3-point bending load based on the first optical image and the second optical image.

[0011] According to some embodiments, another method of testing edge strength of a sheet of material along an edge of the sheet using a test apparatus that comprises a test region is disclosed. The method comprises: applying a surface pattern of visual markers on a surface of the sheet in a region of interest along the edge of the sheet; continuously advancing the sheet of material through the test apparatus wherein the edge of the sheet is advanced through the test region while applying a 3-point bending load to the portion of the sheet passing through the test region; obtaining a first optical image of the surface of the sheet in the region of interest while the edge of the sheet is continuously advancing through the test region but before the region of interest reaches the test region; obtaining a second optical image of the surface of the sheet in the region of interest when the region of interest advances into the test region while the 3-point bending load is being applied; and determining stress on the surface of the region of interest along the edge of the sheet resulting from the application of the 3-point bending load based on the first optical image and the second optical image.

[0012] Additional features and advantages of the disclosure will be set forth in the detailed description which follows, and in part will be readily apparent to those skilled in the art from that description or recognized by practicing the methods as described herein, including the detailed description which follows, the claims, as well as the appended drawings.

[0013] It is to be understood that both the foregoing general description and the following detailed description present various embodiments of the disclosure, and are intended to provide an overview or framework for understanding the nature and character of the claims.

The accompanying drawings are included to provide a further understanding of the disclosure, and are incorporated into and constitute a part of this specification. The drawings illustrate various embodiments of the disclosure and together with the description serve to explain the principles and operations of the disclosure.

BRIEF DESCRIPTION OF THE DRAWINGS

[0014] The following detailed description can be best understood when read in conjunction with the following drawings, where like structures are indicated with like reference numerals where possible and in which:

[0015] FIGS. 1A – 1D are schematic illustration of some examples of the hardware configuration in the standard edge strength measurement system (ESMS) for performing the 3-point or 4-point bending test on an edge of the glass sheet for edge strength.

[0016] FIG. 1E is a schematic illustration for a 3-point bending test arrangement for testing edge strength of a test sample.

[0017] FIG 2 is a plot of variation in load-stress at the tension side of a test panel with change in adhesive location between the panel

[0018] FIG. 3 is a plot of variation of load-stress at the tension side of the test panel with change in roller engagement location

[0019] FIG. 3A is a schematic illustration of the basic principle of digital image correlation (DIC) process that is used in the edge strength testing method described herein.

[0020] FIG. 3B is a stress vs. time plot showing the repeatability study for the DIC at the same location during load cycling.

[0021] FIG. 3C shows the stress distribution along the top edge during 3-point bending.

[0022] FIG. 3D shows the overall load-stress curves of the test samples in the repeatability study for the DIC.

[0023] FIG. 4 is an isometric view of an embodiment of an ESMS as disclosed herein.

[0024] FIG. 5A is a side view of the ESMS of FIG. 4.

[0025] FIG. 5B is a close-up view of the arcuate members of the apparatus of FIG. 5A that are engaging the sheet being tested.

[0026] FIG. 6 is a top view of the apparatus shown in FIGS. 4 and 5A.

[0027] FIG. 7 is a close up view illustration of one arrangement of the assemblies for making the 3-point contact with an edge of the test sheet to bend the test sheet for testing the edge strength according to an embodiment of the present disclosure.

[0028] FIG. 8A is a sample strain field obtained at a load of 6N.

[0029] FIG. 8B is a chart showing the maximum stress through a test in static mode.

[0030] FIG. 8C shows a comparison of stress fields generated using a digital image correlation (DIC) apparatus disclosed herein compared with stress field results generated using finite element analysis (FEA).

[0031] FIG. 8D shows a chart with maximum stress versus displacement calculated using the digital image correlation apparatus disclosed herein and using finite element analysis.

[0032] FIG. 9A is a schematic showing the dynamic mode of an apparatus as disclosed herein.

[0033] FIG. 9B is a schematic showing a sequence of regions being imaged as a sheet of material advances through the plurality of assemblies without a load.

[0034] FIG. 9C is a schematic showing a sequence of regions being imaged as a sheet of material advances through the plurality of assemblies with an applied load.

[0035] FIG. 9D is a schematic illustration showing two ways of using DIC for test sheet stress measurement: measuring the stress on the test sheet's top surface and measuring the stress on the vertical edge surface.

[0036] FIG. 9E shows a 3D stress plot on the edge and top surfaces of a glass test sheet.

[0037] FIG. 10A shows a digital image correlation strain map of an 11N load with 60 steps in between.

[0038] FIG 10B shows a strain map from the same test with only one step, which confirms they are identical.

[0039] FIG. 11A, on the top portion of the figure, shows a first schematic of a sample arrangement for use in calibration of ESMS and, on the bottom portion, shows a top view of the test sheet depicted in the schematic.

[0040] FIG. 11B, on the top portion of the figure, shows a second schematic of a sample arrangement for use in calibration of ESMS and, on the bottom portion, shows a top view of the skewed sheet depicted in the schematic.

[0041] FIG. 11C, on the top portion of the figure, shows a third schematic of a tilted sample arrangement for use in calibration of ESMS and, on the bottom portion, shows a top view of the sheet depicted in the schematic.

[0042] FIG. 11D, on the top portion of the figure, shows a schematic of a fourth sample arrangement for tilted sample arrangement for use in calibration of ESMS and, on the bottom portion, shows a top view of the skewed sheet depicted in the schematic.

[0043] FIG. 12 shows a schematic of belt rollers that can be used in embodiments disclosed herein.

[0044] FIG. 13 shows a schematic of ball rollers that can be used in embodiments disclosed herein.

[0045] FIG. 14 shows schematic side view and top view illustrations of a configuration for cameras for monitoring both the horizontal top surface of the test sheet along the edge and the vertical edge surface of the test sheet according to another embodiment of the DIC system of the present disclosure.

[0046] FIG. 15 is a schematic illustration showing the location of the load cell with respect to the arcuate members and the position of the test sheet **204**.

[0047] FIG. 16 is an applied load vs. sample edge position plot showing the improved load control achieved with the aggregate of the improvements to the ESMS disclosed herein.

[0048] FIG. 17 shows a plot of load vs. time measured on ten sample sheets at a faster speed at which the test sample sheet **204** moves over the rollers with a speed of 10 mm/s.

[0049] FIG. 18 shows a plot of load vs. time measured on ten sample sheets at a slower speed at which the test sample sheet **204** moved over the rollers with a speed of 1 mm/s.

[0050] FIG. 19A is an illustration of the ESMS test system according to an embodiment showing a test sheet mounted on a sample stage.

[0051] FIG. 19B is a detailed close up illustration of the desired roller engagement location along the edge of a test sheet **204** which is at a distance **D** from the edge **E** of the bottom roller **218**.

[0052] FIG. 19C is an illustration showing the positioning of the test sheet **204** at the start of the testing procedure with the ESMS so that the leading edge $\mathbf{E_L}$ of the test sheet rests above the apex of the bottom roller **218**.

[0053] FIG. 20 is an illustration of an example of a test sheet **204** identifying a fly-in zone, measurement length, and a fly-out zone.

[0054] FIG. 21 is a plot showing an example of the load profile starting from the initial period during the lowering of the upper rollers **220a**, **220b**, the Fly-in zone, the Measurement Length, and the Fly-out zone.

[0055] FIG. 22 is a schematic illustration of an example of a test sheet 204 identifying a new crack position being detected.

[0056] FIG. 23A is a schematic illustrating the Phantom Motor technique applied to improve the load control in the ESMS according to an embodiment of the present disclosure.

[0057] FIG. 23B is a plot of the measured load readings taken without the Phantom Motor technique modification.

[0058] FIG. 23C is a plot for the measured load readings taken with the Phantom Motor technique.

[0059] FIG. 24 is a graph illustrating the impact of the roller diameter/polymer thickness on the load-to-stress correlation as determined by finite element analysis.

[0060] FIG. 25 is a plot of Stress (MPa) vs. Load (N) comparing two groups of panels of two different thicknesses 0.2 mm and 0.3 mm measured by DIC and modeled by FEA.

[0061] FIG. 26A is a plot of Stress (MPa) vs. Load (N) showing the modeled load-to-stress correlation for panels having different total thicknesses.

[0062] FIG. 26B is a plot of Normalized change in stress vs. Load (N) showing the normalized change in stress with respect to thickness variations in panels.

[0063] FIG. 27A is a plot of force over time measured with dynamic ESMS for 0.1, 0.15, 0.2, and 0.5 mm thick glass sheets.

[0064] FIG. 27B is a plot of displacement over time measured with dynamic ESMS for 0.1, 0.15, 0.2, and 0.5 mm thick glass sheets.

[0065] FIG. 28 is a schematic illustration of a test panel/sheet showing the distance **d** from the center of the edge of the test panel/sheet to the test location.

[0066] FIG. 29 is a plot showing the impact of roller engagement on the load-to-stress correlation as determined by FEA and DIC measurements

[0067] FIG. 30A is a photograph showing an example of an off-apex breakage in a test panel/sheet during an edge strength test.

[0068] FIG. 30B is a plot of normalized stress vs. distance from the roller apex for an off-apex break in a test panel/sheet.

[0069] FIG. 31 is a plot of ESMS stress profile.

[0070] FIG. 32 is a probability vs. stress plot showing the strength distribution of a batch of panels that were analyzed either by the "Simplified method" or "Right" methods.

[0071] FIG. 33 is a schematic illustration showing the different panel surface nominations

[0072] FIG. 34 shows a schematic illustration of the propagation of a pre-existing crack on the long edge which interfered with the short edge measurement.

[0073] FIG. 35 shows the stress profiles on Surface 1 and Surface 3 when the gap between the sealant to glass edge was 0 mm.

[0074] FIG. 36 shows the stress profiles on Surface 1 and Surface 3 when the distance between the sealant to glass edge is 2 mm.

[0075] FIG. 37 is a schematic illustration of a machine learning neural network for identifying cracks in the test panels/sheets.

[0076] FIG. 38 is a schematic of a panel with its design parameters.

[0077] FIG. 39 is a schematic illustration of terminal, non-terminal edges of a panel engaged with the rollers in the ESMS of the present disclosure.

[0078] FIG. 40 is a flowchart illustrating a method according to an embodiment of the present disclosure.

[0079] FIG. 41 is a flowchart illustrating a method according to another embodiment of the present disclosure.

DETAILED DESCRIPTION

[0080] In glass sheet production for display applications, for example, cut-to-size glass sheets are put through finishing processing to remove sharp edges by grinding and/or polishing and to make beveled edges. During these finishing process, handling or other manipulating steps, residual stresses can remain on the edges of the glass sheets. Such residual stresses and improper handling can cause subsequent breakage of the glass sheet. If the breakage occurs before the glass sheets are shipped to the customers, it reduces glass manufacturing yield and disrupts the glass manufacturing process. If the breakage occurs in customer's possession, typically a manufacturer of display devices that utilize the glass sheets, the breakages will cause yield loss and disruptions in the customer's manufacturing process. Regardless of when such subsequent breakage happens, it is not desired.

[0081] For this reason, edge strength of the glass sheets are tested in the glass manufacturing plant before they are shipped to the customers. A conventional method of edge strength testing is vertical four point bending (V4PTB) method. The V4PTB tests are conducted on small test coupon samples of the glass that are cut from the glass sheets at the end of production. The coupons are roughly 150 mm x 10 mm in dimension and the coupons are individually tested. Because a glass sheet is destroyed to cut out a test coupon, only a small number of glass sheets are tested and assume that they are statistically representative of the population of the glass sheets being manufactured.

[0082] Testing the sample coupons by V4PTB is a manually intensive process that takes about one day to process the samples from one glass sheet and hence very few glass sheets are tested, e.g., on the order of about three sheets for every 22,000 sheets produced. Further, such methods are unable to evaluate laminate structures or panels. Such shortcomings can result in significant leakage in the form of bad product reaching a customer.

[0083] In Corning's U.S. patent application serial No. 15/557,991, published as US 2018/0073967 A1, an edge strength measurement system (ESMS) and the related method of non-destructively testing the edge strength of the glass sheets without cutting out test coupons is disclosed. The ESMS system performs 3-point bending test or 4-point bending test directly on the edges of the glass sheets, thus, providing the ability to test the glass sheets in production without the need for cutting so that a larger portion of the glass sheet production population can be tested.

[0084] FIGS. 1A-1D are schematic illustration of some examples of the hardware configuration in the existing ESMS system for performing the 3-point or 4-point bending test on an edge of the glass sheet for edge strength. FIGS. 1A and 1B are perspective and plan views, respectively, of exemplary configurations that enabled 3-point bending test on the edge **205** of a glass sheet **204**. The roller assemblies **207b** and **213b** via the three rollers **215** associated with them, one roller on top side **226** (See FIG. 1E) of the glass sheet **204** and two rollers on the bottom side of the glass sheet **204** provide a 3-point bending test configuration. The roller assemblies **207c** and **213c** via the three rollers **215** associated with them, two rollers on top side of the glass sheet **204** and one roller on the bottom side of the glass sheet **204** provide a 3-point bending test configuration. As noted in FIG. 1B, the vertical load that bends the glass sheet **204** is applied using the rollers on the topside. As shown in the FIG. 1D, the rollers **215** and the glass sheet **204** are positioned so that the rollers **215** catch the edge **205** of the glass sheet **204** between the top and bottom rollers so that the vertical loading force is exerted on the edge **205**.

[0085] FIG. 1C is a side view of an exemplary configuration that enabled 4-point bending test on the edge **205** of a glass sheet **204**. The roller assemblies **207d** and **213d** via the four rollers **215** associated with them, two rollers on top side of the glass sheet **204** and two rollers on the bottom side of the glass sheet **204** provide a 4-point bending test configuration. The vertical load that bends the glass sheet **204** is applied using the roller assembly **207d** on the top side.

[0086] The ESMS system can be useful for testing glass sheets used in the manufacture of flat panel displays as such glass sheets must meet stringent surface quality requirements in the display area that are usually in the central portions of the glass sheet away from the edges. Contacting the serviceable or "quality" areas of the glass sheet may impart surface defects that make the glass sheet unusable. The arrangement of the rollers **215** in the exemplary configurations shown in FIGS. 1A-1D preserves the surface quality on both sides of the glass sheet **204**.

[0087] The ESMS system can be utilized to test sheet materials other than the glass sheet **204** shown in the illustrated examples. For example, the ESMS system can be used to test strength of laminate structures (also referred to as panels), of other rigid or semi-rigid materials. Laminate structures or panels can include a plurality of glass sheets laminated with one or more intermediate polymeric layers or can also, in alternative embodiments,

include a structure having a thin film transistor glass substrate and color filter glass substrate having one or more films therebetween or adjacent to either or both substrates. For purposes of the present disclosure for the ESMS system and methods of using the ESMS system, the terms "sheet(s)" and "panel(s)" will be used interchangeably. Unless specifically distinguished, whether sheet(s) or panel(s) are being tested by the ESMS system will not fundamentally change the edge strength testing methodology using the ESMS system.

[0088] The structure of an example of panels that can be tested on ESMS will be described. Panels with different designs can be tested. FIG. 38 shows a schematic of a panel identifying some design parameters. W and L are the panel's width and length, respectively. (1) is the protruding length of the terminal edge, (2) is the distance between the sealant and panel edge, (3) is the sealant width, (4) and (5) are the CF, TFT glass thicknesses, respectively.

[0089] There are some preferences on the dimensions and sealant properties of the panels in order to be tested on ESMS. They are as follows: Small size rectangular panels that have a length (L) and/or width (W) of 600 mm or less can be tested. Larger size panels are also measurable. Preferably, the protruding length of the terminal edge (1) is longer than the roller engagement, which can range from 0.5 to 2 mm. Preferably, the distance between the sealant and panel edge (2) is less than 1 mm. Preferably, the sealant width (3) is equal to or wider than 500 um. Preferably, the thickness of the sealant is $\leq$ 10 um and have a Young's modulus of 1 Gpa or greater. Preferably, the interfacial bond strength between the brittle material and the seal should be sufficient so that no delamination occurs during the edge strength testing. Preferably, the total thickness of the CF glass thickness (4) + the TFT glass thickness (5) is $\geq$ 0.2 mm but $\leq$ 0.5 mm. The CF glass thickness (4) and the TFT glass thickness (5) can be equal or different. Preferably, the mechanical stiffness of display layers that are deposited on the TFT surface are negligible.

[0090] Both non-terminal and terminal edges of a panel can be tested. FIG. 39 shows the side view and top view of panels being engaged with the rollers on both non-terminal and terminal side edges. The terminal edge of a panel is where the TFT glass protrudes relative to the CF glass edge.

[0091] One of the drawbacks of the ESMS system described in US 2018/0073967 A1 referenced above is that the stress measurement during the edge strength testing is made using load cells attached to the topside roller assemblies **207b**, **207c** that are used to apply the test load to the glass sheet. This is an indirect way of detecting the stress in the edges. A more direct way of measuring the stress experienced by the test subject glass sheet is desired.

[0092] Previous techniques for measuring edge stress and strength of ultra-thin glass sheets using three-point bending configurations produced highly variable results. These results were subject to substantial levels of variability based on a variety of factors, including, but not limited to, (a) failure prior to testing, (b) residue or dust in the system, (c) product variability (*e.g.*, changes in panel thickness, adhesive properties/location), and (d) alignment, among others. These sources of variability resulted in incorrect strength measurements and resulted in unexpected product failure in the field. FIG. 2 and FIG. 3 show how changes in adhesive location and roller engagement result in variability in stress values. FIG. 2 is a plot of variation in load-stress at the tension side of a test panel with change in adhesive location between the panel. FIG. 3 is a plot of variation of load-stress at the tension side of the test panel with change in roller engagement location. An additional source of variability is the fact that the previous three-point bending configurations obtained results based on models of the glass sheets, not direct measurements of the strain on the surface of the region of the glass sheet at issue.

[0093] In contrast, the measurement apparatuses and methods disclosed herein provide real-time information on stress distributions in the sheet **204** being tested using Direct Image Correlation (DIC) full-field imaging techniques. Using DIC, one can measure strain on the surface of the sheet **204** in both in-plane orthogonal directions simultaneously as a function of time. Then, stresses can be determined from the measured strains and generate stress field map of the sheet. The direct measuring techniques disclosed herein are more accurate than the previous techniques and avoid the need to develop new calibration equations and models each time the glass sheet/panel is redesigned or reconfigured.

[0094] Examples of the uses of the ESMS described herein include, but are not limited to: (a) calibrating currently existing edge strength testers that do not have DIC capability; (b) investigating the failure modes of new glass sheet/panel designs as the test system has the flexibility to change various testing parameters such as roller engagement, sheet/panel

angle, roller diameter, loading rate, etc.; and (c) optically making direct strain measurements during dynamic & continuous edge strength testing suitable for manufacturing plants.

[0095] Examples of benefits and advantages of the devices described herein include, but are not limited to:

- Direct full-field (optical) strain measurement on ultra-thin glass panels.
- Optical imaging for detection along with the full field stress mapping provides insight into the failure modes.
- Real-time stress visualization during dynamic, continuous edge testing suitable for deployment in manufacturing plants
- Improved analytical equations to obtain stress from measured strains.
- Novel material handling assemblies that provide enhanced optical visibility enabling the above-mentioned stress measurement.
- Ability to act as a calibration bench for existing edge strength testing devices.
- Ability to vary the testing parameters like roller diameter, engagement area, roller thickness etc. in order to develop new panel designs.
- Accurate stress measurements with accuracy of ±10% on measured stress

[0096] Referring to FIGs. 4-7, 9B and 9C, an apparatus **200** for testing the edge strength of a sheet **204** of material is disclosed. The structures of the apparatus **200** described herein is an exemplary embodiment that is configured to optically measure strain in the sheet **204** when the sheet is in a no-load condition and when the sheet **204** is in a loaded condition. The loaded condition being produced by a 3-point bending load.

[0097] The apparatus **200** can include a plurality of assemblies **206a, 206b** configured for selectively applying a 3-point bending load along an edge of the sheet **204** of material in a test region **208**. Selectively applying the 3-point bending load means that the plurality of assemblies **206a**, **206b** are configured to apply or not apply the 3-point bending load as desired and also control the amount of load applied. The apparatus **200** also includes a detection mechanism configured for optically measuring strain in the sheet **204** in the test region **208** when the sheet **204** of material is in a no-load condition and when the sheet **204**

of material is in a loaded condition. The strain in the loaded condition is produced by the applied 3-point bending load. The apparatus **200** also includes a processor **214** (see FIG. 9C) for determining stress in the sheet **204** based on the measured strain. The applied 3-point bending load on the sheet **204** produces a strain on the surface of the sheet **204** because the applied 3-point bending load bends the sheet **204**.

[0098] The plurality of assemblies **206a**, **206b** (see FIG. 7) comprise two opposing assemblies **206a** and **206b**, where the first **206a** of the two opposing assemblies comprise a single arcuate member **218** for engaging a first side of the sheet **204**. The second **206b** of the two opposing assemblies comprise two spaced-apart arcuate members **220a**, **220b** for engaging a second side **230** of the sheet **204** opposite the first side. The two spaced-apart arcuate members **220a**, **220b** define the test region **208** between the two spaced-apart arcuate members.

[0099] The arcuate members **218**, **220a**, and **220b** can be rotatably mounted rollers, as shown in FIG. 9A, belt rollers, bearing rollers, or fixed bushings. Fixed bushing (e.g. non-rotating) structures are shown in FIGs. 4 and 5B. The fixed bushings are configured with an arcuate surface formed from a material having a low coefficient of friction (e.g., a fluropolymer resin). In a preferred embodiment of the test apparatus **200** of the present disclosure that incorporates the DIC feature, the two spaced-apart arcuate members **220a** and **220b** are fixed bushing structures for engaging the second side **230** of the sheet **204** as shown in FIGs. 4 and 5B. The non-rotating bushing structures are configured to have narrower width than the rotating roller embodiments so that the bushing structures provide wider space between the two arcuate members while the two contact points on the surface of the test sheet **204** are the same distance apart.

[00100] In some embodiments, the detection mechanism comprises a first optic system **222** for determining the strain on the surface of the test sheet **204** in the test region **208**. The first optic system **222** utilizes the DIC technique to determine the strain. DIC technique is described in more detail below but essentially, DIC determines the strain by acquiring two images of an interested region of the test sheet **204**: first image taken in a no-load condition, and a second image taken with the interested region of the test sheet in a loaded condition, i.e., under a 3-point bending load in the context of the present disclosure. The surface of the interested region is provided with some visual markers so that when the two images are

compared, any displacement of the visual markers in the loaded condition image caused by strain (deformation) can be detected.

[00101] As mentioned, the sheet **204** can be a brittle material such as glass or glass ceramic. The 3-point bending load is enough to deform the sheet **204** of material. As shown in FIGS. 4-5B, and 7, in some embodiments, the plurality of assemblies **206a**, **206b** comprises a first assembly **206a** positioned below the sheet **204** comprising a single arcuate member **218** for engaging a first side (the lower side) of the sheet **204** and a second assembly **206b** positioned above the sheet **204** comprising two arcuate members **220a**, **220b** for engaging a second side (the top/upper side) **226** (see FIGs. 11A, 11B) of the sheet **204** opposite the first side. The two arcuate members **220a**, **220b** are separated by a minimum spacing **S** in order to provide a clear view of the test region **208** for the optic system. The actual dimension of the minimum spacing **S** will depend on the particular type of cameras and the size of the test region **208** that is determined by the particular arrangement of the arcuate members **220a**, **220b**, and **218** chosen.

[00102] The arcuate members **218**, **220a**, and **220b** are preferably structures that contacts the sheet **204** while the arcuate members and the sheet are moving relative to each other while imparting low friction at the contact surface. Some examples of such arcuate members are cylindrical rollers, as shown in FIGS. 7, 9A-9C, and 11A-11D, and bearing rollers as shown in FIG. 13.

[00103] In belt roller embodiments, such as shown in FIG. 12, the arcuate members **218**, **220a**, **220b** can be belt rollers **240c**, **240a**, **240b**. In the belt roller embodiment, a belt **240a**, **240b**, **240c** extends around a drive shaft **242a**, **242b**, **242c** and an arcuate tensioner **244a**, **244b**, **244c**. In some embodiments, the arcuate tensioner can be a cylindrical roller or a static, arcuate tensioner (such as a polished metal finger with an arcuate portion contacting the belt). In bearing roller embodiments, such as shown in FIG. 13, the arcuate members **218**, **220a**, **220b** are bearing rollers **246a**, **246b**, **246c**. In such embodiments, the bearing rollers **246a**, **246b**, **246c** are formed from a roller ball **248a**, **248b**, **248c** disposed and retained within a socket **250a**, **250b**, **250c**.

[00104] In some embodiments, as shown in FIG. 9A, the single arcuate member **218** is vertically aligned between the two spaced-apart, arcuate members **220a**, **220b**. As used herein, "longitudinally" refers to the direction of motion of a sheet **204** passing through the test apparatus **200** (*e.g.*, the machine direction).

[00105] Referring to FIG. 9B, in some embodiments, the optic system **222** comprises a first set of stereo (i.e. a pair) CCD cameras **222a**, **222b** positioned above the second side **226** of the sheet **204** to inspect the surface of the sheet **204** in the test region **208** between the two spaced-apart arcuate members **220a**, **220b**. The test region **208** is the region between the arcuate members **220a**, **220b**, under the two cameras **222a**, **222b** where the two cameras **222a**, **222b** are aimed to take digital images to make optical measurements. In other words, the test region **208** represents the field of view of the two cameras **222a**, **222b**. Also, the test region **208** is the region where the three arcuate members **221**, **220**, and **218** can apply a 3-point bending test load. Thus, the test region **208** represents the target area of the test apparatus for applying a 3-point bend test on a test sample. A test sheet **204** to be tested needs to be brought into the test region **208** for edge strength testing. The pair of cameras **222a**, **222b**

[00106] In some embodiments, the test apparatus **200** can be operated in a dynamic mode. In a dynamic mode, the edge strength testing of the sheet **204** is conducted by passing the sheet **204** through a test region **208** of the testing apparatus **200**. Alternatively, the testing apparatus **200** can be configured so that the edge strength testing of the sheet **204** is conducted by keeping the sheet **204** stationary and having the testing apparatus traverse over the sheet **204**.

[00107] can include a plurality of assemblies **206a, 206b** configured for continuously advancing the sheet of material through the test region **208** along an edge of the sheet **204**. The plurality of assemblies **206a**, **206b** are further configured for applying a 3-point bending load on the edge of the sheet of material passing through the test region **208**. The apparatus **200** also includes a detection mechanism configured for optically measuring strain on a surface of the sheet passing through the test region **208**, where the strain is produced by the applied 3-point bending load. The apparatus **200** also includes a processor **214** for determining the stress in the sheet **204** passing through the test region **208** resulting from the applied. The stress is determined based on the measured strain. The applied load on the test region **208** produces a strain on the surface of the test region **208** because the applied 3-point bending load bends the sheet **204** in the test region **208**.

[00108] **[Digital Image Correlation (DIC)]**

[00109] The DIC feature of the testing apparatus **200** will now be described in more detail with reference to FIGS. 9B and 9C. DIC involves point tracking. It is a full-field optical

technique for obtaining displacements and thereby strains. In some embodiments, the surface of the second side **226** is applied with a surface pattern **230** as visual markers to facilitates the strain measurements in both no-load state and the loaded state. In the loaded state measurement mode, the load imposed on the sheet **204** in the test region **208** causes the surface of the second side **226** of the sheet **204** to deform which, in turn, distorts and displaces the surface pattern **230** on the second side **226** of the sheet **204**. The surface pattern **230** can be an array of dots or points applied on the surface being monitored that will serve as visual markers for the purposes of measuring the strain in the sheet **204**. The array of dots or points can be in any pattern, regular or random. The image of the surface pattern **230** on the sheet **204** taken in the no-load condition serves as the reference point for determining the displacement of those reference points caused by the distortion of the surface pattern **230** resulting from the subsequent application of the 3-point bending load. The first set of stereo cameras **222a**, **222b** in the optic system **222** observes the distortion of the surface pattern **230** and the image data can be used to determine the amount of strain in the sheet **204**.

[00110] In order to make the determination of the amount of strain in the sheet **204** from the distortion of the surface pattern **230**, the amount of the distortion needs to be quantified. This is achieved by comparing the image bearing the distorted surface pattern **230** on the top surface **226** of the test sheet **204** to a reference/registration image of the second side **226** in a no-load state where the surface pattern **230** is not distorted.

[00111] Whether the apparatus **200** is operating in a static mode or a dynamic mode, an image of the surface pattern **230** in a no-load state is recorded as a reference or a baseline state using the optic system **222**. The reference image is used to register the original location of the various points in the surface pattern **230**. Then, the new location of the registered points is tracked in the loaded state image. If the top surface **226** is distorted from the applied load stress, many of the registered points on the top surface **226** will have displaced from their original location. By correlating the registered points in the two-image data, the processor **214** can determine and quantify the deformation, *i.e.* the strain. The algorithms for performing such digital image correlation is well known in the art and more detailed discussion is not necessary here.

[00112] The surface pattern **230** can be printed on the top surface **226** or projected as an image on the top surface **226** or sprayed on as random pattern on the top surface **226** or

etched on using chemical treatment on the top surface **226** or pasted on with manufactured thin film having a pattern on the top surface **226**. Nanoparticles can be sprayed on the top surface **226** using airbrush. The pattern **230** can be a speckle pattern or a grid pattern.

[00113] In some embodiments, the surface pattern **230** can comprise a coating of a mixture, or a blend of black and white dots to form a speckle pattern. The stereo cameras **222a**, **222b** and/or **224a**, **224b** with proper lensing are used to record the image of the surface pattern **230** during the test. The coating of the speckle pattern **230** can be made using oil based black and white spray that produce fine mist resulting in speckles with each speckle covering 5-7 μm. The paint layer was ensured to be less than a few microns so that it doesn't affect the results. A white light LED lamp was used to illuminate the region of interest for optical inspection by the stereo cameras.

[00114] There are two ways of using DIC for edge strength measurement: one is measuring the strain on the sample's top surface and the second is measuring the strain on the edge surface. The illustration in FIG. 9D identifies the top surface **226** and the edge surface **204e** on a test sheet **204**. The edge strength measured from both approaches should be the same since the stress is continuous at the edge boundary. This is illustrated in FIG. 9E which shows a 3D stress plot on the edge and top surfaces of a test sheet. The gradients in the image represented by the difference in the darkness of the shading show that the stresses on the top and edge surfaces are continuous. The darkness of the shading in the gradients represent different stress levels but the actual stress values are not important for the purposes of this disclosure.

[00115] [<u>Alternative way of speckle coating and method to perform dynamic DIC thereof</u>]

[00116] If the test sheet **204** is coated with visible speckle dot surface pattern **230**, that glass sheet is not usable for consumer application even if it survives the edge strength test screening. To circumvent this, one could use non-visible speckles that are only visible to specialized optical systems employed by the apparatus (*e.g.*, ultraviolet light, fluorescent imaging, infrared light, or another non-visible portion of the electromagnetic spectrum). Alternatively, one can project speckle dots on the test sheet **204** using lasers and these speckle dots can be tracked by the cameras during the test. The dot pattern can be random.

[00117] Exemplary embodiments have been described directed to a method for the continuous measurement of the breaking strength of a glass edge by putting only the edge

under stress, such that stresses away from the edge are significantly less than the breaking strength at their respective locations. Additionally, using exemplary embodiments both sides of an edge can be subject to substantially the same tensile stress during the measurement. One method to provide this continuous stress has been described in detail (e.g., opposed and offset rollers), but the claims appended herewith should not be so limited as it is envisioned that acoustic energy and/or infrared energy (both coherent and incoherent) can also be used for the same purpose to induce stress at the edge of a glass sheet. For example, focused ultrasound can be used to induce stress at a glass edge and measurements taken therefrom using the apparatuses and methods disclosed herein. Further, IR irradiation using a laser or other means (at a spectrum in which a respective glass material may have significant absorption) may also be used to induce stress at a glass edge and exemplary measurements taken therefrom using the apparatuses and methods disclosed herein. Additionally, exemplary embodiments provide a continuous high speed nature which results in at least a 30x increase in processing speed, at least a 3x increase in the amount of edge tested, and orders of magnitude of sheets processed and tested over conventional methods. This increase in statistical sampling can thus guarantee less leakage to the customer and is amenable to online configurations.

[00118] [Top Surface DIC]

[00119] The basics of the optical methodology DIC is shown in FIG. 3A. By comparing the images at each time intervals (over increasing load or before and while load is applied), the displacement of the speckle dots can be tracked. This provides a displacement map which can be differentiated to obtain strains. This 3D DIC technique can be used to obtain 3D strain fields. Using the two (**x** and **y** directions) in-plane strain fields the bending stresses can be determined using Equation (1):

$$\sigma_{xx} = \frac{E(\epsilon_{xx} + \upsilon\epsilon_{yy})}{1-\upsilon^2} \qquad (1)$$

where, **E** is the Elastic modulus, ϵ_{xx} is the strain along the bending direction (x), ϵ_{yy} is the strain along the other in-plane principal axis (y), and υ is the Poisson's ratio. The previous practice of stress conversion neglects the biaxiality of the stress state and uses the Hooke's law for uniaxial stress condition. This provides less information than the DIC technique described herein and oversimplifies the results.

[00120] [Vertical Edge surface DIC]

[00121] Referring to FIG. 14, a series of 3-point bending tests were carried out on test sheets **204** while monitoring the vertical edge surface **204e** of each test sheet **204** using DIC. In these tests, the test sheets **204** had laminated structures such as display panels. The thickness of the test sheets was about 200 μm. Speckle patterns **230** were made on the vertical edge surface **204e** of the test sheet **204**. When testing certain types of test sheets **204** such as those having laminated structures, it may be more desirable to conduct the optical monitoring on vertical edge surface **204e** rather than the top (horizontal) surface of the test sheet **204**.

[00122] FIG. 14 shows a schematic illustration of an embodiment of the camera configuration for the optic system **222** of the test apparatus **200** enabling DIC that can optically measure the strain along the vertical edge surface **204e** during 3-point bending test according to an embodiment. In this embodiment of the test apparatus **200**, a second set of at least one camera **222c**, **222d** is provided aimed at the vertical edge surface **204e** of the test sheet **204**. The at least one camera **222c**, **222d** is aimed at the vertical edge surface **204e** in the test region **208** between the two spaced-apart arcuate members **220a**, **220b**. In a static operation mode of the test apparatus **200**, the at least one camera **222c**, **222d** can be used to obtain optical images of the vertical edge surface **204e** in both the no-load condition and the loaded condition. Although, a pair of cameras **222c**, **222d** are illustrated in FIG. 14 observing the vertical edge surface **204e** in the test region **208**, when observing the vertical edge surface **204e**, a single camera can be utilized because the vertical edge surface **204e** is flat even when the 3-point bending load is applied. Because the vertical edge surface **204e** is flat, a 3D view using two cameras is not necessary.

[00123] FIG. 14 also shows a second set of at least one camera **224c**, **224d** that is aimed at the vertical edge surface **204e** but at a location away from the test region **208**. Similar to the pair of cameras **224a**, **224b**, the second set of at least one camera **224c**, **224d** can be used for obtaining optical image of the vertical edge surface **204e** in a no-load condition when the test apparatus **200** is operating in a dynamic mode. Again, although a pair of cameras **224c**, **224d** are illustrated in FIG. 14, a single camera can be utilized for observing the vertical edge surface **204e**. The processor **214** is connected to the cameras **222c**, **222d**, **224c**, and **224d** and the processor **214** can control the cameras as well as receive and process the optical images from the cameras.

[00124] The inventors developed two ways of making fine speckle patterns. The first one, the inventors used a fine brush with liquid paint to make a layer of paint on the edge surface. Then, a lens tissue was used to make a pattern on the edge surface. The lens tissue has a fine random pattern at microscale, and the area with fiber absorb paint, and the area without fiber leaves the paint on the edge surface. This technique provides good speckle pattern for imaging. Another technique for making fine speckle pattern is using nanoparticles for speckle pattern manufacturing. However, the agglomeration affects the quality of the speckle pattern. The quality is not very reliable and stable.

[00125] FIG. 3B shows the repeatability study for the DIC at the same location during load cycling. It shows that the repeatability of DIC on the edge is stable. The accuracy of DIC is in ±10 MPa as we can see at load-free state. Using edge surface DIC, it was observed that the failure mode of the panel is mostly due to stress concentration. FIG. 3C shows the stress distribution along the top edge during 3-point bending. The individual curves are the stress distribution along the top edge at different loads. FIG. 3C shows the stress distribution from loading to the point of the test sheet **204** breaking. From those curves, it can be seen that the defects along the edge affect the stress distribution. FIG. 3D shows the overall load-stress curves of the test samples. It should be noted that edge surface DIC is done at high magnification. The resolution of one pixel is about 0.5 μm, the stress is localized at the Apex location. The variation is due to edge defects, accuracy of Apex location, and sample variations such as thickness, intrusion, layer different, sealing stage and others,

[00126] In some embodiments, a conventional acrylic paint can be used to form very thin (few microns) coating of the speckle surface pattern **230** on the glass sheet **204**. As the modulus of the paint is at least an order less than the glass sheet **204** and its thickness is couple of orders lower than the glass sheet **204**, the effect of the pattern on the measurements is negligible. The use of such surface patterns in digital image correlation is well known in the art and more detailed discussion is not necessary here.

[00127] The top surface and edge surface DIC can be performed statically or dynamically. Static DIC measures the load-to-stress correlation at a fixed location along the edge of the test sheet **204**. Dynamic DIC measures the load-to-stress correlation along the entire length of the edge of the test sheet **204**. Static DIC is easy to perform, but can only measure a single location at a time. Dynamic DIC is more complex to perform, but can measure the entire length of the edge of the test sheet **204**. Static DIC works best for samples such as

monolithic glass where the correlation doesn't change with respect to edge location. Dynamic DIC works best for samples such as panels having laminated structure where the correlation may vary.

[00128] **[ESMS Static Mode - Edge strength tester with real time stress measurement]**

[00129] In a static mode embodiment, the first set of stereo cameras **222a**, **222b** are used to obtain both the no-load measurement and the loaded measurement in a stepwise manner. A surface pattern **230** of visual markers is provided on the top surface **226** of the test sheet **204**. The test sheet **204** is moved in a stepwise manner through the test region **208** of the test apparatus stopping when the particular region of the sheet **204** to be tested is brought into the test region **208** so that the no-load and loaded measurements can be taken.

[00130] In this example, four different regions to be tested (**Regions 1, 2, 3,** and **4**) along an edge of the sheet **204** are brought into the test region **208** by moving the sheet **204** from right-to-left motion as illustrated in FIG. 9B. To test the test **Region 1**, which is on the left-most portion of the bottom edge of sheet **204**, is brought into the test region **208**. To test the test **Region 2**, which is a little to the right of **Region 1**, the sheet **204** is moved to the left in the direction of the arrows in FIG. 9B. Similar steps are repeated to test **Regions 3** and **4**. This initial step is carried out without any vertical load being applied by the upper arcuate members **220a**, **220b**. For 3-point bending test, the load applied is increased until a predetermined load is reached or until a failure of the sheet **204** is detected. The first optic system **222** includes at least two cameras **222a**, **222b** in order to optically inspect and detect deformation of the sheet in the no-load measurement and the loaded measurement.

[00131] The loaded state of the test apparatus for each of the test **Regions 1-4** illustrated in FIG. 9C. In the loaded state, a vertical load is applied either by the two top arcuate members **220a**, **220b** or by the single lower arcuate member **218**. Either way, the applied load causes the sheet between the arcuate members to bend. Each of the four loaded states corresponding to the **Regions 1-4** are labeled as **Deformation 1, 2, 3**, and **4**, respectively.

[00132] In the static mode, the no-load measurement and the loaded measurement can be made back to back at each of the four test regions. Alternatively, the no-load measurements for the four **Regions 1-4** can be made first, then the sheet **204** can be moved back to the initial position and then the loaded measurements can be made for each **Deformation 1, 2, 3, 4** states by moving the sheet **204** through the test region **208**.

[00133] Combining the 3-point bending based edge strength testing technique and the optical method of DIC with appropriate design modifications, it is possible to make real time stress measurements while strength testing the edge of an ultra-thin monolithic or laminate glass structure (e.g., a sheet of material).

[00134] Any form of optical measurement, including DIC feature, requires a clear direct optical view of region of interest on the test sheet **204** in the test region **208** for the measurement. In earlier systems (*e.g.*, U.S. Patent Application Publication No. 2018-0073967) there was no direct stress measurement and their design did not allow for a clear optical pathway to the region of interest because the rollers blocked the path. According to the present disclosure for DIC implemented embodiment of the testing apparatus **200**, the arcuate members **220a**, **220b** are modified to allow clear optical pathway to the region of interest for the cameras. See FIGS. 4-7, 9A-9C, and 11A-11D. This modification and the resulting improvements are also present for the testing apparatus **200** whether the apparatus is operated in a static DIC mode or a dynamic DIC mode. The key design considerations were:

- The top rollers (the arcuate members) **220a**, **220b** were changed from a wheel to a partial section. Specifically, the partial section width was minimized for maximum optical pathway while maintaining the required contact area on the glass sheet **204** of a full roller. See FIGS. 5A and 5B.
- Fine micrometer level adjuster **232** was incorporated for x, y, z axis control to enable precision alignment of glass to rollers/upper partial sections for studying the effects of engagement. See FIGS. 5A and 5B.
- Fine micrometer level adjustment **234** was incorporated for axis control to enable precision alignment of glass to rollers/upper partial sections for studying the effects of skew. See FIGS. 5A and 5B.
- The two halves of the fixture and the partial sections were all pinned with dowels **236a**, **236b** to insure initial test alignment. See FIGS. 5A and 5B.

[00135] With a clear optical pathway to the test region **208** now available, an optical system was designed that employs the techniques of DIC to make real time direct stress measurements. Two 4 megapixel commercial monochrome cameras fitted with specialized lens systems were used to view a 7 mm x 7 mm test region **208** near the edge of the glass sheet **204**. The samples were coated with a random black and white dot surface pattern **230**

so that the dots were about 5-7 pixels in size and the thickness of the coating did not exceed few microns. Using the stereo camera system, a series of images (150-200 pairs of images at 4 frames per second) was recorded during an edge testing experiment. This series of images was correlated to yield the strain fields and thereafter using the Equation (1), stresses were obtained. An example of the stress field obtained at a load step of 6N along with the history of maximum stress throughout a test is shown in FIG 8C. It is believed that this kind of stress visualization/measurement was never done before. The results were correlated with numerical simulation (e.g., finite element analysis) and a good agreement is seen as shown in FIG. 8C.

[00136] Referring to the flowchart **500** in FIG. 40, an example of the method of testing edge strength of a sheet of material along an edge of the sheet **204** of material can be outlined as follows: the method comprises: (a) applying a surface pattern of visual markers **230** on a surface **226** (the second side) of the sheet **204** in a region of interest along the edge of the sheet **204** (see box **510**); (b) obtaining a first optical image of the surface of the sheet **204** in the region of interest along the edge of the sheet without any 3-point bending load applied to the region of interest (see box **520**); (c) applying a 3-point bending load to the region of interest along the edge of the sheet (see box **530**); (d) obtaining a second optical image of the surface of the region of interest along the edge of the sheet while the 3-point bending load is being applied to the region of interest (see box **540**); and (e) determining stress on the surface of the region of interest along the edge of the sheet resulting from the application of the 3-point bending load based on the first optical image and the second optical image (see box **550**).

[00137] In some embodiments of the method of flowchart **500**, the step (e) of determining stress on the surface of the region of interest along the edge of the sheet comprises: measuring strain in the sheet **204** of material in the region of interest in a no-load condition based on the first optical image; measuring strain in the sheet of material in the region of interest in a loaded condition, where the 3-point bending load is applied, based on the second optical image; and comparing the measured strain in the no-load condition to the measured strain in the loaded condition to determine the strain in the sheet induced by the applied 3-point bending load.

[00138] In some embodiments of the method, the step of measuring strain in the sheet of material in the region of interest in the loaded condition based on the second optical image

comprises determining the displacement of the visual markers **230** in the second optical image compared to the visual markers' location in the first optical image. In some embodiments, the step of determining stress on the surface of the region of interest along the edge of the sheet comprises calculating the stress that would be required to produce the measured strain in the sheet of material in the region of interest.

[00139] In some embodiments of the method, applying the surface pattern of visual markers comprises printing, coating, spraying, etching, pasting, or projecting an image on the surface of the sheet.

[00140] In some embodiments of the method, the first optical image and the second optical image are obtained using an optic system comprising at least one camera **222a**, **222b**.

[00141] [**Dynamic Mode - Edge strength tester along with algorithm for real-time stress measurement**]

[00142] Referring to FIG. 9C, in some embodiments, the apparatus **200** can operate in a dynamic mode where the apparatus **200** can obtain both the no-load measurements and the loaded measurement while the test sheet **204** is continuously moving through the test apparatus **200** without pausing. In preferred embodiments, both the no-load measurements and the loaded measurements are made during a single pass of the test sheet **204** through the test apparatus **200**. In order to achieve this, the optic system **222** can further comprise a second set of stereo cameras **224a**, **224b** positioned ahead of the test region **208** for obtaining the no-load condition measurement by recording an image of the test sheet **204** without any 3-point bending load applied to it.

[00143] The second set of stereo cameras **224a**, **224b** are positioned above the second (top) side **226** of the test sheet **204** and because they are looking at a section of the test sheet **204** ahead of the test region **208** as the test sheet **204** passes by before moving into the test region **208**, the second set of cameras **224a**, **224b** can record the image of the section of the test sheet **204** at no-load condition. This is illustrated by the **Deformation 1** case, the left most illustration in FIG. 9C.

[00144] In the illustrated 3-point bending test configuration imposed by the arcuate members **220a**, **220b**, and **218**, the second side **226** of the test sheet **204** experiences tension as the sheet passes under the topside arcuate members **220a**, **220b** and over the

bottom arcuate member **218**. In some embodiments, as shown in FIGS. 9A, 9B, and 9C, the arcuate members **218**, **220a**, **220b** are rollers.

[00145] The method for testing edge strength of a sheet **204** of material along an edge of the sheet using the test apparatus **200** operating in a dynamic mode can be summarized using the flowchart **600** in FIG. 41. The method comprises: (a) applying a surface pattern of visual markers **230** on a surface of the sheet in a region of interest along the edge of the sheet **204** (see box **610**); (b) continuously advancing the sheet of material through the test apparatus **200** wherein the edge of the sheet is advanced through the test region while applying a 3-point bending load to the portion of the sheet passing through the test region **208** (see box **620**); (c) obtaining a first optical image of the surface of the sheet in the region of interest while the edge of the sheet is continuously advancing through the test region **208** but before the region of interest reaches the test region (see box **630**); (d) obtaining a second optical image of the surface of the sheet's region of interest when the region of interest advances into the test region while the 3-point bending load is being applied (see box **640**); and (e) determining stress on the surface of the region of interest along the edge of the sheet resulting from the application of the 3-point bending load based on the first optical image and the second optical image (see box **650**).

[00146] In some embodiments of the method summarized in flowchart **600**, the step of determining the stress on the surface of the region of interest along the edge of the sheet **204** comprises: measuring strain in the sheet of material in the region of interest in a no-load condition based on the first optical image; measuring strain in the sheet of material in the region of interest in a loaded condition, wherein the 3-point bending load is applied, based on the second optical image; and comparing the measured strain in the no-load condition to the measured strain in the loaded condition to determine the strain in the sheet induced by the applied 3-point bending load.

[00147] In some embodiments of the method of flowchart **600**, the step of measuring strain in the sheet of material in the region of interest in the loaded condition based on the second optical image comprises: determining the displacement of the visual markers **230** in the second optical image compared to the visual markers' location in the first optical image.

[00148] In some embodiments of the method, the step of determining stress on the surface of the region of interest along the edge of the sheet comprises calculating the stress that

would be required to produce the measured strain in the sheet of material in the region of interest.

[00149] In some embodiments of the method of flowchart **600**, the first optical image and the second optical image are obtained by an optic system comprising at least two cameras **222a**, **222b**, **224a**, **224b**. In some embodiments, applying the surface pattern **230** of visual markers comprises printing, coating, spraying, etching, pasting, or projecting an image on the surface of the sheet.

[00150] In some embodiments of the methods described above, the stress is determined in at least two dimensions. The two-dimensional stress is displayed as a surface plot. FIG. 8A shows the two-dimensional surface strain on a sheet when loaded by the 3-point contacts. **216** denotes the peak strain location with high stress and **217** denotes a far field location with low stress. FIG. 8B is an exemplary plot showing the applied load vs. maximum stress on the test sheet measured multiple times. FIG. 8C is also a 2-dimensional surface stress field on a sheet when loaded by the 3-point contacts. The left image is measured by DIC and the right image is modeled by FEA. FIG. 8D shows the normalized stress values as a function of vertical distance from the peak stress location to the inward sheet direction (shown as black arrow). The stress increases as a function of applied load.

[00151] In an embodiment of this system apart from being a calibration unit in its static condition, can also be used in a manufacturing environment (or otherwise) with continuous edge testing in a dynamic mode. As discussed throughout, the direct optical pathway to the surface of the material being tested facilitates the more accurate direct strain measurements relied upon herein.

[00152] The ability to make dynamic mode measurements is a design improvement on the existing edge measurement techniques and also adds the capability of real-time direct stress measurement. In some embodiments, the setup described above can be modified by switching the partial rollers (e.g., arcuate members) with 3 fully functional rollers that can intake the sample continuously feeding into it as shown in FIGS. 9A-9C and 11A-11D. Such a system will have the rollers in a position such that the incoming glass edge will continuously be subjected to a required bending/load. In such a system, the spacing between the rollers and their diameters are controlled to provide a minimum spacing **S** between the two rollers **220a**, **220b** so that there is a clear optical path for camera to inspect.

[00153] FIGs. 9B-9C describes the methodology to accomplish real-time stress measurement in such a dynamic type of edge strength testing setup. The edge strength tester needs to pre- inspect the edge (without any load/bending, the sample passes through the rollers) before testing so that preexisting breakages can be detected. If such a breakage is not detected, then the system would malfunction or overestimate the edge strength. During such an inspection, the stereo cameras **222a**, **222b** can take series of pictures along the length of the edge as shown in FIG. 9B. Then, in the second pass when a load is applied on the sample edge, the cameras take another set of images at exact locations on the edge are the first series of images as shown in FIG. 9C by pairing corresponding images from same location and then correlating, one could obtain strain fields and thereby stresses as described previously, *i.e.* by correlating identically numbered images in FIG. 9B and 9C.

[00154] Alternatively, an embodiment of the testing apparatus **200** with two sets of stereo cameras **222a**, **222b** and **224a**, **224b** can be used to make dynamic measurements in a single pass. An example of such embodiment is shown on the left-most schematic of FIG. 9C. The system includes the first set of stereo cameras **222a, 222b** and the second set of stereo cameras **224a, 224b**. In such systems, both sets of stereo cameras are connected to a processor **214** that controls the cameras **222a**, **222b**, **224a**, **224b** and also processes the image data from the cameras. The system can also include a display **228** for displaying any of the analytical information on the measured stress in the sheet **204** as well as displaying the image of what the cameras see.

[00155] The obvious question that arises is can an algorithm and image correlation obtain strain from zero stress to peak stress state without any intermediate images (150-200 images for static tests). FIGS. 10A and 10B show the results obtained from proof testing this concept and confirm that it is possible to obtain accurate results without the intermediate images. The series of 150-200 images taken during a static test at 11N load were correlated to obtain the stress distribution map shown in FIG. 10A. FIG 10B, on the other hand, shows the stress distribution map obtained by correlating the 1st image with the 200th image without any of the intermediate images. The two stress distribution maps are identical, showing that the absence of the intermediate steps does not affect the result. Thus, this embodiment describes the dynamic system of edge strength measurement for ultra-thin monolithic and laminate glass samples with real time stress visualization.

[00156] The test apparatus **200** described herein can be used for performing the method. This is referring to a dynamic DIC method. Dynamic DIC refers to when it obtains strain measurement in real-time while the 3 points "roll" along the edge. Obtaining strain after a no-load measurement is required in such scenarios.

[00157] An example of the dynamic method of testing edge strength of a sheet **204** of material along an edge of the sheet using the test apparatus **200** that comprises a test region **208** can be outlined as follows. The method comprises: providing a surface pattern **230** of visual markers on a surface **226** of the sheet **204** that includes the edge of the sheet; continuously advancing the sheet of material through the test apparatus wherein the edge of the sheet is advanced through the test region **208** of the test apparatus while applying a 3-point bending load to the portion of the sheet passing through the test region; obtaining a first optical image of the surface of a region of interest along the edge of the sheet while the edge of the sheet is continuously advancing through the test region **208** of the test apparatus but before the region of interest reaches the test region **208**; obtaining a second optical image of the surface **226** of the region of interest of the sheet when the region of interest has advanced within the test region **208** while the 3-point bending load is being applied; and determining stress on the surface of the region of interest along the edge of the sheet resulting from the application of the 3-point bending load by comparing the first optical image and the second optical image.

[00158] In some embodiments, stress can be determined in a time resolved domain, *i.e.*, the history of stress evolution is obtained. This can be true in either a static mode, where the measurement is taken on a location along the edge of the test sheet **204** while the test sheet **204** is stationary, or in a dynamic mode where the measurement is taken along a length of the edge of the test sheet **204** while the test sheet **204** is continuously fed through the test apparatus **200** while a predetermined load is applied.

[00159] It should be noted that while some embodiments are described with reference to a sheet **204** formed of glass, the claims appended herewith should not be so limited as the test apparatus **200** described herein can be used to accept or accommodate and analyze laminate structures or panels. Suitable laminate structures can include plural glass sheets having one or more intermediate polymeric layers or can also, in alternative embodiments, include a structure having a thin film transistor glass substrate and color filter glass substrate having one or more films there between or adjacent to either or both substrates. Thus, where

reference is made to a sheet **204** or glass sheet herein, reference can also be made to glass, glass-ceramic, plastic, as well as, laminate structures and other panels. For the sake of brevity, reference will only be made to a sheet **204** herein.

[00160] The test apparatus **200** can test sheets of various sizes. For example, the test sheet **204** can have length/width dimensions ranging from about 5 mm / 5 mm, to about 100 mm / 100 mm, to about 600 mm / 600 mm, to about 1000 mm / 1000 mm, to about 2300 mm / 2600 mm, to about 4000 mm / 4000 mm and all subranges there between. Glass sheets in panels or laminate structures may also have length/width dimensions ranging from about 5 mm / 5 mm, to about 100 mm / 100 mm, to about 600 mm / 600 mm, to about 2300 mm / 2600 mm, to about 4000 mm / 4000 mm and all subranges there between. Further, adjacent glass sheets in panels or laminate structures may have different length/width dimensions which can result in an overlap of one sheet on the other and on one or more sides of such sheets. Exemplary glass thicknesses for a single glass sheet testing or individual glass sheet contained in a panel or laminate structure can be less than 0.1 mm (e.g., as low as 10 microns) to thicknesses greater than 5 mm, between 0.1 mm to 3 mm, between 0.4 mm to 2 mm, between 0.5 mm to 1 mm, between 0.5 mm to 0.7 mm.

[00161] The table **202** may include a plurality of driving mechanisms which are configured to move the glass sheet **204** into a predetermined position to commence a measurement cycle or to continuously advancing the glass sheet **204** through the test region **208** for the dynamic mode testing.

[00162] A predetermined portion of an edge of the glass sheet **204** can be tested. A width of this predetermined portion can range from about 1 mm to about 5 mm, from about 1.5 mm to about 3.5 mm, from about 2 mm to about 3 mm, and all subranges there between. Since the primary purpose of testing the glass sheet **204** is to test the strength of the sheet material along its edge, it is generally desired to test the areas close to the edge as possible. To that end, for the glass sheets having the dimensions mentioned above, engaging the final 2 mm of the surface of the glass sheet **204** along its edge with the arcuate members **220a**, **220b**, and **218** would generally ensure stress concentration is at the glass sheet edge. This set up is also beneficial in minimizing any chances of catching extraneous particles (such as dust) between the glass sheet **204** and the arcuate members **220a**, **220b**, and **218** which can introduce unwanted surface cracks. In embodiments where the sheet **204** is a panel or laminate structure measured for edge strength and where adjacent glass sheets in these

panels or laminate structures are different (e.g., one or more edges of the structure have an overlapping feature), then the predetermined portion is measured with respect to the smaller of the glass sheets in the structure (i.e., the non-overlapping sheet).

[00163] In some embodiments, the arcuate members **220a**, **220b**, and **218** in each or any of the assemblies **206** can be made of compliant materials to minimize the risk of creating a break in the glass sheet **204** during non-destructive testing (e.g., not evaluating maximum stress). The arcuate members or rollers can be selected to have sufficient compliance while being able to provide a long life to minimize maintenance and downtime as well as sufficient friction to allow the roller to roll freely on the glass surface. Exemplary arcuate member materials can include hardened steel rollers, steel rollers, urethane rollers, polyetheretherketone (PEEK) rollers, Shore 80 hardness urethane rollers, polycarbonate (PC) rollers (e.g., Lexan or the like), high-density polyethylene (HPDE) rollers, Shore 90 hardness urethane rollers, urethane coated rollers, or the like. Exemplary urethane rollers can also be employed to reduce rolling noise which can contaminate any signals used by the system, feedback or otherwise. Additionally, urethane or urethane coated rollers can be used to accommodate debris in the roller path and to make y-direction stress profiles have no inboard stress concentrations. In embodiments used to measure edge strength of panels and laminate structures, it was discovered that less compliant rollers (e.g., PC, HPDE, etc.) were required to achieve adequate edge strength testing results.

[00164] Exemplary dimensions for each arcuate member or roller can vary depending on the particular embodiment of the present subject matter. For example, roller dimensions can range from a 5 mm to a 15 mm outside diameter (OD), from a 7 mm to a 12 mm OD, from a 9 mm to a 10 mm OD. In some embodiments, an exemplary roller dimension can be about 9 mm OD so that stress can be applied nearly all the way to a corner of a glass sheet which is important as many customer issues occur in this area. Exemplary systems can also traverse a glass edge at speeds ranging from 5 mm/s to 500 mm/s or more, or from 2 mm/s to 400 mm/s or more. Exemplary systems are robust and can be used on glass having thicknesses as small as 0.1 mm to thicknesses as great as 1 mm depending on the durability of the polymer material used for the rollers.

[00165] In some embodiments, a high speed closed loop stress control mechanism can be employed to detect cracks as well as ensure applied stress is within a predetermined value of a target, e.g., 2 MPa of target. For example, a load can be applied to a glass sheet **204**

using the single arcuate member **218** whereby a load cell signal can be sent to a high speed controller (not shown) which continuously monitors for cracks. This load cell signal can also be used to control the applied load while traversing the edge at a predetermined speed (e.g., 5 mm/sec to 100 mm/sec or more).

[00166] The use of the edge strength test apparatus **200** is not limited to interrogation of just edge features. It is envisioned that embodiments can interrogate surface features as well for conducting defect screening in manufacturing lines. For example, some features on the surface of the glass sheet, e.g., particle contamination and/or visible types of surface defects such as pits, chips or scratches, can be employed with embodiments of the present subject matter. In such embodiments, however, rather than providing strength distributions, the embodiments would utilize size, shape and/or depth distributions, i.e., a dimensional metric, of such surface defects. Exemplary and non-limiting surface features include surface proximity regions (e.g., approximately 20 mm inboard from the edge) and interface regions (where the surface meets the edge) and any size, shape or depth feature of surface defects. Such dimensional metrics can be used alone or with strength metrics obtained from edge features.

[00167] In some embodiments, the test length may span the entirety of a glass sheet edge or may be conducted on a portion(s) of a glass sheet edge. Thus, the test length may span from as little as about 1 mm to 5 mm to as much as about 2600 mm, 3000 mm, 4000 mm or more depending upon the length of the glass edge.

[00168] **Edge strength testing based on 3-point bending**

[00169] FIGS. 4-7B, 9A-9C, and 11A-11D show schematics of an edge strength test apparatus **200** using three-point bending method. In a destructive failure test mode, the test sample glass panel **204** is placed under increasing load until failure and the peak load at the failure point is recorded. This peak load is mapped to a stress based on prior empirically developed calibration curve from strain gaging. This technique provides strains/stresses along two directions (x-axis and y-axis), which is a significant improvement over the current practice of using only strains along the bending direction via strain gauging.

[00170] **[Optical System (Camera) calibration]**

[00171] Referring to FIGS. 11A-11D, system calibration is completed prior to performing actual tests on glass panel. By performing this operation, the image correlation software

gets to know the angle and distance at which camera is positioned with respect to the test sample. This will help in translating the movements of dot pattern in terms of image pixels to physical dimensions in the 3D space. This calibration step is described schematically in FIGS. 11A-11D. FIG. 11A shows the relative positions of the cameras (**222a**, **222b**), rollers and the test panel. The top rollers are farther away from the panel as the test have not started yet. Now we switch the test panel with predetermined (known to image correlation software) pattern printed on a flat surface. Camera takes a series of photographs of this pattern with the pattern being swiveled around in 3D space yet within camera's focal region as depicted in FIG. 11B-11D. A series of images and appropriate software can be used to develop a calibration file that will be used during the actual test on the panel to obtain strains.

[00172] [Capabilities of the static test setup]

[00173] The static mode has following design features that helps it to act as a calibration device (or benchmarking device) for studying panel/laminate sheet design along with other parametric studies.

a) Interchangeable rollers (roller material and diameter)
b) Ability to change the feed angle. This helps in addressing the edge testing for non-rectangular display panels.
c) Adjustment of the roller assembly closer to or further away from the test edge. This enables inspection of specific regions of the edge along with testing smaller panels (mobile device).
d) The rollers can be replaced with partial roller profiles, which increases viewable area, especially near the contact points and enables studying stress distribution in that region without additional stress from rollers.

It incorporates alignment techniques, such as alignment pins **236a**, **236b**, that align various components precisely which is very critical for the test to be accurate.

[00174] [Improvement of stress measurement accuracy in non-DIC ESMS testing]

[00175] [Load Cell Position] In the existing ESMS the load cell is positioned in adjunct with the topside roller assembly. Inventors found that an improvement on load control can be achieved by moving the load cell to below the bottom side roller **218**. FIG. 15 is a

schematic illustration showing the new location of the load cell. No load cell drift was observed with the new configuration.

[00176] [Speed Control] The stress on the sheet **204** is a function of the load applied on it. Thus, the stress measurement accuracy depends on the load measurement accuracy. One factor in improving the accuracy in the non-DIC ESMS testing where the test sample sheet **204** is continuously fed into the test region **208** of the tester is the speed at which the test sheet **204** is moved through the test region **208**. The conveyance of the test sheet **204** is achieved by using rollers for the arcuate members **218**, **220a**, **220b**. Thus, the material for the roller can affect the friction between the rollers and the test sheet which can affect the ability of the rollers to move the test sheet **204**. Compliant rollers shrink and expand as they rotate against the test sheet **204** and can induce variation in the load applied by the bottom roller **218**. When the test sheet is moving through the rollers fast, the ESMS test system **200** has little time to adjust for the load variation. Inventors investigated the impact of the speed at which the test sheet **204** moved over the rollers vs. load control using a commercially available load frame Instron. The results are shown in the plots in FIGs. 17 and 18. The data was generated with ten (10) specimens. The plot in FIG. 17 shows the measured load over time with a speed of 10 mm/s. The plot in FIG. 18 shows the measured load over time with a speed of 1 mm/s. The load control was significantly improved when the speed was reduced from 10 mm/s to 1 mm/s. The load control also depends on the speed and accuracy in which the ESMS test system's software can adjust for the load variation. Thus, an optimal speed should be selected taking these factors into consideration. With the current improved ESMS set up inventors were able to achieve good load control with speeds between 1 mm/s up to 40 mm/s. Using 5 mm/s speed, for a 0.2 mm monolithic glass, inventors were able to achieve ± 0.1N or lower load variation for a 2N target which equated to 100 ± 5 MPa stress variation. While a faster speed will result in shorter test time, some maximum limit is required so as not to compromise the ability to control the load.

[00177] [Polymer coating on the rollers] In the embodiments where the arcuate members **218**, **220a**, **220b** are rollers, the rollers preferably have a polymeric coatings on the rolling surface that comes in contact with the test sheet **204** to aid in moving the test sheet **204**. Because the polymers are viscoelastic, the material can shrink and expand during rolling. Therefore, the inventors had expected that thinner polymer coating on the rollers would be better for controlling the load applied on the test sheet **204**. However, inventors

unexpectedly found that thicker polymer coating provided better load control with less variability in the applied load. The total diameter of the roller (roller bearing + polymer coating) was 9 mm. The thickness of the polymer coating was 1.32 mm.

[00178] The inventors further investigated the impact of roller diameter and polymer coating thickness on the load-to-stress correlation to understand the potential variability in dynamic measurement. Modeling results showed that for a given roller inner diameter L2 and outer diameter L1, the change in the correlation was negligible up to 400 MPa as the roller inner diameter varied from 4 mm to 14 mm and the polymer thickness varied from 0.5 to 2.5 mm. FIG. 24 is a plot of the load-to-stress correlations as a function of roller outer diameter L1 / roller inner diameter L2 as determined by FEA. The correlations are invariant up to 400 MPa for wide ranges of L1 and L2. From the study, inventors were able to understand that the potential variability in the load-to-stress correlation was minimal for dynamic measurement

[00179] [Software Improvements]

[00180] Improvements were made to the control software for the ESMS system **200** to fully automate the system operation in order to make the testing operation more reliable. The system targets small, ~200 x 130 x 0.2 mm, test sheets/panels. Test samples as thin as 0.2 mm require a much more accurate load control to accurately measure the stress because even small changes in the load induces relatively large changes in stress. Therefore, improvements needed to be made to the control software by improving the control loop to maintain better load control. The control software allowed the ESMS to perform the following automated procedures. One of the initial steps in the edge strength testing procedure is alignment of the test sheet **204**. The desired roller engagement is at the distance **D** (typically at about 2 mm) from the edge **E** of the test sheet **204**. This roller engagement position is shown in FIG. 19B.

[00181] Before the edge strength test can begin, some pre-scan routines are carried out. Such routines comprise generating a thickness profile of the edge of the test sheet **204** to be tested. Referring to FIG. 19A, the length of the test sheet **204** is moved slowly through a pair of thickness sensors **410a**, **410b** that measures the thickness of the test sheet **204** and generates a thickness profile of the edge of the test sheet **204** to be tested. The thickness data allows for an accurate post measurement analysis of failure stress if the test sheet **204** cracks. This routine also finds the leading edge $\mathbf{E}_L$ and trailing edge $\mathbf{E}_T$ of the test sheet **204**

and the sample sheet length so that the actual dimensions can be used during the edge strength test rather than recipe dimensions. The test sheet **204** is placed so the leading edge $\mathbf{E_L}$ is positioned above the apex of the bottom roller **218** at the start of the edge strength testing procedure. FIG. 19C shows this configuration.

[00182] Next, the ESMS drives the test sheet **204** in the direction indicated by arrow **M** until the apex of the bottom roller **218** is aligned with the starting offset position. The starting offset position refers to a horizontal edge alignment as shown in FIG. 19C. FIG. 20 is an illustration of an example of test sheet **204** identifying a fly-in zone, measurement length, and a fly-out zone. To begin the edge strength test procedure, the ESMS drives top roller assembly **220a**, **220b** slowly downward towards the top surface of the test sheet **204** until small force is detected which signifies that the top rollers **220a**, **220b** have made a contact with the test sheet **204**.

[00183] Next, the loading force and the glass test sheet speed are ramped up synchronously through a **Fly-in zone** over a specified fly-in distance within a specified time frame. The loading force is maintained along a **Measurement Length** until **Fly-out zone** is reached. The length of the fly-out zone is defined by a fly-out distance and the loading force the glass test sheet speed are ramped down do complete the testing procedure. FIG. 21 is a plot showing an example of the load profile starting from the initial period during the lowering of the upper rollers **220a**, **220b**, the **Fly-in zone**, the **Measurement Length**, and the **Fly-out zone**.

[00184] [Crack Detection] Under the updated control software, the ESMS carries out the following crack detection procedure. User specifies threshold around target load. If threshold is breached, the ESMS immediately disengages the rollers **218**, **220a**, **220b** and stops the test sheet **204**. The position of the lower roller **218** (i.e. the apex of the roller **218**) where the test sheet **204** is under the applied stress is defined as a new crack position. The edge strength testing is continued if enough space is left along the test sheet **204** edge considering the user defined crack offset. FIG. 22 is a schematic illustration of the test sheet **204** showing the position of the detected crack position. Crack offset refers to the distance the rollers are to be moved away from the detected crack position before the rollers can reengage with the test sheet edge to resume dynamic testing. If the crack offset is too short, the crack would propagate and disturb the measurement. If the crack offset is too large,

testable edge real estate can be wasted. According to the modeled magnitude and shape of the stress field, the inventors used a minimum 25 mm distance for the crack offset.

[00185] After reengaging the test sheet **204**, the ESMS loops through all of the user defined loading forces as long as there is sufficient length of the edge region of the test sheet remains to be tested. ESMS applies a constant force as it traverses along the edge. When a break occurs, the strength of the test sheet **204** can be anywhere between 0 and the stress corresponding to the applied force. Therefore, to accurately determine the strength of the sheet, one must apply multiple step loads in an incremental fashion to better understand the lower bound of the strength. The user can define these step forces based on the level of measurement accuracy he desires. The system must loop through all of the user defined step loads until a break occurs.

[00186] [Load Control] For controlling the 3-point bending stress load applied to the test sheet **204** by the rollers **218**, **220a**, **220b**, a Phantom Motor technique (also known as Cascading Servo Loop) was incorporated into the ESMS control software. The Phantom Motor technique was applied to the load cell analog input. The technique allowed the ESMS to read the load cell input signal and make changes to the moving sample stage **202** to control the load being applied to the test sheet **204** in real time.

[00187] FIG. 23A is a schematic illustrating the Phantom Motor technique. The Delta Tau's Power PMAC motion controller can be configured in such a way where the output of an individual servo loop can be used as an input to another. This allows the system to join the capabilities of both loops on a single actuator and allows the engineer to take full advantage of controller tuning parameters for a device that was not specifically intended to control motion. In this case, the output of a load cell was integrated into the motion system such that its analog output was pointed to the output of a servo loop inside the controller. This is known as the "inner loop". The servo loop that actually controls physical motion of the actuator is then fed the inner loops output to command physical motion. By scaling the relationship between the two loops with the motor tuning parameters provided by the Delta Tau system, an optimal balance was achieved that allowed the motion controller to respond to real time deviations from the target load and apply the necessary corrections, making for a stable load application across the sample.

[00188] FIGS. 23B and 23C show plots of the measured load reading from the load cell vs. time comparing the load cell readings from a test run. The plot in FIG. 23B is for the

measured load readings taken without the Phantom Motor technique modification and the plot in FIG. 23C is for the measured load readings taken with the Phantom Motor technique. The plot in FIG. 23C show substantially less variations in the load cell readings with the Phantom Motor technique implemented.

[00189] [Method to estimate the strength of a batch of panels.]

[00190] According to some embodiments, a method of measuring the average strength of identically manufactured panels that have the same design but manufacturing tolerance will be disclosed. There can be two ways to measure the strength of multiple panels to obtain the average strength of the batch:

- Directly measure the strength of all individual panels by using the optical strain measurement technique disclosed in this invention;
- Use a nominal load-to-stress correlation determined by measuring a few samples using the optical strain measurement technique to estimate the strength of all remaining panels consisting the batch;

The first method has the advantage of being more accurate than the second, but can be time consuming since all samples must be measured using the optical strain measurement technique which can have multiple process steps and longer time. The second method involves less processing time since it can use the load directly to estimate the strength, but will have an error bar in the estimate since the same nominal correlation is adopted for panels having a certain manufacturing tolerance. Still, the second method is preferred in practice since less test time has the advantage over the additional accuracy obtained from utilizing the first method. Here we detail more about the second method.

[00191] The nominal load-to-stress correlation can be obtained by conducting multiple optical strain measurements (i.e., DIC) on multiple panels by using either a static or dynamic DIC approach. A higher number of measurements will provide a more accurate estimate of the nominal correlation. As the number of measurements increases, the error bar will also increase due to the manufacturing tolerance of the panels.

[00192] For example, FIG. 25 shows a load vs. stress plot for two different batches of panels having average thicknesses of 0.2 and 0.3 mm measured by DIC and modeled with FEA. While DIC measurement results have a scatter due to the panel manufacturing

tolerance, FEA model shows only a single result since the nominal panel design parameters were used for the calculation.

[00193] To minimize the errors from using a nominal load-to-stress correlation for all panels, correction factors can be applied to the nominal load-to-stress correlation on each panel based on its measured variability.

[00194] [Panel correction factors]

[00195] Thickness – For example, if a nominal load-to-stress correlation derived from a panel batch having an average thickness of 0.3 mm is applied to a panel having a thickness of 0.29 mm, the stress could be underestimated. Therefore, a correction factor can be applied based on the measured thickness of 0.29 mm. In this case, the correction factor is a function of the measured panel thickness and the average thickness of the panel batch. The mathematical form of the correction factor can be derived from a sensitivity study conducted by DIC and/or FEA modeling.

[00196] It may be difficult to characterize the influence of panel manufacturing tolerance using experimental methods such as DIC if the tolerance is small. In such cases, FEA modeling can be used to understand the sensitivity and derive correction factors. FIG. 26A shows the modeled load-to-stress correlation for panels having different thicknesses of 0.1, 0.2, 0.21, 0.22, and 0.25 mm, while FIG. 26B shows the normalized change in stress vs. load (N) for the different thicknesses. By using these graphs and measuring the thickness variation of each panel, one can apply the appropriate correction factor to the nominal load-to-stress correlation.

[00197] Similarly, correction factors could be applied for other panel design parameter that has a certain manufacturing tolerance.

[00198] [Measurement process correction factors]

[00199] Measurement location – The measurement process may also involve measurement variability that should be accounted for as correction factors. For example, FIGs. 27A and 27B show the force and displacement curves vs. time for 0.1, 0.15, 0.2 and 0.5 mm thick glass sheets as they are tested at a constant load on dynamic ESMS. While the force was maintained constant for all thicknesses, the displacement curves showed significantly different behavior as the rollers approached closer to the corners, as shown by the rising behavior as time progresses. This indicated that the stiffness at the corners became lower as the thickness of glass became thinner, which implied that the load-to-

stress correlation had to be corrected for measurement location along the edge. Referring to FIG. 28, the measurement location **d** along the edge of the panel is measured from the center ***C*** of the edge of the panel **204** to the center of the test region **208** marked by "X" in FIG. 28.

[00200] Roller engagement – The variability in roller engagement can also be accounted for as a correction factor. Roller engagement refers to the engagement length between the roller and the panel edge. While roller engagement is typically set to a nominal value, it may vary depending on the straightness of edge and alignment process. FIG. 29 shows an example of the impact of roller engagement on the load to stress correlation. When the engagement varied between 0.7 and 1.7 mm, it had a 10% impact on the load to stress correlation.

[00201] Off-apex failure (Static ESMS only) – For static ESMS, the off-apex failure location must be considered as a correction factor for accurate stress measurement since the stress sharply drops off as it gets further away from the roller apex. FIG. 30A is a photograph of an example of an off-apex break in the test panel and FIG. 30B is a plot of the stress profile with respect to the off-apex break location.

[00202] Mathematically, for example, the correction factors can be applied to the nominal load-to-stress correlation as following:

$$\text{Stress} = F(N) \times C1(t) \times C2(x) \times C3(R) \times C4(L) \times \ldots$$

Here, F is the nominal load to stress correlation, and C1~C4 are correction functions that account for each individual variable, thickness (t), measurement location (x), roller engagement (R) and off-apex break location (L).

[00203] Error bars – Variabilities in certain panel design parameters or measurement processes that cannot be easily measured due to practical reasons can be accounted for as error bars. For example, the variability of the sealant width, position, or individual glass thicknesses comprising a panel can be accounted for as error bars. In addition, measurement process variabilities such as errors from the load cell, operator, etc. can also be accounted for as error bars. The final load-to-stress correlation accounting for both correction factors and error bars are shown below:

$$\text{Stress} = F(N) \times C1(t) \times C2(x) \times C3(R) \times C4(L) \times \ldots \pm \text{Error bars}$$

[00204] [Method to estimate the failure probability of a panel]

[00205] [1. Deriving strength distributions and predicting product reliability based on ESMS]

Traditional ways of predicting the reliability of glass in a specific application include deriving a strength distribution based on strength tests, and then scaling the probability of failure for a given reference size to the entire production size. This approach has been successfully used for many years, however it relies on the strength distribution being referenced to a given size. Traditional means of testing glass strength, like 4-point bend and ring on ring, that are performed on glass specimens of adequate thickness have the benefit that the stress field in the tested area is constant. Therefore, if a strength distribution is obtained from this data, the resultant distribution is referenced to the area tested (inside the inner ring for ring on ring tests, and inside the inner knives for four-point bend tests). Using these distributions for reliability predictions is straight forward in this case since the reference size of the strength distribution relative to the product size is known and therefore the probability of failure can be readily scaled to the product size by utilizing the Weibull scaling (or closure) property. To utilize this approach, the reference size to which the Weibull strength distribution applies must be known.

[00206] Various new test approaches, such as ESMS, are being used for strength measurements of thin glass. While ESMS is well suited for thin glass edge strength evaluation, it does not have a constant stress field. In the static ESMS test, the stress field is symmetric around the center roller, and is shown in FIG. 31, which illustrates the stress along the edge of the panel/sheet. Here, the failure site location and stress are shown with a star. A common mistake is to generate a strength distribution based only on the stress at the failure location. The problems with this approach are:

- Since the stress is maximum at the center roller location and monotonically decreases away from this location, the resulting strength is dictated by the weakest site within the location "center ± failure site to center distance." Therefore, the distribution is of the weakest flaw within the location of failure. Since the location of this weakest flaw varies, the tested length from which the distribution is obtained also varies. Therefore, the distribution is not referenced to a specific length.
- The edge length that survived stresses higher than the failure stress can dramatically affect the strength distribution, and must be accounted for.

As a result, the distribution based only on the stress at the failure site cannot be used for product reliability predictions. Therefore, special methods are required to derive a valid strength distribution. To adequately determine a strength distribution for ESMS, the effects of length and stress must be deconvolved, and the distribution must be referenced to a

specific unit length. A methodology to accomplish this has been developed. This methodology includes defining a small reference length (or reference areas in the case of surface reliability), identifying the specific reference length (or area) that failed, the stress at which it failed, and the stress to which the surviving reference lengths (or areas) were exposed. The resulting data is then statistically analyzed to derive a valid strength distribution relative to a known length (or area). This distribution, in turn, can be used for reliability prediction purposes. Details of this approach are not provided here.

[00207] ["Simplified method" for data analysis of dynamic ESMS]

For dynamic ESMS, inventors also implemented a simplified method to derive the strength distribution by using the first failure data. The simplified method assumes that the stress profile is constant for dynamic ESMS across the entire test area. FIG. 32 shows a Probability vs. Stress plot showing the strength distribution of a batch of panels that were analyzed either by the "Simplified method" or "Special" method outlined in the previous section above. Results from both methods have no significant difference because at each step load, the stress of the gauge areas at the whole test length is almost the same, and the step stress is small. This enabled the inventors to use conventional Weibull statistics and not rely on the "special" method for dynamic ESMS data analysis.

[00208] [Panel failure modes]

Panel failure modes describe the different ways or locations a panel may break when tested on the ESMS. It is generally preferred to have consistent or predictable break locations on a panel in order to classify breaks. However, due to complications in the panel structure and flaw populations, the identification of break locations and understanding the exact failure stress maybe challenging. Here we provide examples of failure modes found in panels and ways to estimate their failure stresses.

[00209] Edge failures - Edge failure is when the edge on **Surface 1** breaks under tension (FIG. 33). Edge failure on surface 1 under tension is the intended failure mode to be obtained from the ESMS test. To obtain this failure mode, however, it is required that the two pieces of glass comprising a panel behaves collectively like a single piece of glass. In the case where the two pieces of glass comprising a panel behaves like two separate pieces of glass, the edge failure may also occur at the edge on **Surface 3**, which will complicate the identification of the break location. The single-piece-of-glass behavior of a panel can be accomplished by ensuring that the sealant adhering the two pieces of glass is well cured, sufficiently wide and sufficiently close enough to the panel edge being measured. For

example, the sealant must not delaminate from the shear stress being applied by the test, the modulus of the sealant should be sufficiently high, typically over 1 GPa, and the sealant must well adhere the area around the vicinity of the edge where a load is being applied.

[00210] This behavior of the panel with respect to sealant properties can be better explained by the change in stress profiles on **Surfaces 1** and **3** with respect to varying sealant to edge distances. FIG. 35 shows the stress profiles on **Surface 1** and **Surface 3** when the gap between the sealant to glass edge is 0 mm. The sealant width is about 1 mm and the stiffness is 3 Gpa. The peak stress is at the edge of **Surface 1** while the edge stress on **Surface 3** is less than half, which implies that breaks will only occur on **Surface 1**. FIG. 36 shows the stress profiles on **Surfaces 1** and **3** when the distance between the sealant to glass edge is increased to 2 mm. As the sealant moves away from the loading area, the peak stresses are now located on both edges of **Surfaces 1** and **3**. The probability of having a failure on the edge of **Surface 3** is now the same as that on **Surface 1**.

[00211] In some cases, it may be preferred to test both edges on **Surfaces 1** and **3** simultaneously. If so, one could design a panel whose sealant does not have the aforementioned properties. The failure stress for both edges would be calculated based on the same correlation since the glasses would behave like two identical pieces of glass as shown in FIG. 36.

[00212] Surface failures - Surface failures are breaks that occur at the surface of **Surface 1** under tension near the edge, typically within 3 mm of it (FIG. 33). In cases when the panel behaves like two separate pieces of glass, the failure may also occur at the surface of **Surface 3**. Similar to edge failures, if it is preferred to test both **Surfaces 1** and **3** simultaneously, one could design a panel whose sealant does not have the aforementioned properties and use the same correlation to estimate the stress.

[00213] Failures from the compressive side surface - Failures from the compressive side surface refer to failures that occur at the edge or surface of **Surface 4** due to the small tensile stress being applied by the two outer rollers (FIG. 33). Due to force balance, the tensile stress beneath each outer roller is half of that being applied by the center roller. Despite the smaller stresses on surface 4, breaks may still occur at the edge or surface of **Surface 4** if there are large flaws. While it is still generally desired to have breaks only on **Surface 1**, others may take advantage of this and test flaws on both **Surfaces 1** and **4** simultaneously. This potentially eliminates the need for having two sets of rollers to test both A side and B sides.

[00214] Adjacent cracks - Adjacent cracks are ones that occur when a pre-existing crack extends out to the loading area (FIG. 34). In effect, a pre-existing crack propagates into an adjacent test region and subsequently becomes the origin of failure. This failure mode usually occurs when the distance between test regions are too close. The way to mitigate this failure mode is to ensure that enough distance is provided between adjacent breaks and test locations.

[00215] [Gauge failure modes] Gauge failure modes describe the ways the gauge may fail to detect a break or falsely detect a break on a panel.

[00216] Missed break detection - Missed break detection refers to when the ESMS fails to detect a break on a panel. The inventors found that this usually occurs when the breaking energy from the crack is small relative to the sensitivity of the load cell. In some cases, the crack could still be adhered by the underlying sealant that bonds the two pieces of glass together.

[00217] False break detection - False break detection refers to when the ESMS detects a break when no actual break occurred. The inventors found that this usually occurs when the sensitivity of the load sell is too high relative to the noise from the environment.

[00218] Machine learning to identify a break

[00219] In ESMS crack detection, the panel samples are captured with cameras with different illumination and magnification. The hand-crafted features are difficult to identify to define panel crack from image frames. The captured video samples have most of the image frames as un-cracked glass. There are very limited cracked glass image frames from collected data. This problem is handled as abnormality detection using unsupervised learning. In other words, the machine learning model is trained with normal images and find common features. Then, encoder and decoder are used to detect outlier, the outlier images are treated as abnormal images. The crack image would be detected as abnormal image in this case. FIG. 37 illustrates the machine learning model.

[00220] There are three convolutional neural networks. Two of the networks G and D are adversarial and unsupervised learning using the training data, which is composed of only the target class. Specifically, G learns to reconstruct the positive samples and tries to fool the detector D with feature weighting z and G(z). Whereas, D learns to distinguish original (positive) samples from the reconstructed ones. In this way, D learns merely the concept characterized by the space of all positive samples, and hence it can be used for distinguishing between positive and novelty classes. There is another neural network E

which has been trained to mirror the behavior of G which would be able to extract feature weighting from image. On the other hand, G learns to efficiently reconstruct the positive samples, while for negative (or novelty) samples it is unable to reconstruct the input accurately, and hence, for negative samples it acts as a decimator (or informally a distorter). In the testing phase, D operates as the actual novelty detector, while G improves the performance of the detector by adequately reconstructing the positive or target samples and decimating (or distorting) any given negative or novelty samples.

[00221] For our ESMS case, if our input image is x (image), it would go to the neural network E and generate feature weighting E(x). Then we define Z equal to E(x), and Z go through neural network G and it becomes G(z)(image). If (G(z), z) and (x, E(x)) achieve similar score through neural network D, and (G(z), z) achieve high score through D, the input x is normal/positive case. Otherwise, it is abnormal/negative case.

[00222] Embodiments and the functional operations described herein can be implemented in digital electronic circuitry, or in computer software, firmware, or hardware, including the structures disclosed in this specification and their structural equivalents, or in combinations of one or more of them. Embodiments described herein can be implemented as one or more computer program products, i.e., one or more modules of computer program instructions encoded on a tangible program carrier for execution by, or to control the operation of, data processing apparatus. The tangible program carrier can be a computer readable medium. The computer readable medium can be a machine-readable storage device, a machine readable storage substrate, a memory device, or a combination of one or more of them.

[00223] The term “processor” or “controller” can encompass all apparatus, devices, and machines for processing data, including by way of embodiment a programmable processor, a computer, or multiple processors or computers. The processor can include, in addition to hardware, code that creates an execution environment for the computer program in question, e.g., code that constitutes processor firmware, a protocol stack, a database management system, an operating system, or a combination of one or more of them.

[00224] A computer program (also known as a program, software, software application, script, or code) can be written in any form of programming language, including compiled or interpreted languages, or declarative or procedural languages, and it can be deployed in any form, including as a standalone program or as a module, component, subroutine, or other unit suitable for use in a computing environment. A computer program does not necessarily

correspond to a file in a file system. A program can be stored in a portion of a file that holds other programs or data (e.g., one or more scripts stored in a markup language document), in a single file dedicated to the program in question, or in multiple coordinated files (e.g., files that store one or more modules, sub programs, or portions of code). A computer program can be deployed to be executed on one computer or on multiple computers that are located at one site or distributed across multiple sites and interconnected by a communication network.

[00225] The processes described herein can be performed by one or more programmable processors executing one or more computer programs to perform functions by operating on input data and generating output. The processes and logic flows can also be performed by, and apparatus can also be implemented as, special purpose logic circuitry, e.g., an FPGA (field programmable gate array) or an ASIC (application specific integrated circuit) to name a few.

[00226] Processors suitable for the execution of a computer program include, by way of embodiment, both general and special purpose microprocessors, and any one or more processors of any kind of digital computer. Generally, a processor will receive instructions and data from a read only memory or a random access memory or both. The essential elements of a computer are a processor for performing instructions and one or more data memory devices for storing instructions and data. Generally, a computer will also include, or be operatively coupled to receive data from or transfer data to, or both, one or more mass storage devices for storing data, e.g., magnetic, magneto optical disks, or optical disks. However, a computer need not have such devices. Moreover, a computer can be embedded in another device, e.g., a mobile telephone, a personal digital assistant (PDA), to name just a few.

[00227] Computer readable media suitable for storing computer program instructions and data include all forms data memory including nonvolatile memory, media and memory devices, including by way of embodiment semiconductor memory devices, e.g., EPROM, EEPROM, and flash memory devices; magnetic disks, e.g., internal hard disks or removable disks; magneto optical disks; and CD ROM and DVD-ROM disks. The processor and the memory can be supplemented by, or incorporated in, special purpose logic circuitry.

[00228] To provide for interaction with a user and as shown in the Figures contained herein, embodiments described herein can be implemented on a computer having a display device, e.g., a CRT (cathode ray tube) or LCD (liquid crystal display) monitor, and the like for displaying information to the user and a keyboard and a pointing device, e.g., a mouse or a trackball, or a touch screen by which the user can provide input to the computer. Other kinds of devices can be used to provide for interaction with a user as well; for embodiment, input from the user can be received in any form, including acoustic, speech, or tactile input.

[00229] Embodiments described herein can be implemented in a computing system that includes a back end component, e.g., as a data server, or that includes a middleware component, e.g., an application server, or that includes a front end component, e.g., a client computer having a graphical user interface or a Web browser through which a user can interact with an implementation of the subject matter described herein, or any combination of one or more such back end, middleware, or front end components. The components of the system can be interconnected by any form or medium of digital data communication, e.g., a communication network. Embodiments of communication networks include a local area network ("LAN") and a wide area network ("WAN"), e.g., the Internet.

[00230] The computing system can include clients and servers. A client and server are generally remote from each other and typically interact through a communication network. The relationship of client and server arises by virtue of computer programs running on the respective computers and having a client-server relationship to each other

[00231] It will be appreciated that the various disclosed embodiments may involve particular features, elements or steps that are described in connection with that particular embodiment. It will also be appreciated that a particular feature, element or step, although described in relation to one particular embodiment, may be interchanged or combined with alternate embodiments in various non-illustrated combinations or permutations.

[00232] It is also to be understood that, as used herein the terms "the," "a," or "an," mean "at least one," and should not be limited to "only one" unless explicitly indicated to the contrary. Thus, for example, reference to "a component" includes examples having two or more such components unless the context clearly indicates otherwise.

[00233] Ranges can be expressed herein as from "about" one particular value, and/or to "about" another particular value. When such a range is expressed, examples include from

the one particular value and/or to the other particular value. Similarly, when values are expressed as approximations, by use of the antecedent "about," it will be understood that the particular value forms another aspect. It will be further understood that the endpoints of each of the ranges are significant both in relation to the other endpoint, and independently of the other endpoint.

[00234] The terms "substantial," "substantially," and variations thereof as used herein are intended to note that a described feature is equal or approximately equal to a value or description. Moreover, "substantially similar" is intended to denote that two values are equal or approximately equal. In some embodiments, "substantially similar" may denote values within about 10% of each other, such as within about 5% of each other, or within about 2% of each other.

[00235] Unless otherwise expressly stated, it is in no way intended that any method set forth herein be construed as requiring that its steps be performed in a specific order. Accordingly, where a method claim does not actually recite an order to be followed by its steps or it is not otherwise specifically stated in the claims or descriptions that the steps are to be limited to a specific order, it is no way intended that any particular order be inferred.

[00236] While various features, elements or steps of particular embodiments may be disclosed using the transitional phrase "comprising," it is to be understood that alternative embodiments, including those that may be described using the transitional phrases "consisting" or "consisting essentially of," are implied. Thus, for example, implied alternative embodiments to an apparatus that comprises A+B+C include embodiments where an apparatus consists of A+B+C and embodiments where an apparatus consists essentially of A+B+C.

[00237] It will be apparent to those skilled in the art that various modifications and variations can be made to the present disclosure without departing from the spirit and scope of the disclosure. Since modifications combinations, sub-combinations and variations of the disclosed embodiments incorporating the spirit and substance of the disclosure may occur to persons skilled in the art, the disclosure should be construed to include everything within the scope of the appended claims and their equivalents.

WE CLAIM:

1. An apparatus for testing edge strength of a sheet of material comprising:

a plurality of assemblies configured for selectively applying a 3-point bending load along an edge of the sheet of material in a test region of the apparatus, whereby the plurality of assemblies can establish a loaded condition on the sheet of material in the test region by applying the 3-point bending load and establish a no-load condition on the sheet of material in the test region by not applying the 3-point bending load;

a detection mechanism configured for optically measuring strain in the sheet of material in the test region when the sheet of material is in the no-load condition and when the sheet of material is in the loaded condition, wherein the strain in the loaded condition is produced by the 3-point bending load; and

a processor that is configured for determining stress in the sheet of material based on the measured strain.

2. The apparatus of claim 1, wherein the plurality of assemblies comprises two opposing assemblies, wherein a first of the two opposing assemblies comprising a single arcuate member for engaging a first side of the sheet and a second of the two opposing assemblies comprising two spaced-apart arcuate members for engaging a second side of the sheet opposite the first side,

wherein the two spaced-apart arcuate members define the test region between the two spaced-apart arcuate members.

3. The apparatus of claim 2, wherein the single arcuate member is vertically aligned between the two spaced-apart arcuate members.

4. The apparatus of claim 1, wherein the detection mechanism comprises a first pair of cameras positioned to acquire one or more images of the surface of the second side of the sheet in the test region between the two spaced-apart arcuate members,

wherein the detection mechanism optically measures the strain in the sheet of material from the image of the surface of the second side of the sheet acquired using the first pair of cameras.

5. The apparatus of claim 2, wherein the arcuate members are non-rotating bushings, cylindrical rollers, belt rollers, or bearing rollers.

6. The apparatus of claim 1, wherein a pattern provided on the surface of the sheet in the test region facilitates optically measuring the strain in the sheet of material.

7. The apparatus of claim 4, wherein the detection mechanism further comprises a second pair of cameras positioned to acquire an image of the surface of the second side of the sheet at a region other than the test region.

8. The apparatus of claim 1, wherein the detection mechanism comprises at least one camera positioned to acquire one or more images of the a vertical edge surface of the sheet in the test region between the two spaced-apart arcuate members,

wherein the detection mechanism optically measures the strain in the sheet of material from the image of the vertical edge surface of the sheet acquired using the at least one camera.

9. The apparatus of claim 8, wherein the detection mechanism further comprises at least one additional camera positioned to acquire an image of a vertical edge surface of the sheet at a region other than the test region.

10. A method of testing edge strength of a sheet of material along an edge of the sheet, the method comprising:

applying a surface pattern of visual markers on a surface of the sheet in a region of interest along the edge of the sheet;

obtaining a first optical image of the surface of the sheet in the region of interest without any 3-point bending load applied to the region of interest;

applying a 3-point bending load to the region of interest along the edge of the sheet;

obtaining a second optical image of the surface of the sheet in the region of interest while the 3-point bending load is being applied to the region of interest; and

determining stress on the surface of the region of interest along the edge of the sheet resulting from the application of the 3-point bending load based on the first optical image and the second optical image.

11. The method of claim 10, wherein the step of determining stress on the surface of the region of interest along the edge of the sheet comprises:

measuring strain in the sheet of material in the region of interest in a no-load condition based on the first optical image;

measuring strain in the sheet of material in the region of interest in a loaded

condition, wherein the 3-point bending load is applied, based on the second optical image; and

comparing the measured strain in the no-load condition to the measured strain in the loaded condition to determine the strain in the sheet induced by the applied 3-point bending load.

12. The method of claim 11, wherein the step of measuring strain in the sheet of material in the region of interest in the loaded condition based on the second optical image comprises:

determining the displacement of the visual markers in the second optical image compared to the visual markers' location in the first optical image.

13. The method of claim 12, wherein the step of determining stress on the surface of the region of interest along the edge of the sheet comprises calculating the stress that would be required to produce the measured strain in the sheet of material in the region of interest.

14. The method of claim 10, wherein applying the surface pattern of visual markers comprises printing, coating, spraying, etching, pasting, or projecting an image on the surface of the sheet.

15. The method of claim 10, wherein the first optical image and the second optical image are obtained using an optic system comprising at least one camera.

16. A method of testing edge strength of a sheet of material along an edge of the sheet using a test apparatus that comprises a test region, the method comprising:

applying a surface pattern of visual markers on a surface of the sheet in a region of interest along the edge of the sheet;

continuously advancing the sheet of material through the test apparatus wherein the edge of the sheet is advanced through the test region while applying a 3-point bending load to the portion of the sheet passing through the test region;

obtaining a first optical image of the surface of the sheet in the region of interest while the edge of the sheet is continuously advancing through the test region but before the region of interest reaches the test region;

obtaining a second optical image of the surface of the sheet's region of interest when the region of interest advances into the test region while the 3-point bending load is being applied; and

determining stress on the surface of the region of interest along the edge of the sheet resulting from the application of the 3-point bending load based on the first optical image and the second optical image.

17. The method of claim 16, wherein the step of determining the stress on the surface of the region of interest along the edge of the sheet comprises:

measuring strain in the sheet of material in the region of interest in a no-load condition based on the first optical image;

measuring strain in the sheet of material in the region of interest in a loaded condition, wherein the 3-point bending load is applied, based on the second optical image; and

comparing the measured strain in the no-load condition to the measured strain in the loaded condition to determine the strain in the sheet induced by the applied 3-point bending load.

18. The method of claim 17, wherein the step of measuring strain in the sheet of material in the region of interest in the loaded condition based on the second optical image comprises:

determining the displacement of the visual markers in the second optical image compared to the visual markers' location in the first optical image.

19. The method of claim 18, wherein the step of determining stress on the surface of the region of interest along the edge of the sheet comprises calculating the stress that would be required to produce the measured strain in the sheet of material in the region of interest.

20. The method of claim 16, wherein the first optical image and the second optical image are obtained by an optic system comprising a pair of stereo cameras.

21. The method of claim 16, wherein applying the surface pattern of visual markers comprises printing, coating, spraying, etching, pasting, or projecting an image on the surface of the sheet.

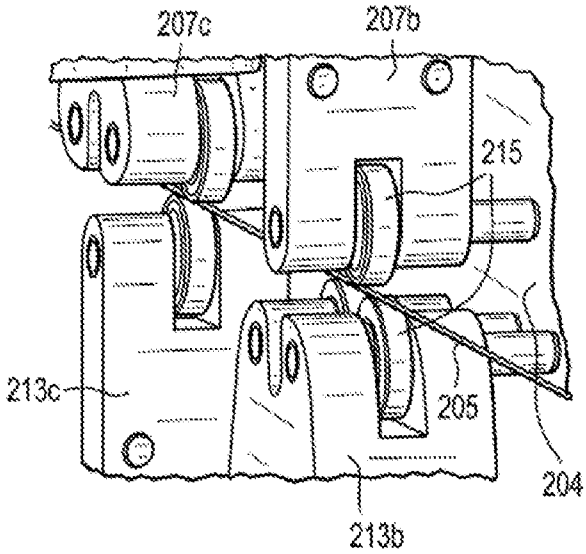


FIG. 1A
(Prior Art)

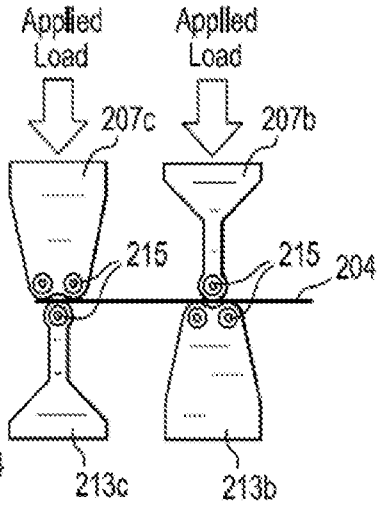


FIG. 1B
(Prior Art)

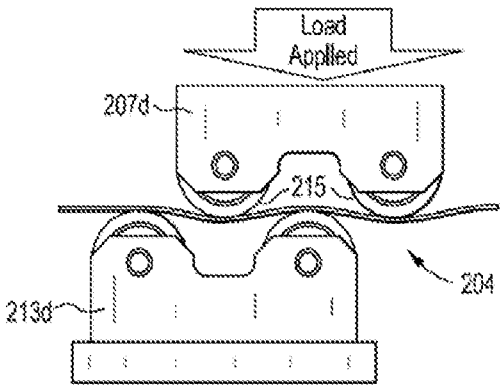


FIG. 1C
(Prior Art)

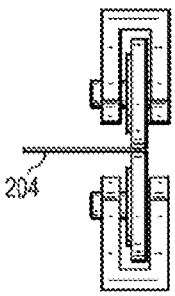


FIG. 1D
(Prior Art)

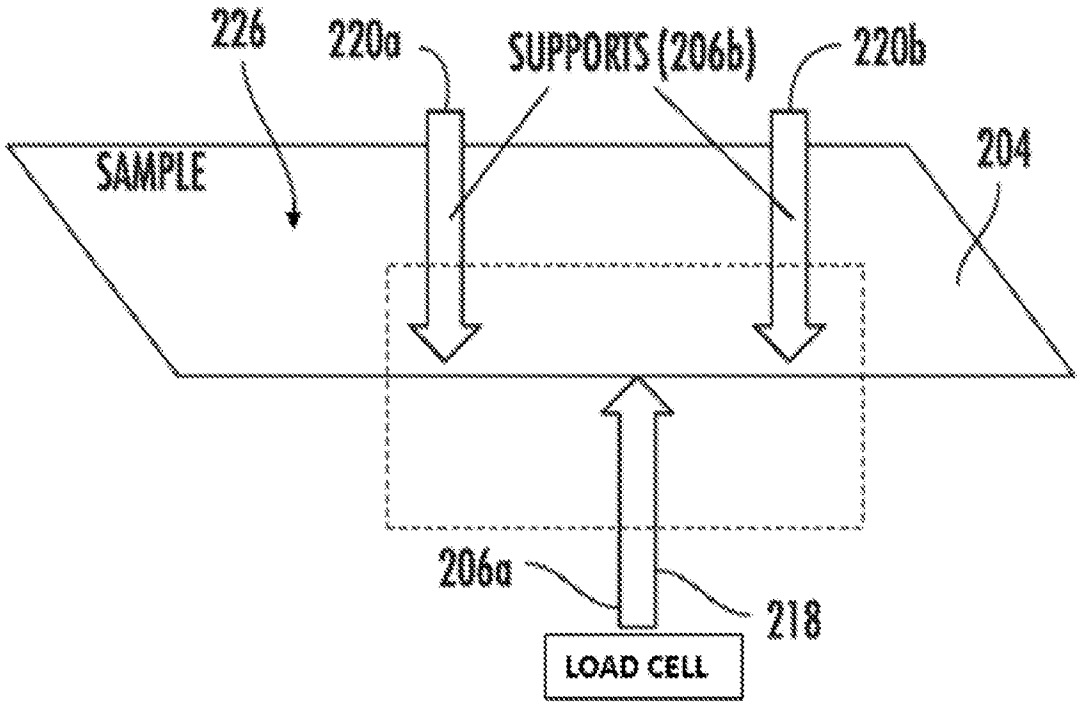


FIG. 1E

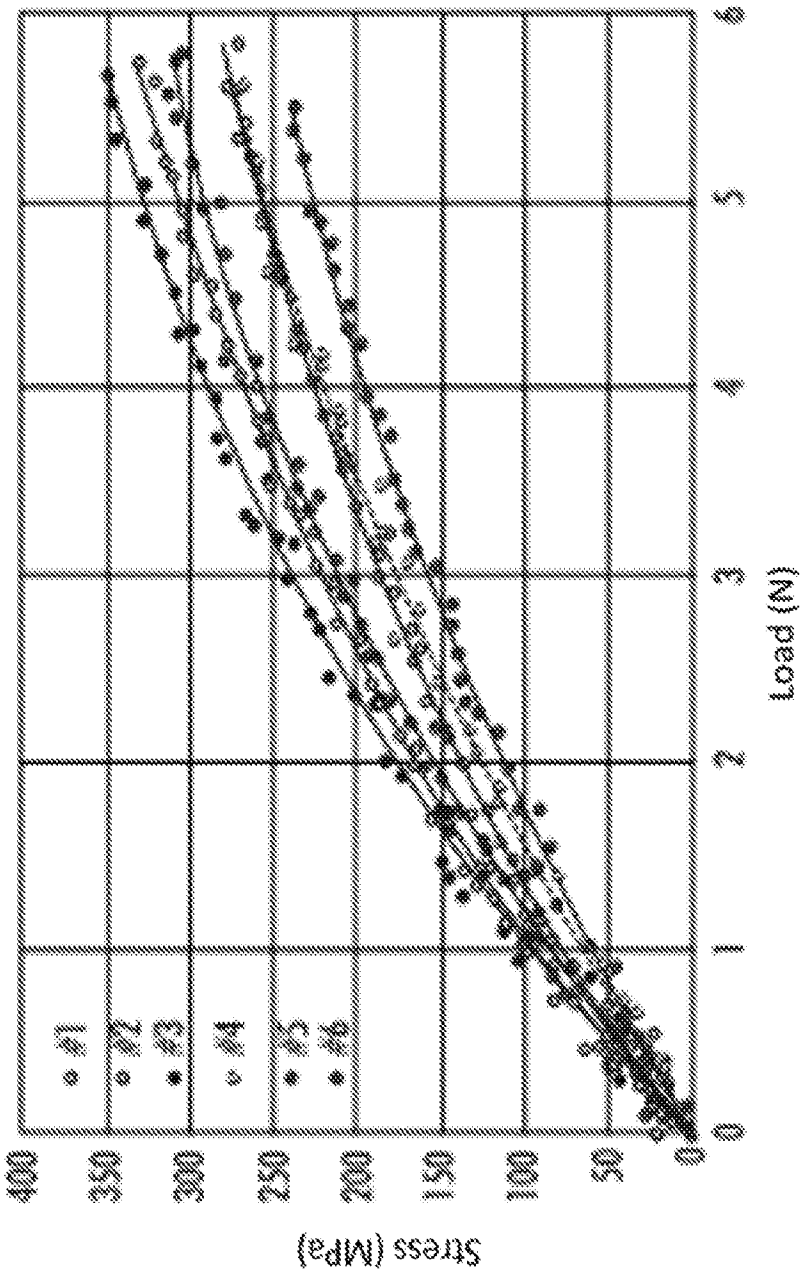

Stress (MPa)
400
350
300
250
200
150
100
50
0
1
2
3
4
5
6
Load (N)
#1
#2
#3
#4
#5
#6

FIG. 2

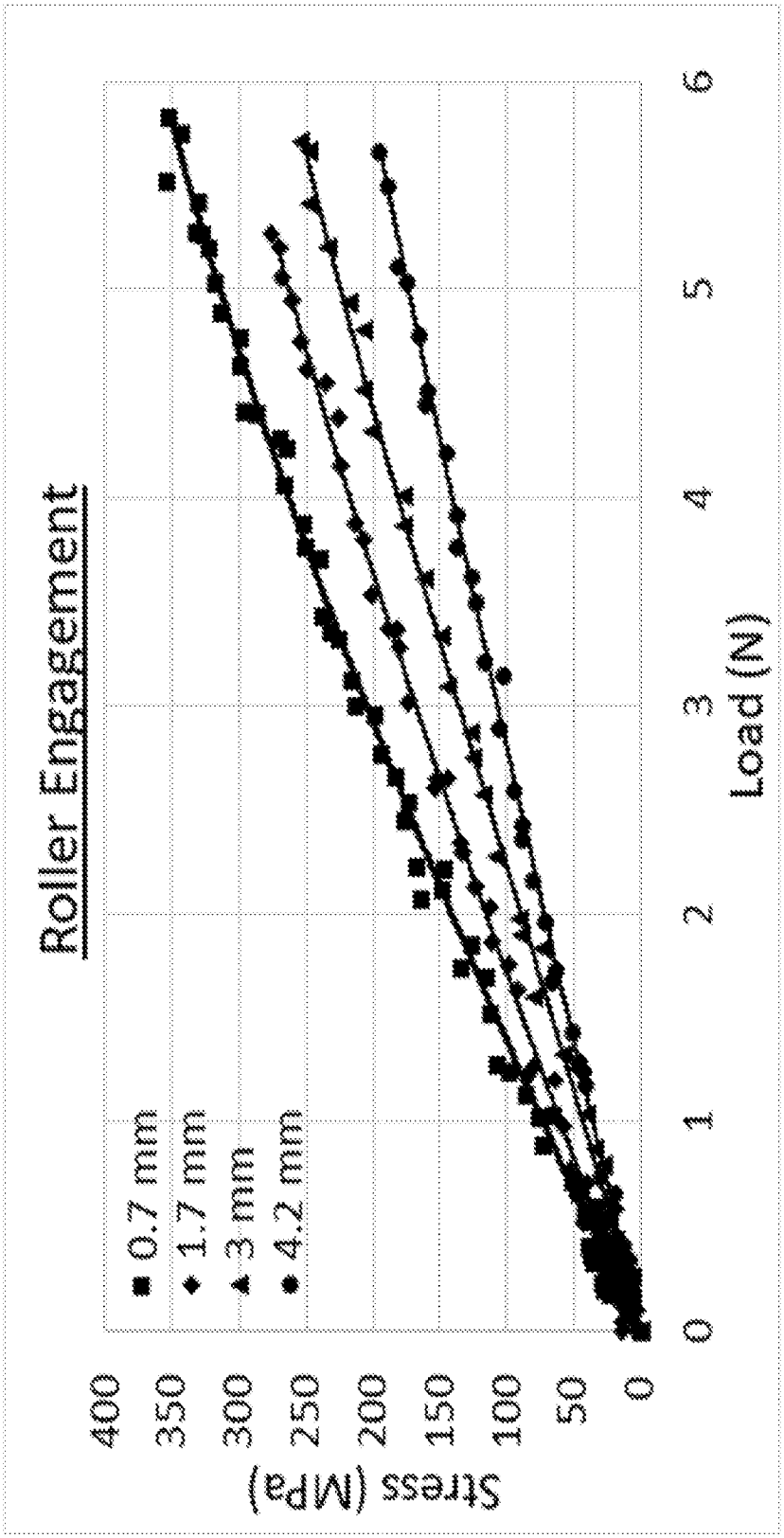

Roller Engagement
Stress (MPa)
Load (N)
0.7 mm
1.7 mm
3 mm
4.2 mm
0
50
100
150
200
250
300
350
400
0
1
2
3
4
5
6

FIG. 3

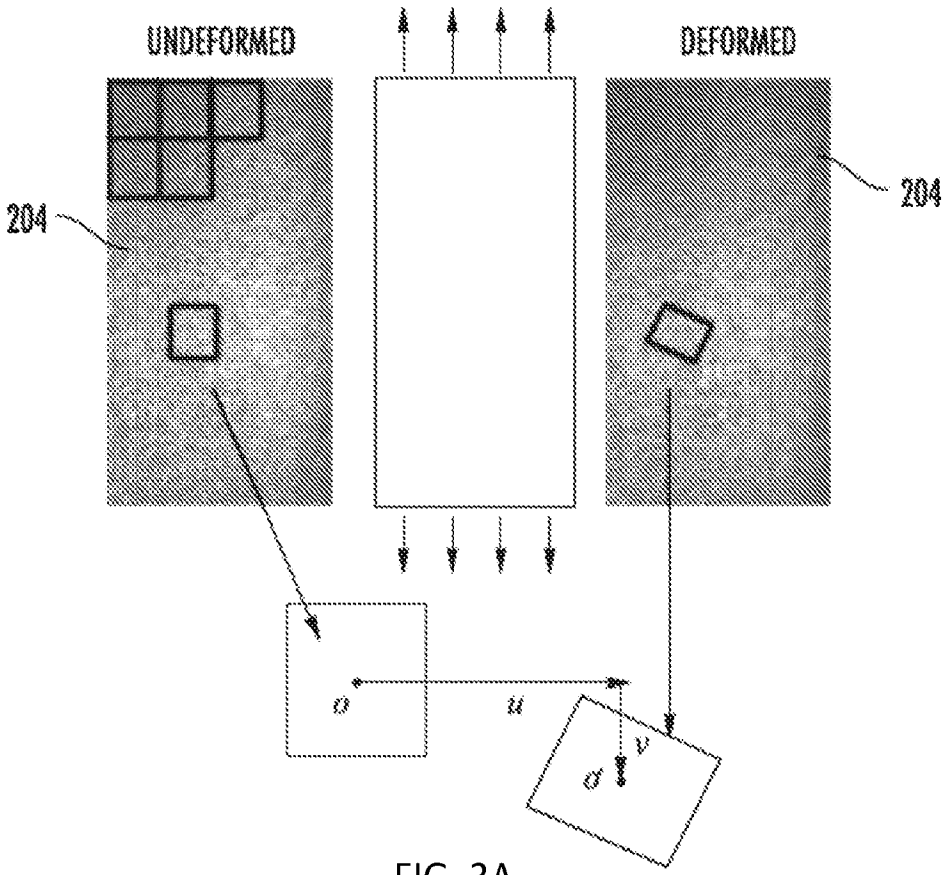


FIG. 3A

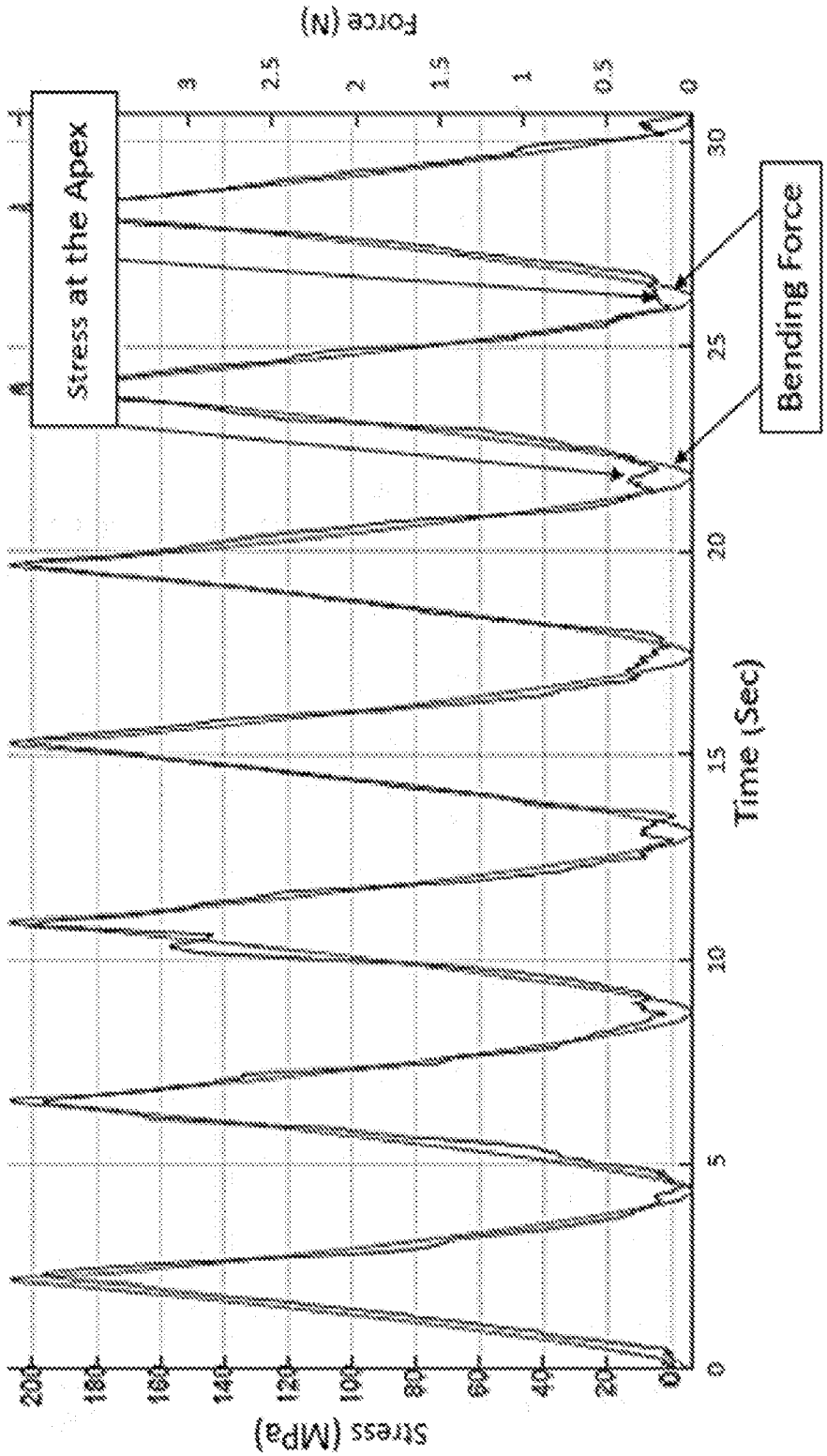


FIG. 3B

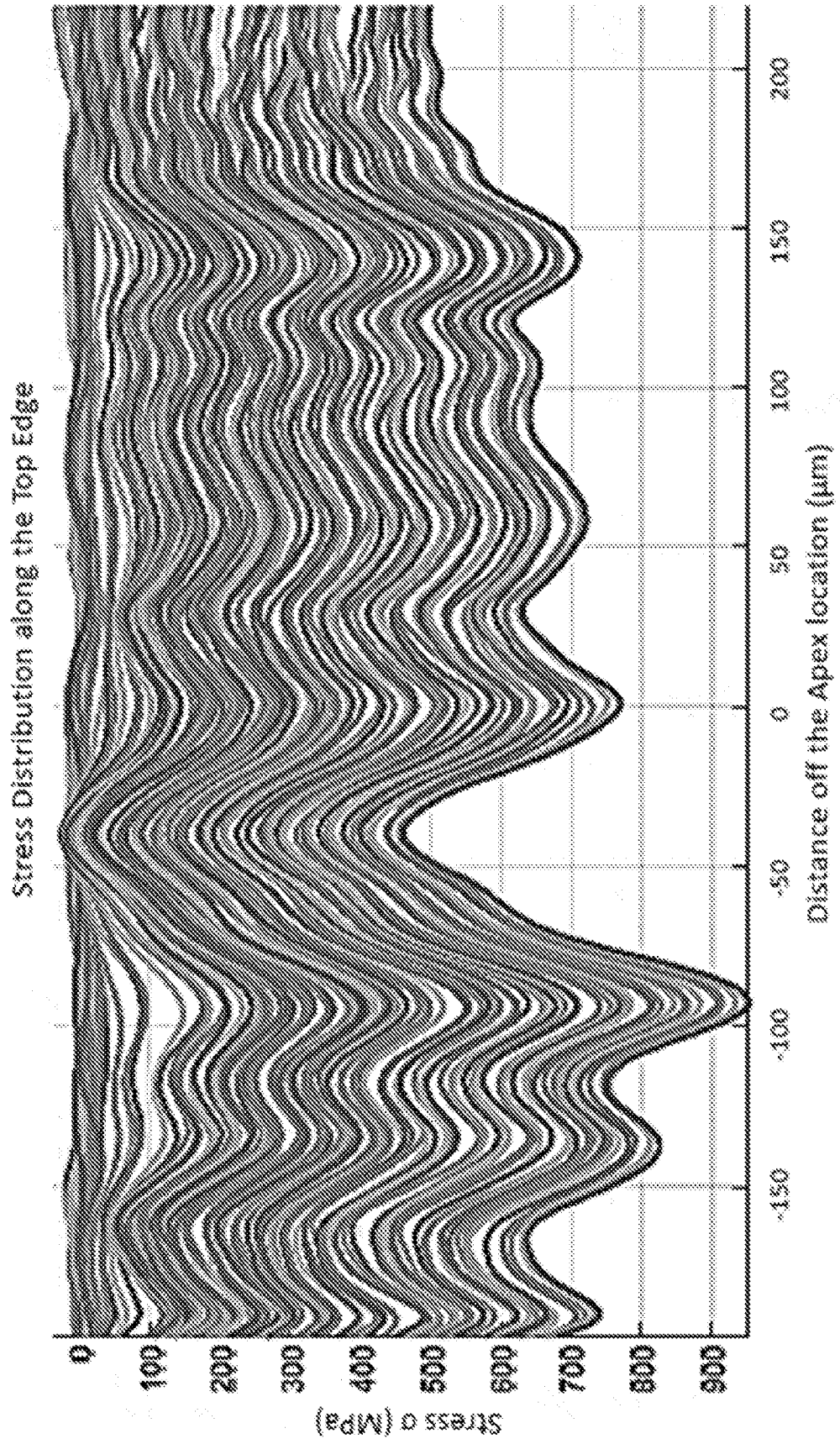

Stress Distribution along the Top Edge
Stress σ (MPa)
0
100
200
300
400
500
600
700
800
900
Distance off the Apex location (μm)
-150
-100
-50
0
50
100
150
200

FIG. 3C

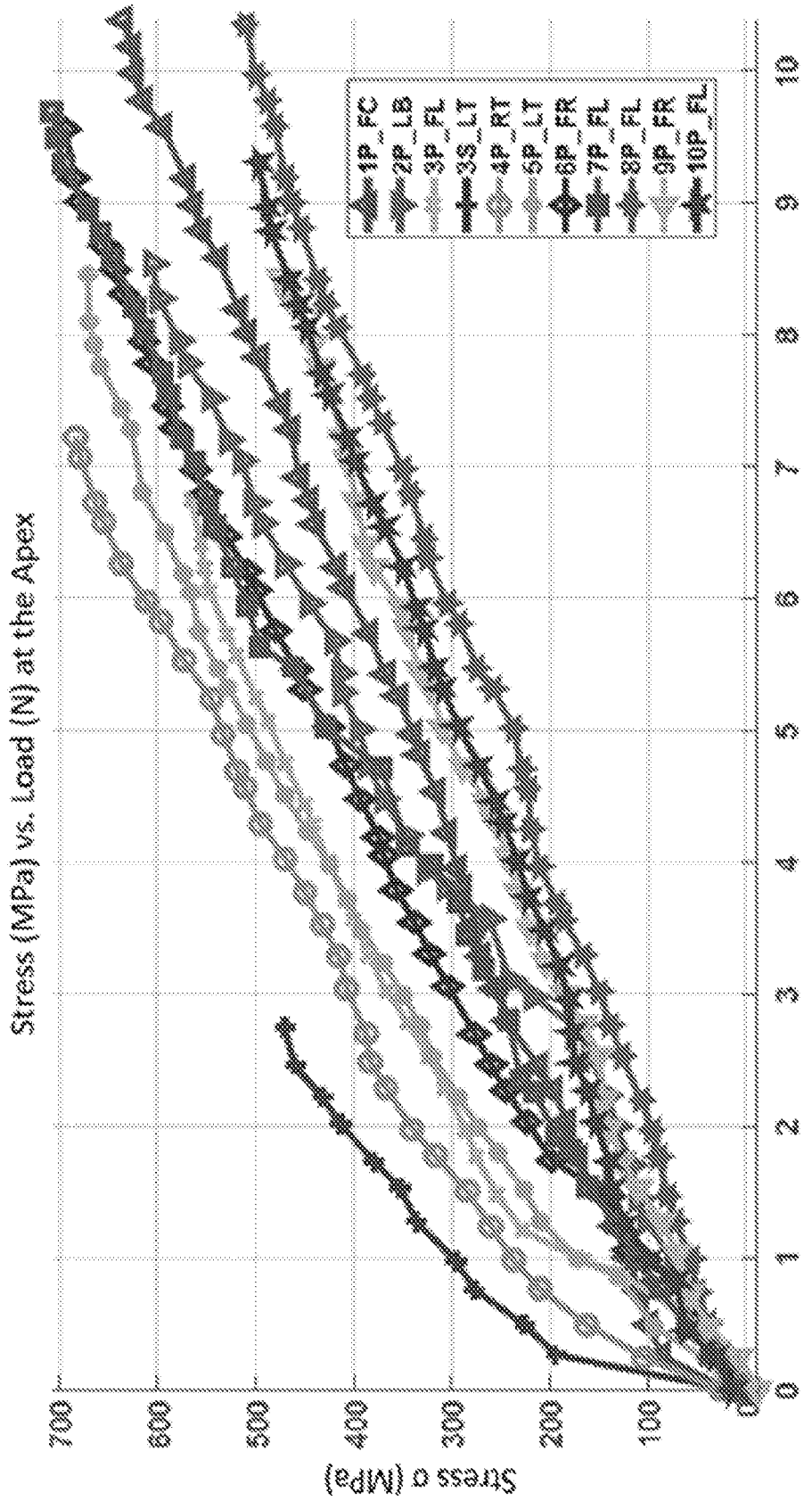

Stress (MPa) vs. Load (N) at the Apex
Stress σ (MPa)
Force (N)
0
1
2
3
4
5
6
7
8
9
10
100
200
300
400
500
600
700
1P_FC
2P_LB
3P_FL
3S_LT
4P_RT
5P_LT
6P_FR
7P_FL
8P_FL
9P_FR
10P_FL

FIG. 3D

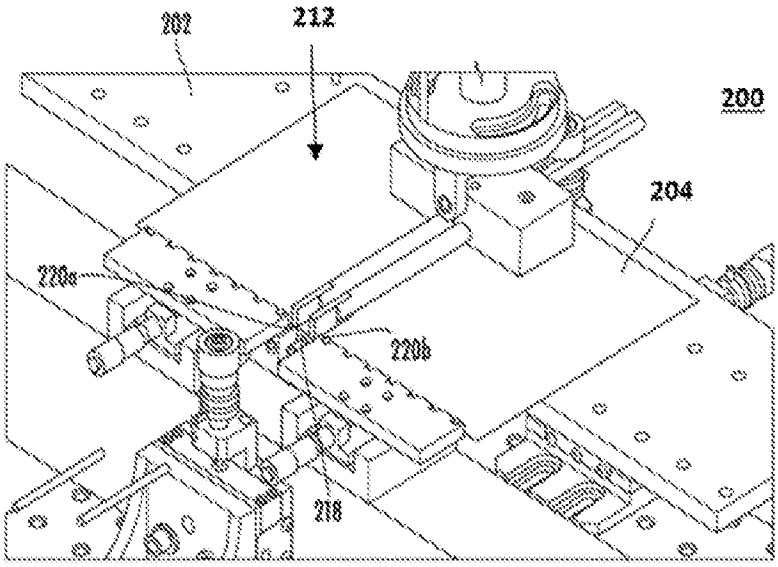


FIG. 4

FIG. 5B

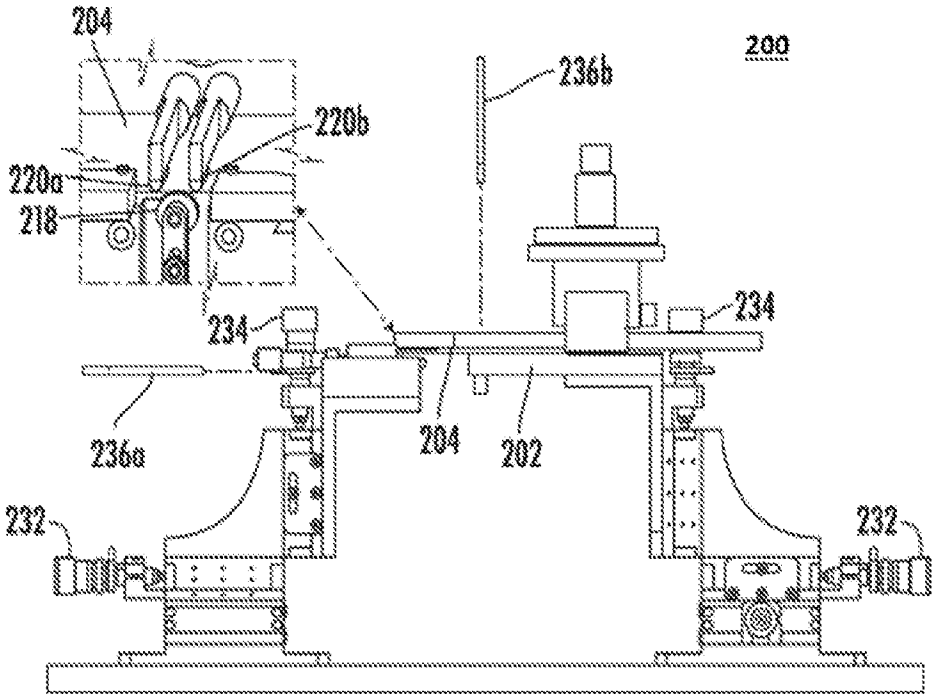


FIG. 5A

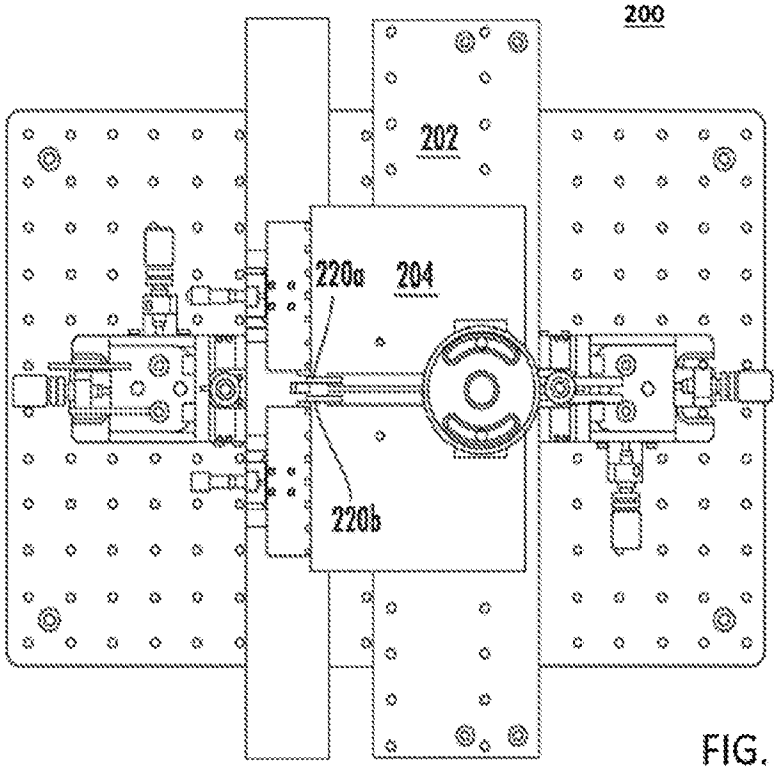


FIG. 6

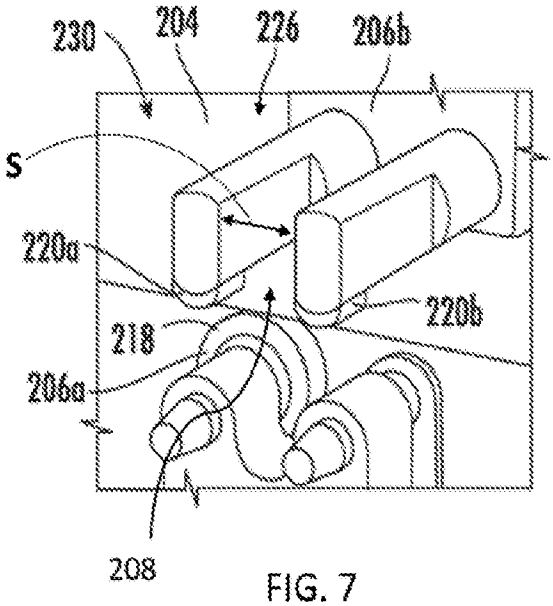


FIG. 7

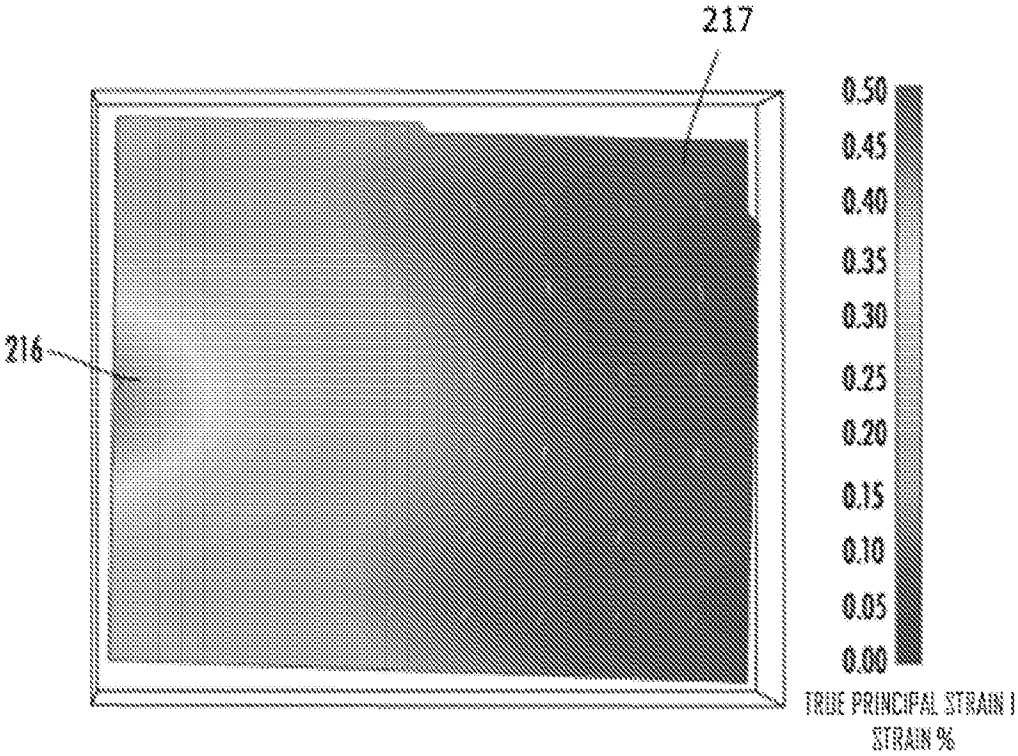

217
216
0.50
0.45
0.40
0.35
0.30
0.25
0.20
0.15
0.10
0.05
0.00
TRUE PRINCIPAL STRAIN I
STRAIN %

FIG. 8A

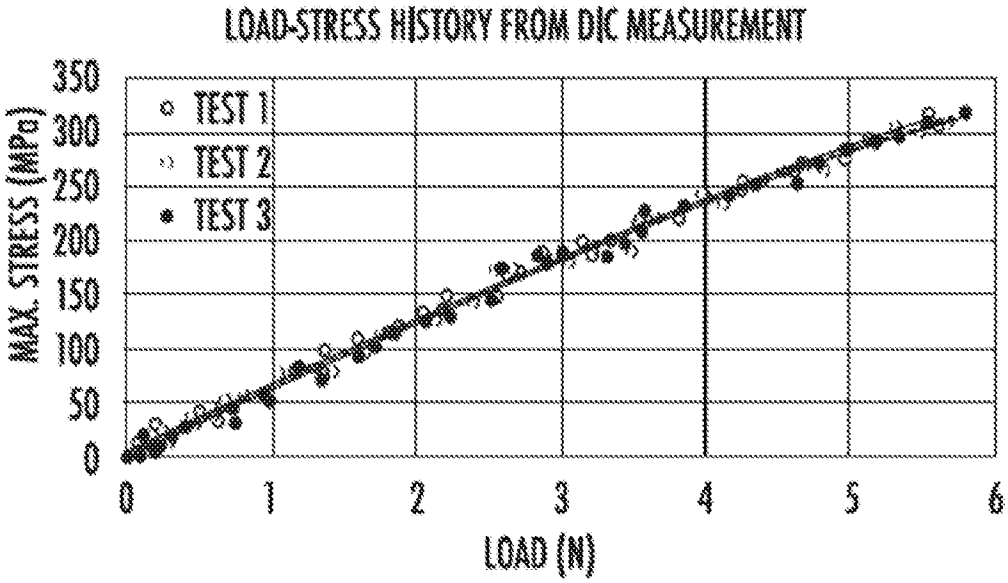

LOAD-STRESS HISTORY FROM DIC MEASUREMENT
MAX. STRESS (MPa)
350
300
250
200
150
100
50
0
TEST 1
TEST 2
TEST 3
0
1
2
3
4
5
6
LOAD (N)

FIG. 8B

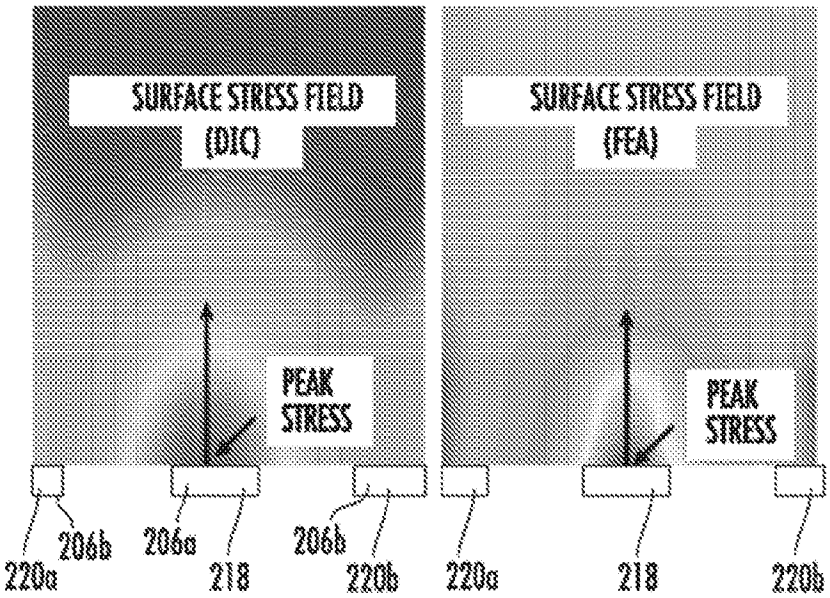

SURFACE STRESS FIELD
(DIC)
PEAK
STRESS
SURFACE STRESS FIELD
(FEA)
PEAK
STRESS
220a
206b
206a
218
206b
220b
220a
218
220b

FIG. 8C

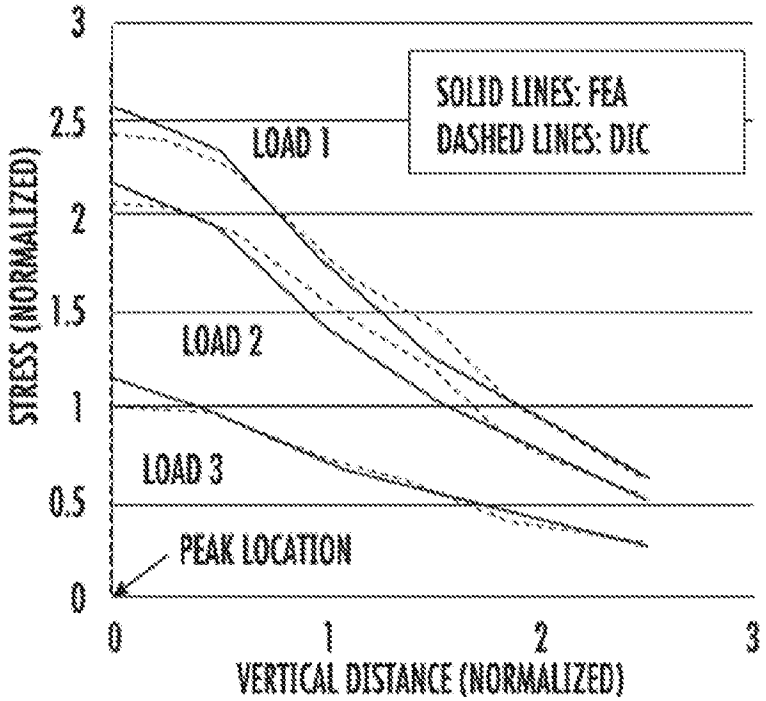

SOLID LINES: FEA
DASHED LINES: DIC
LOAD 1
LOAD 2
LOAD 3
PEAK LOCATION
STRESS (NORMALIZED)
VERTICAL DISTANCE (NORMALIZED)
0
0.5
1
1.5
2
2.5
3
0
1
2
3

FIG. 8D

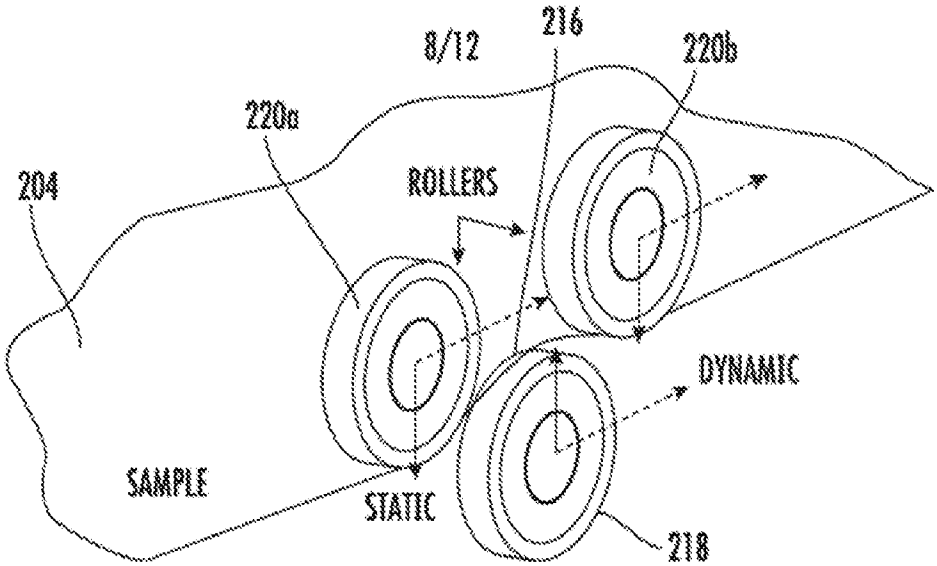


FIG. 9A

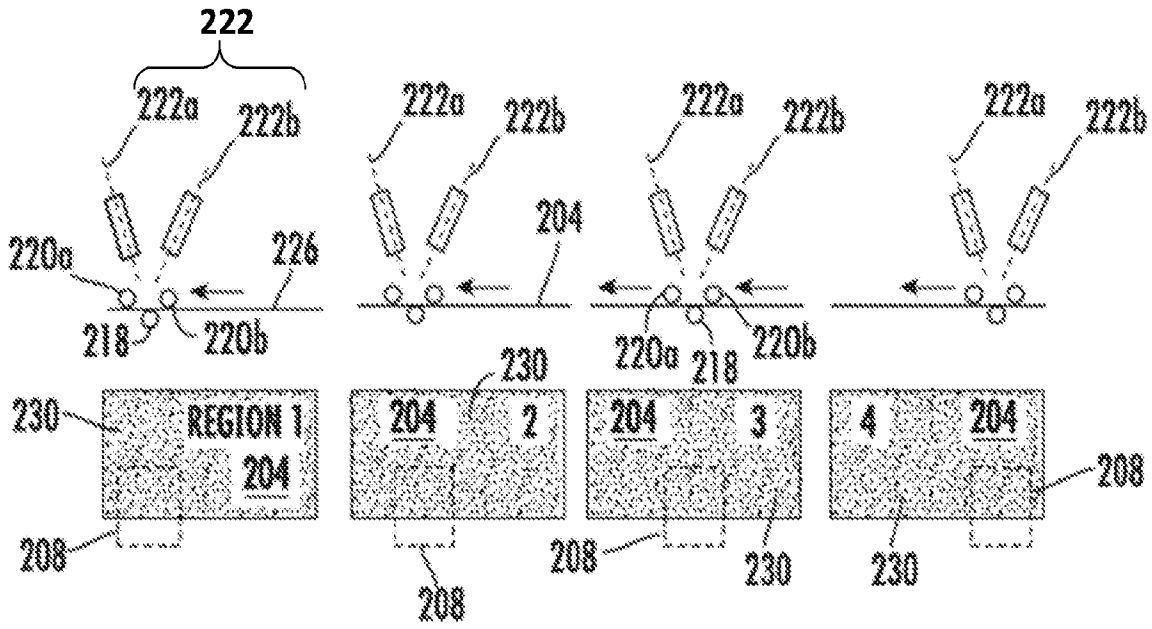

222
222a
222b
220a
226
218
220b
204
230
REGION 1
204
2
3
4
208

FIG. 9B

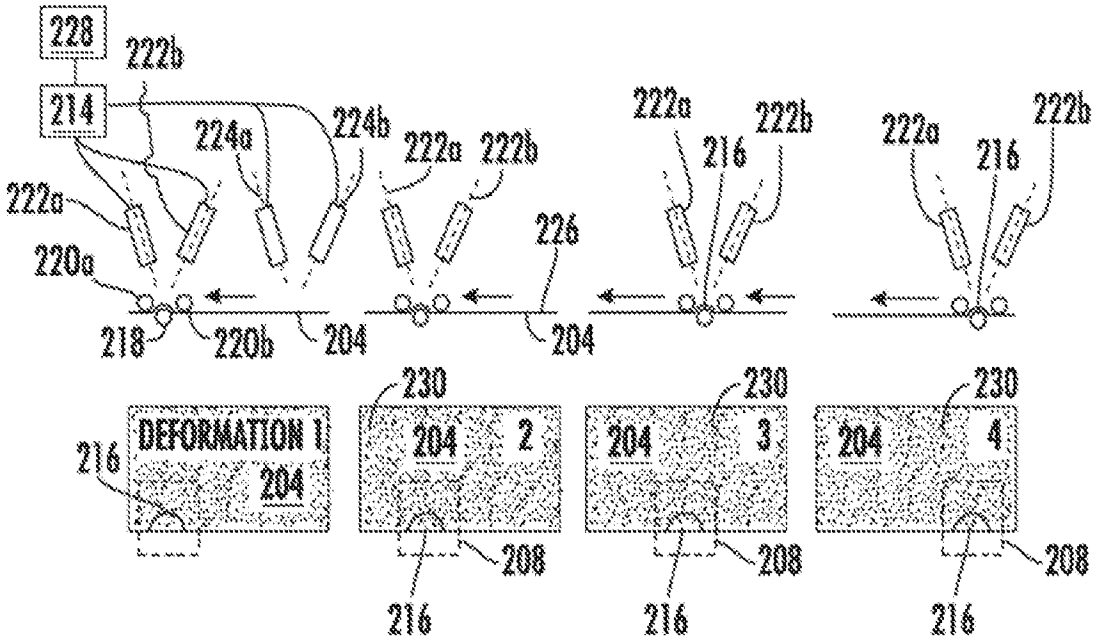

228
214
222b
224a
224b
222a
216
226
220a
218
220b
204
DEFORMATION 1
230
208

FIG. 9C

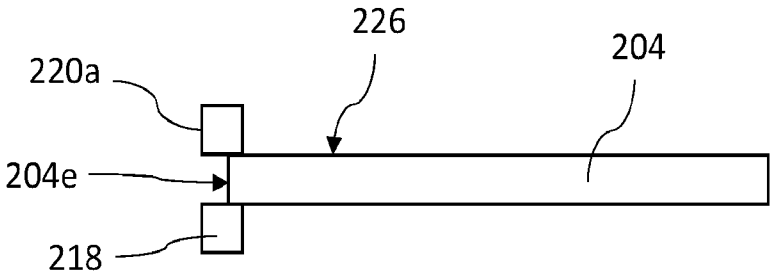


FIG. 9D

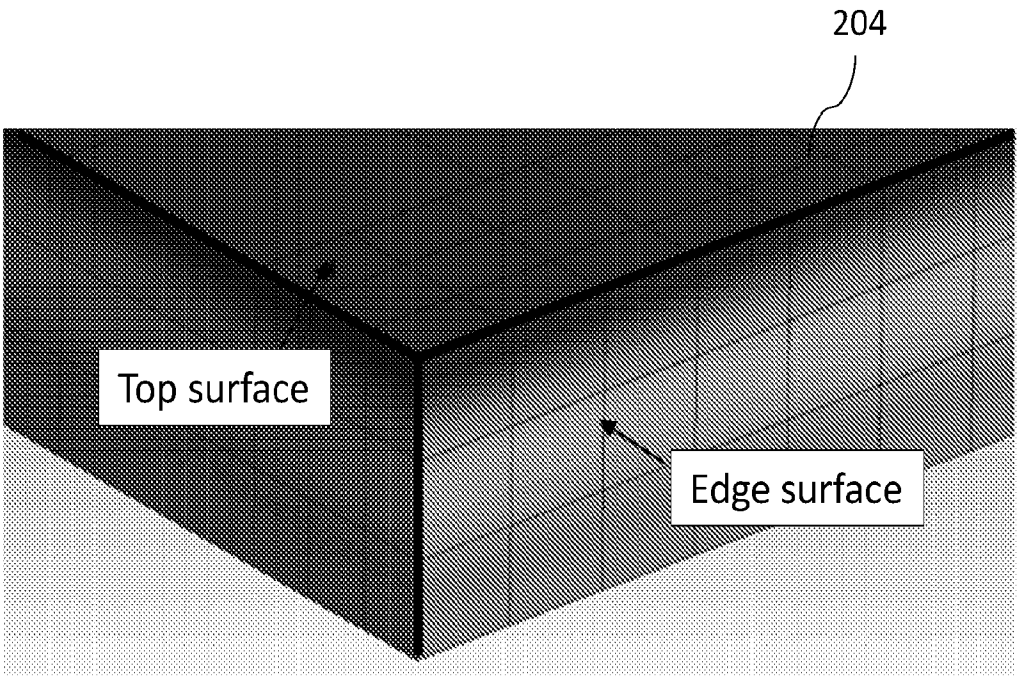


FIG. 9E

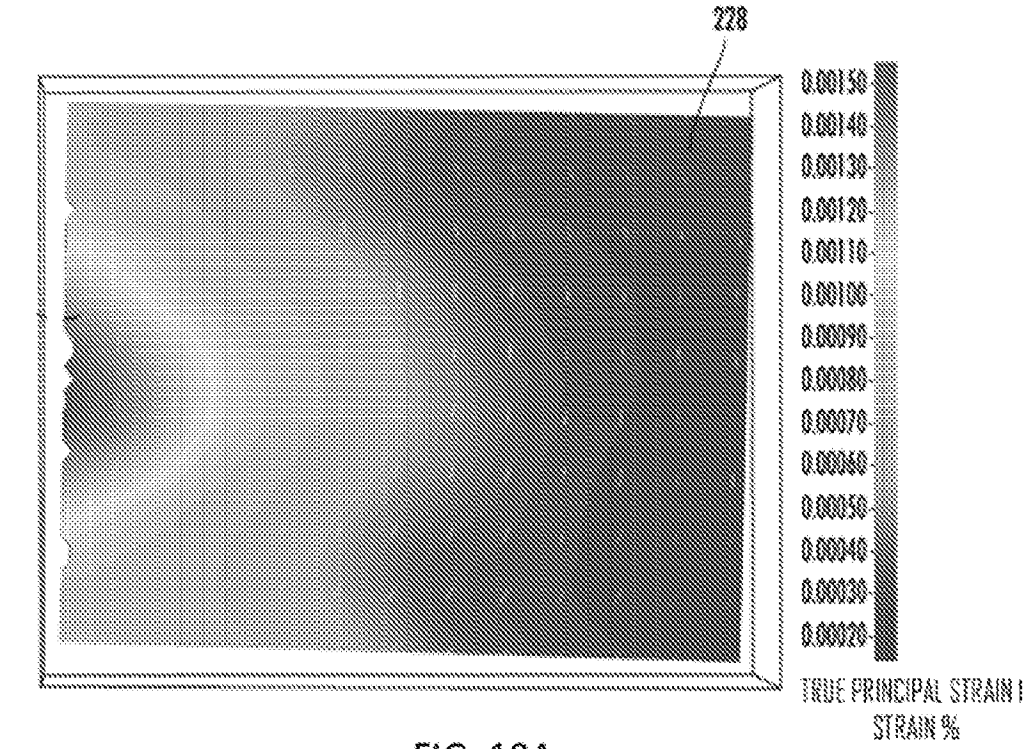


FIG. 10A

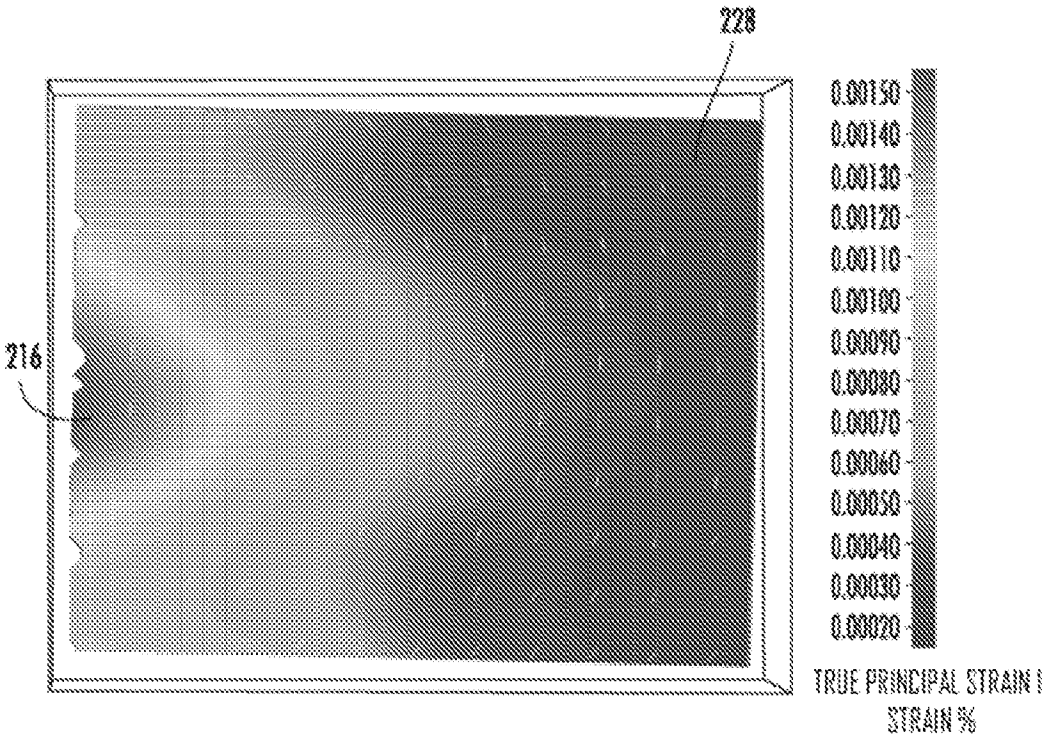


FIG. 10B

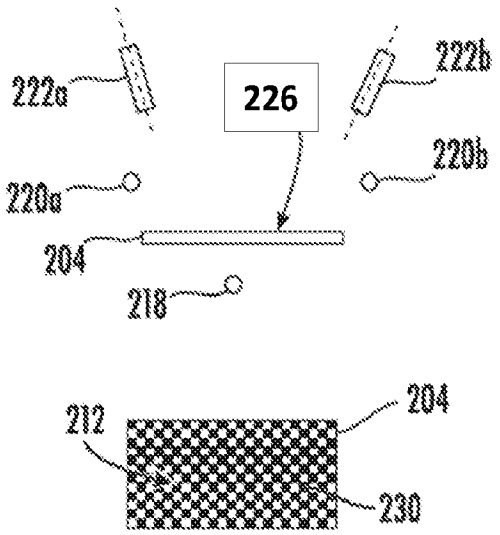


FIG. 11A

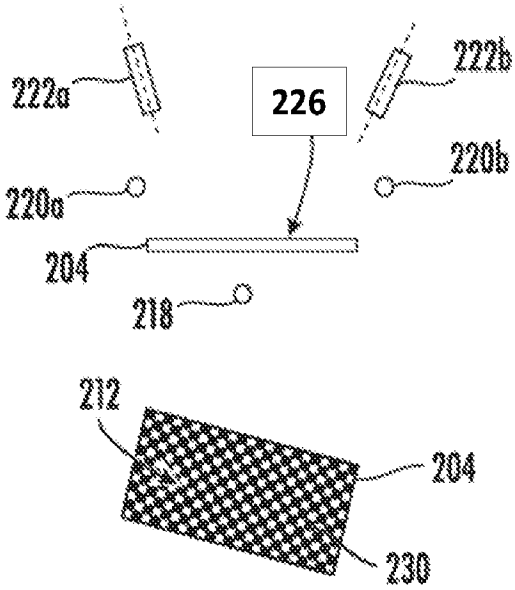


FIG. 11B

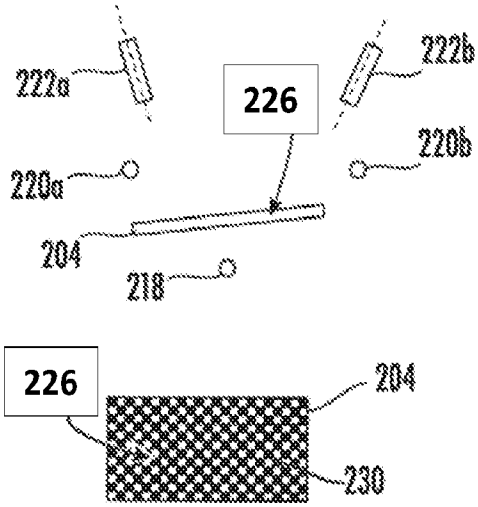


FIG. 11C

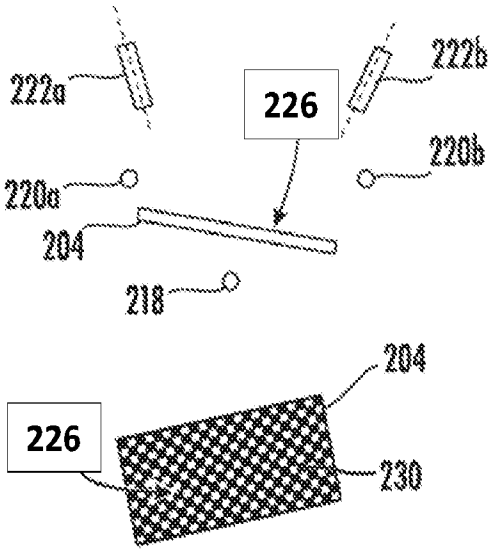


FIG. 11D

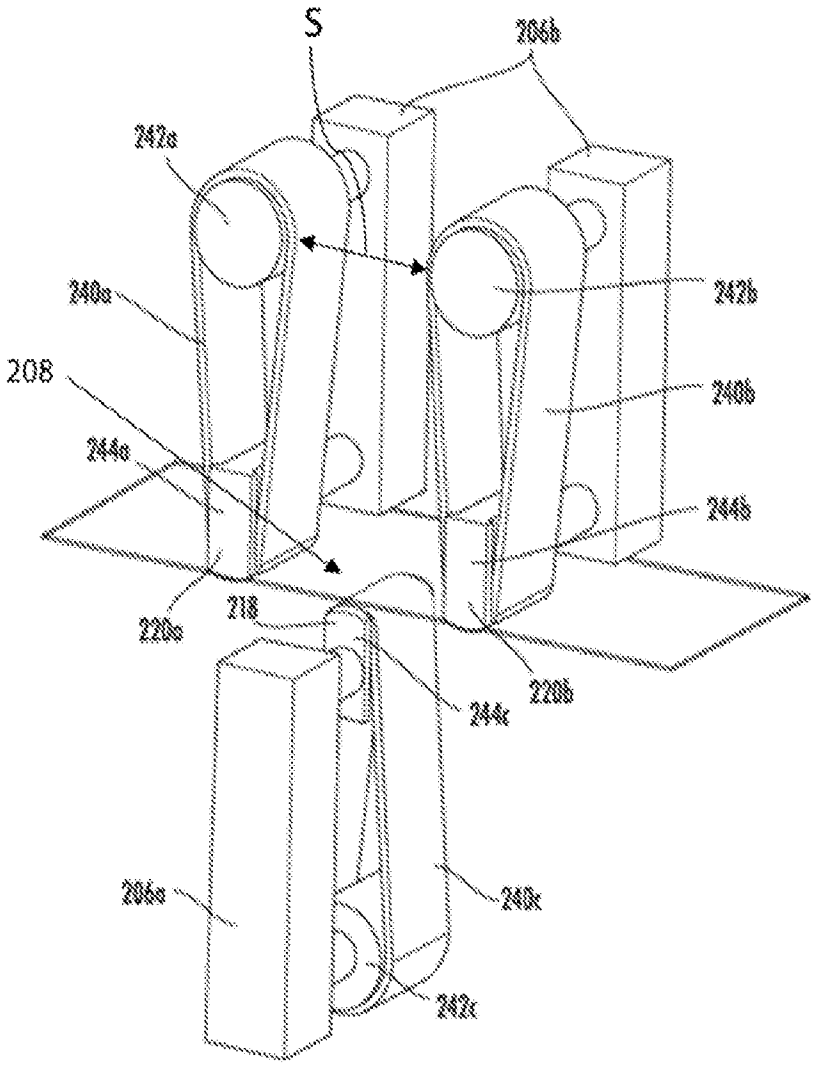

S
206b
242a
240a
208
244a
220a
218
242b
240b
244b
220b
244c
206a
240c
242c

FIG. 12

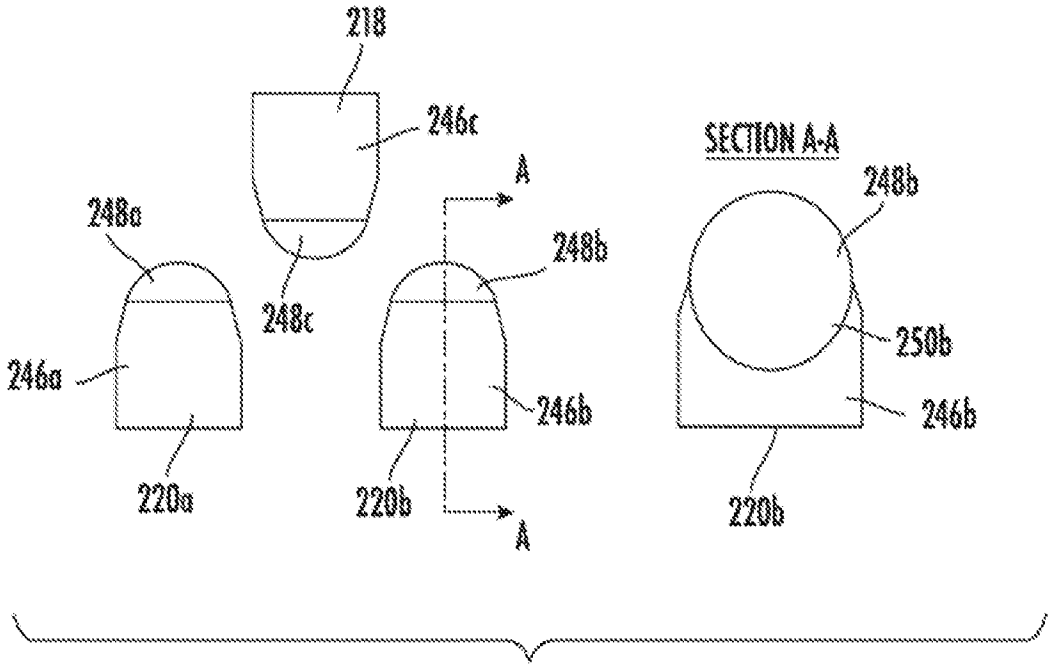

218
246c
248a
248c
246a
220a
A
248b
246b
220b
A
SECTION A-A
248b
250b
246b
220b

FIG. 13

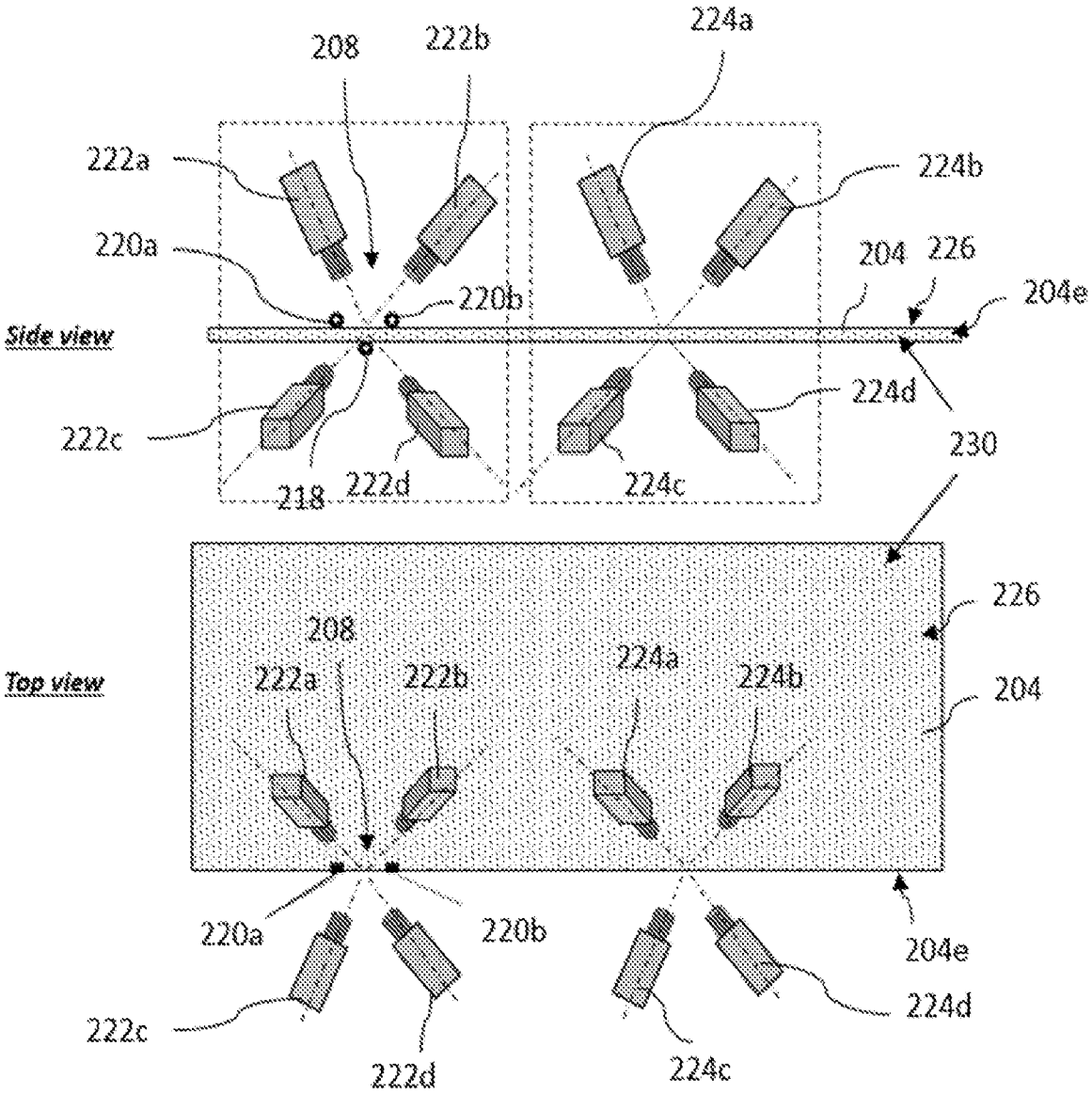

208
222b
224a
222a
224b
220a
204
226
220b
204e
Side view
224d
222c
230
218
222d
224c
226
Top view
208
222a
222b
224a
224b
204
220a
220b
204e
222c
224d
222d
224c

FIG. 14

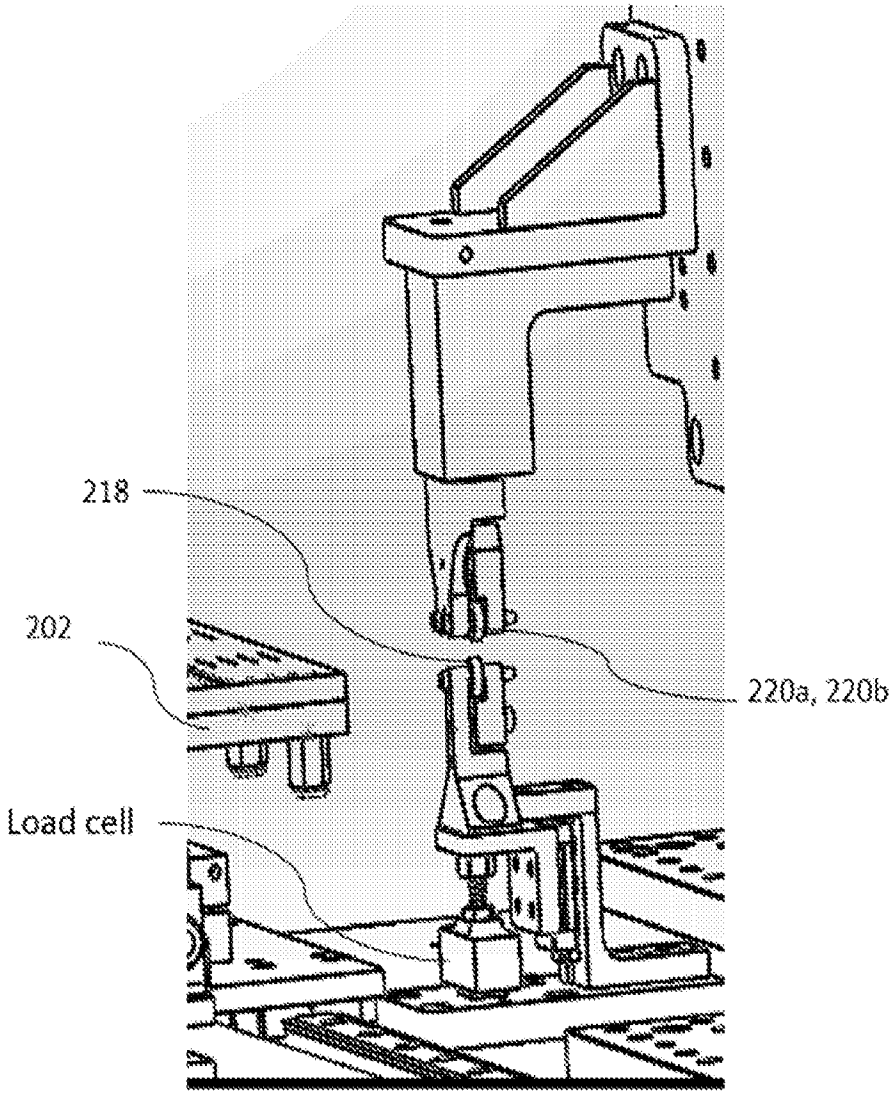
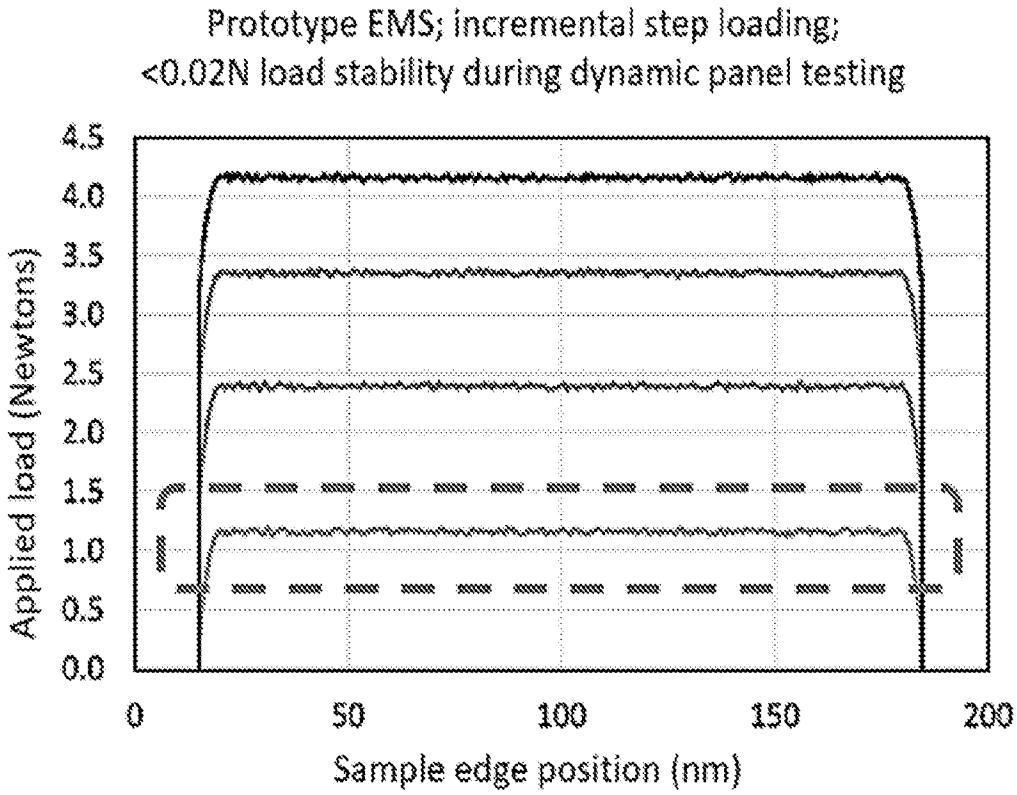


FIG. 15



Load control performance improvement 1.2 ± 0.02 N

FIG. 16

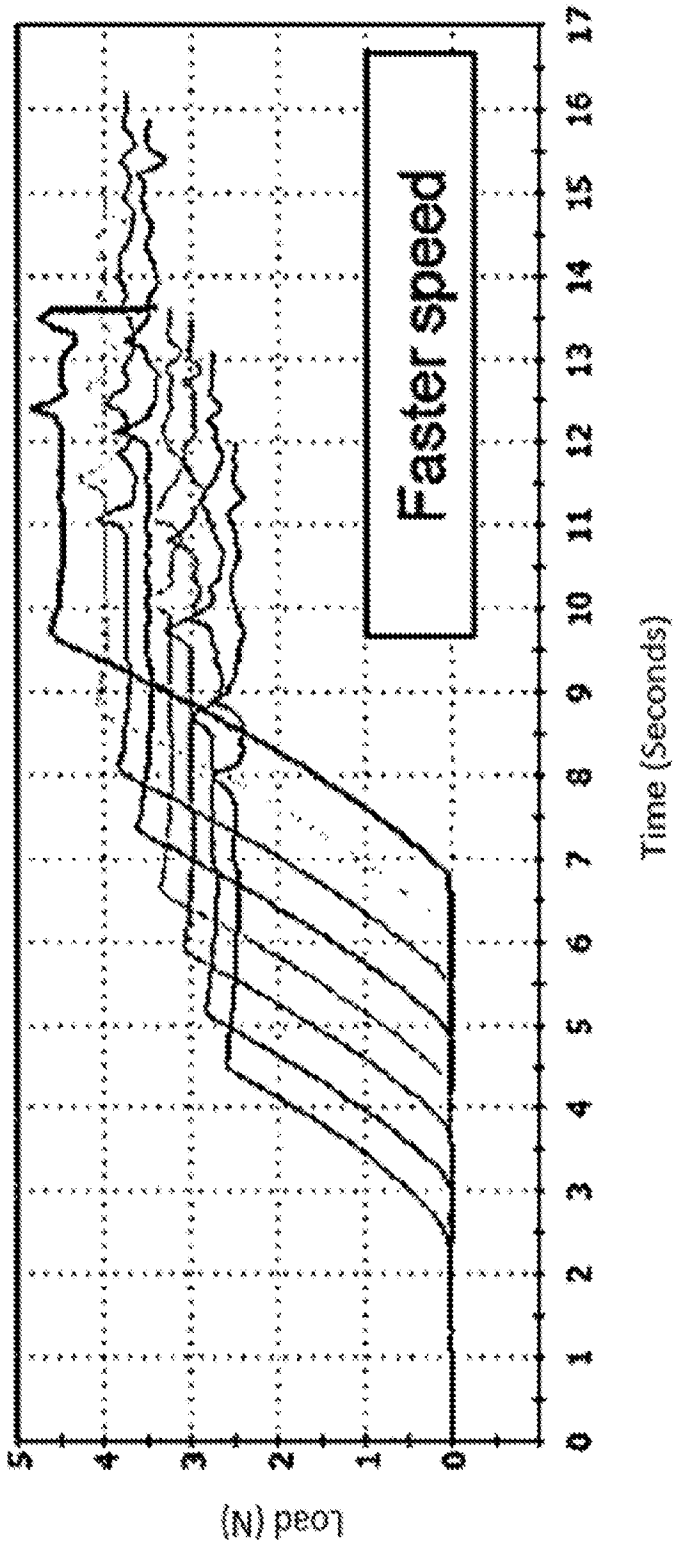

Faster speed
Load (N)
Time (Seconds)
0
1
2
3
4
5
6
7
8
9
10
11
12
13
14
15
16
17

FIG. 17

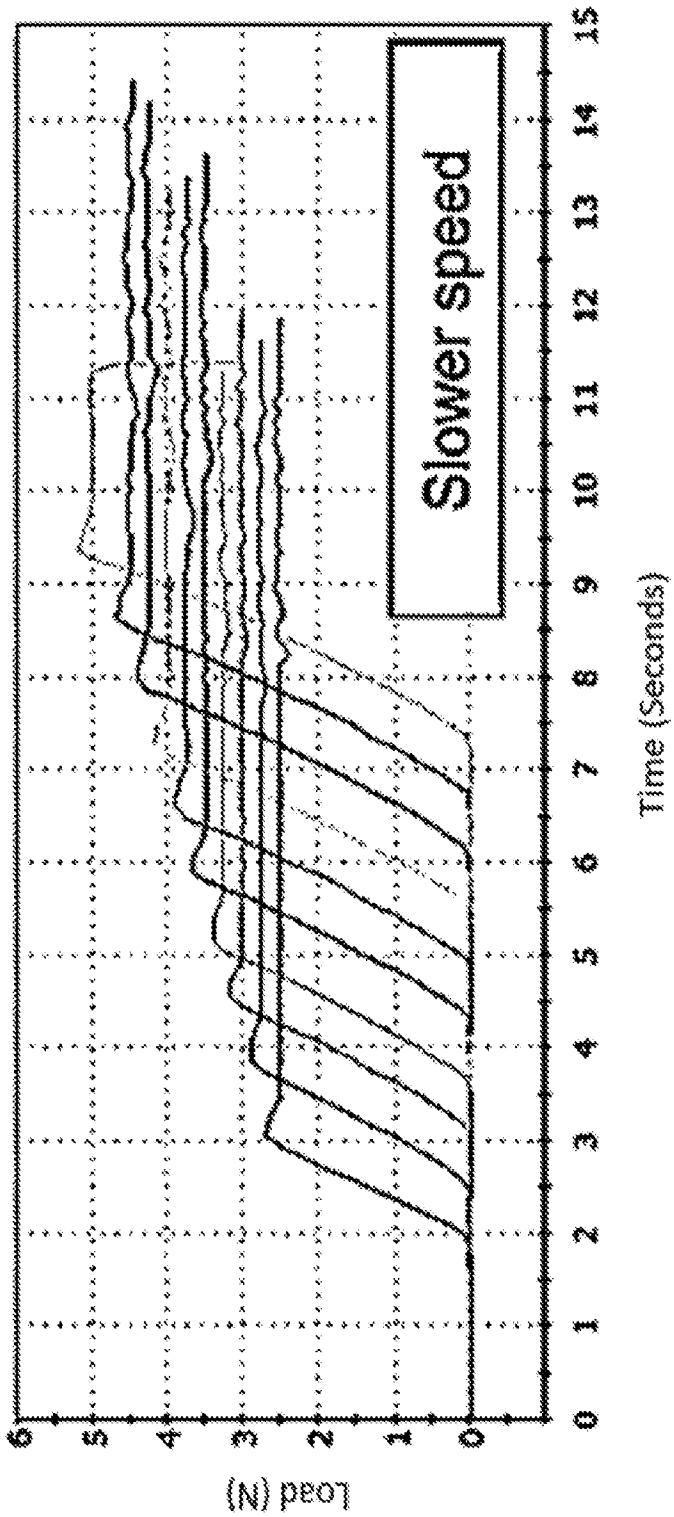

Slower speed
Load (N)
Time (Seconds)
0
1
2
3
4
5
6
0
1
2
3
4
5
6
7
8
9
10
11
12
13
14
15

FIG. 18

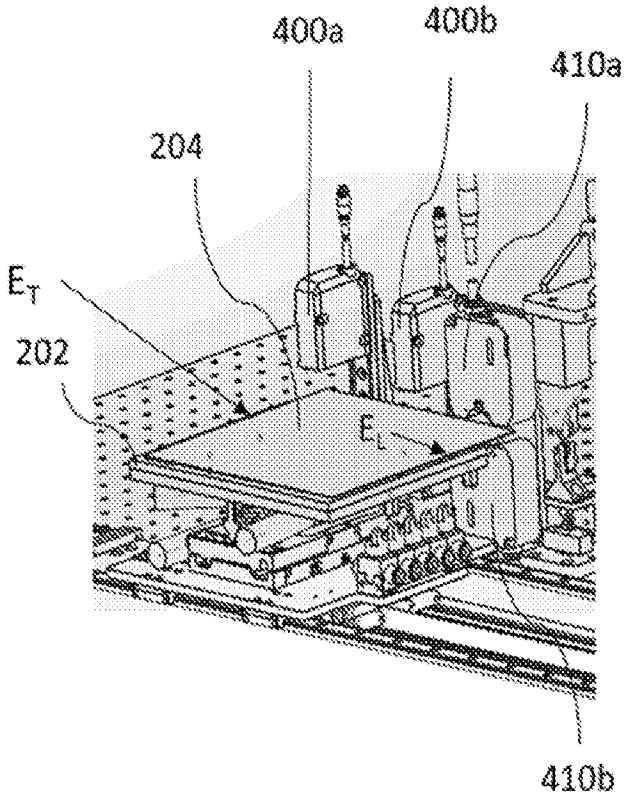


FIG. 19A

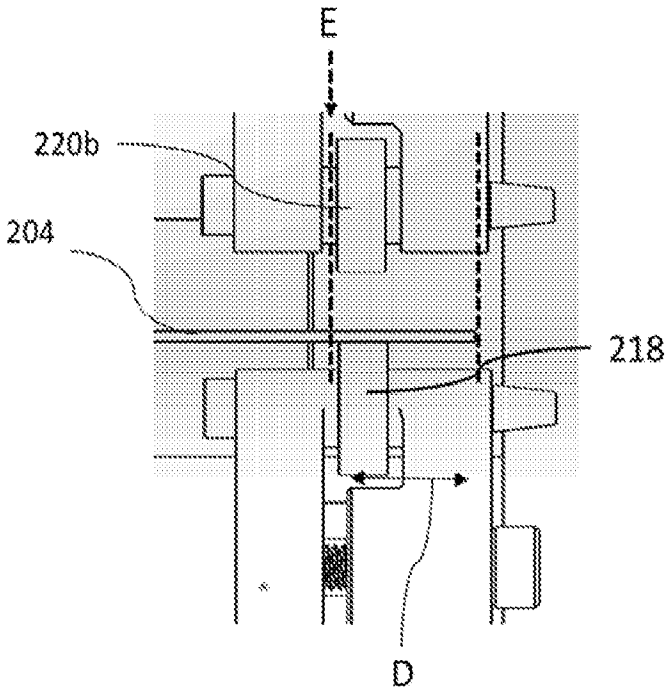


FIG. 19B

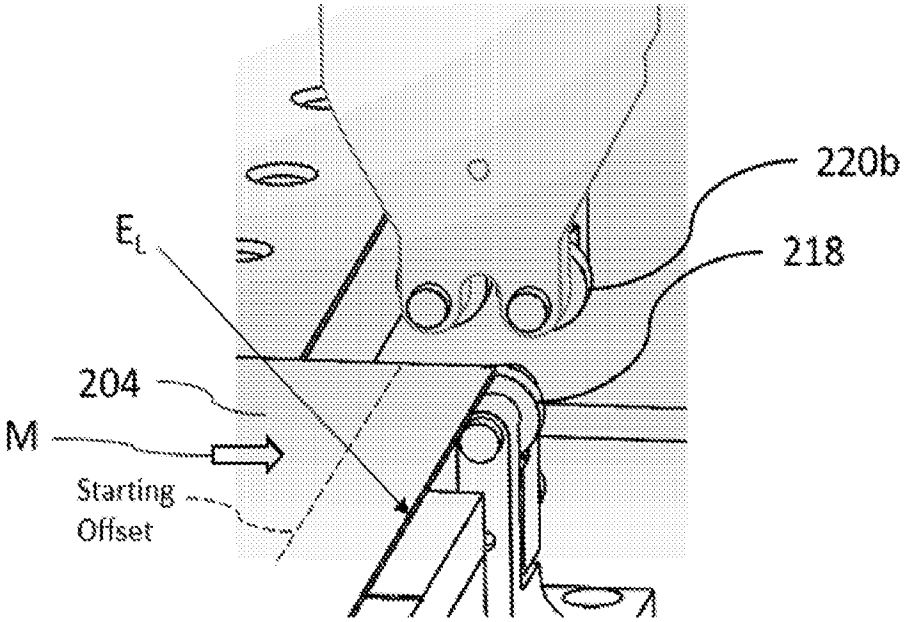


FIG. 19C

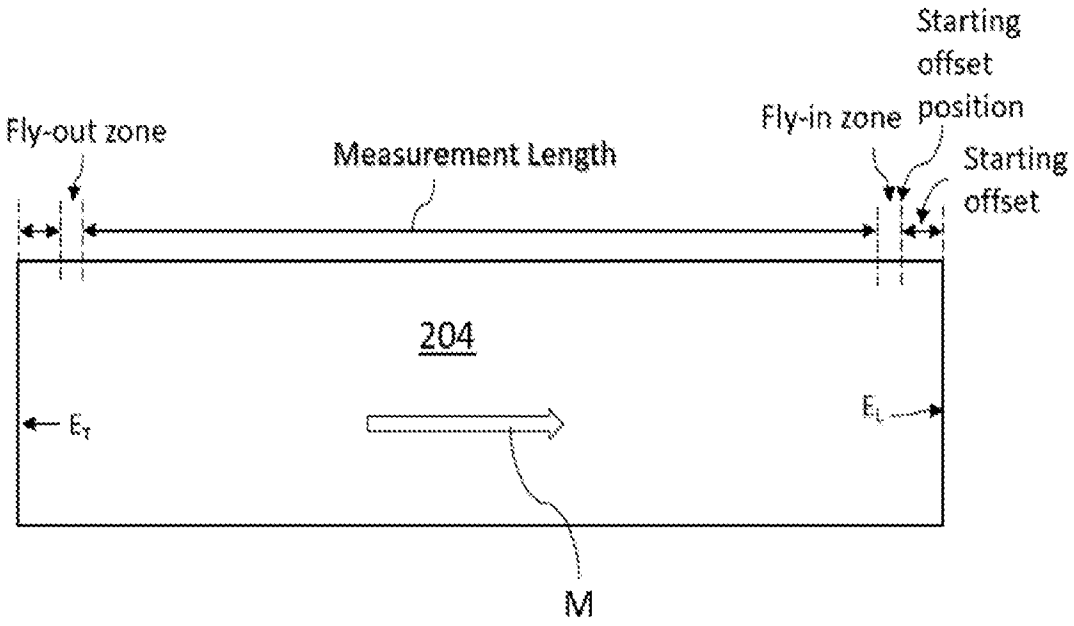

Starting offset position
Fly-out zone
Measurement Length
Fly-in zone
Starting offset
204
M

FIG. 20

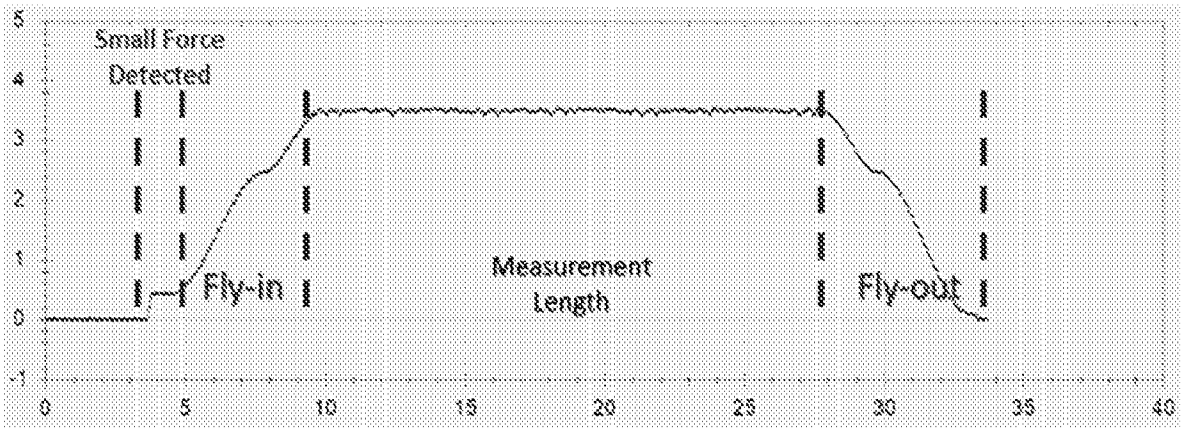

Small Force Detected
Fly-in
Measurement Length
Fly-out
Time (msec) (10^3)

FIG. 21

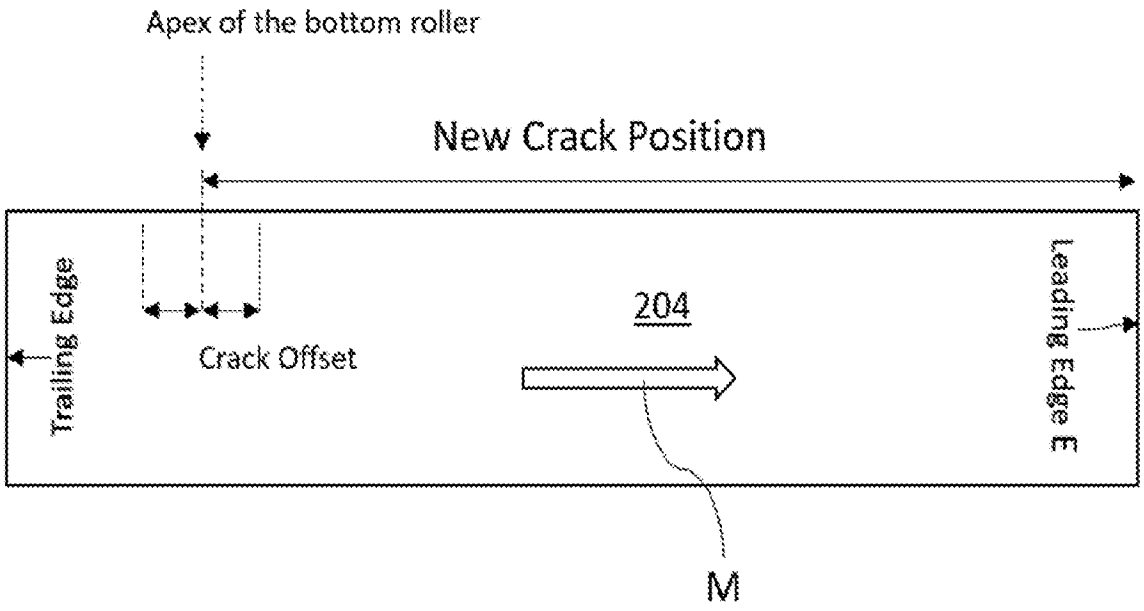

Apex of the bottom roller
New Crack Position
Trailing Edge
Crack Offset
204
Leading Edge
M

FIG. 22

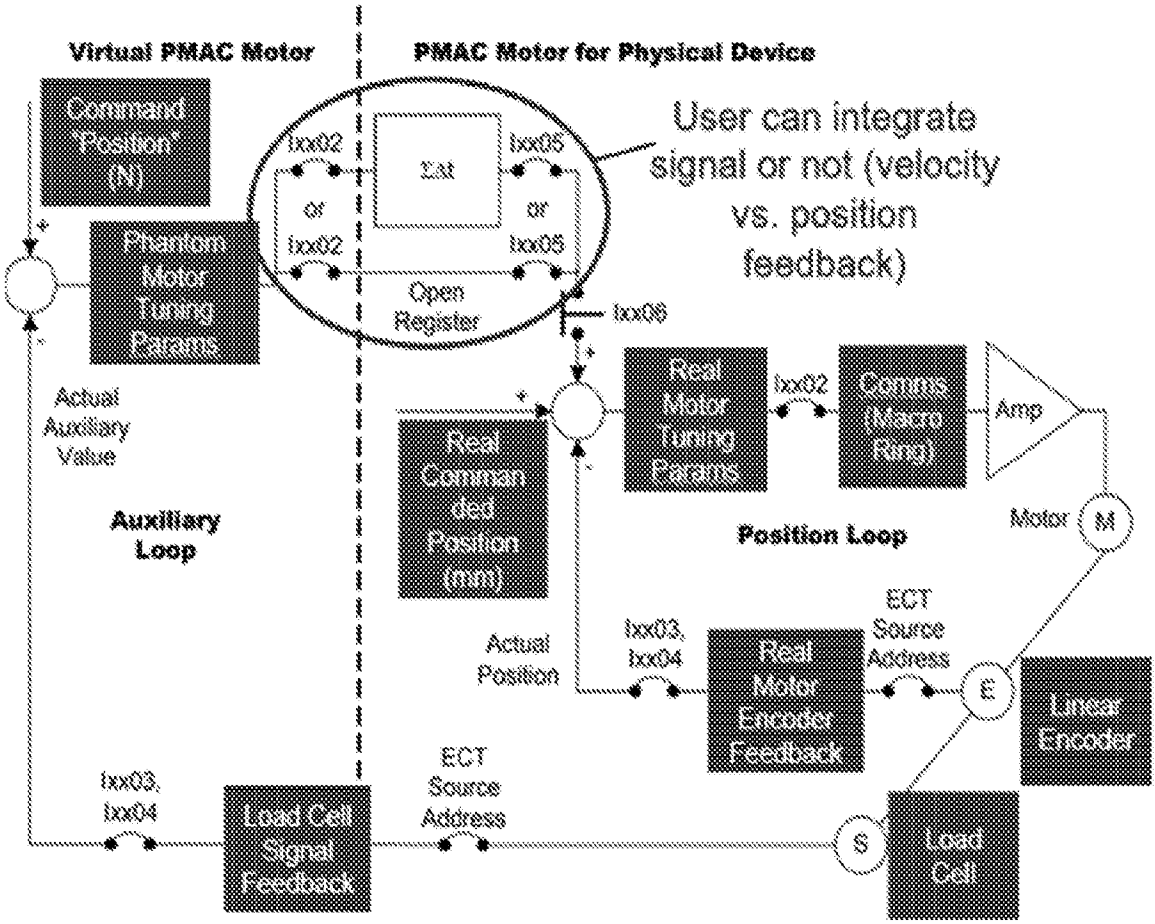

Virtual PMAC Motor
PMAC Motor for Physical Device
Command Position* (N)
Ixx02
or
Ixx02
Σ.ut
Ixx05
or
Ixx05
User can integrate signal or not (velocity vs. position feedback)
Phantom Motor Tuning Params
Open Register
Ixx08
Actual Auxiliary Value
Auxiliary Loop
Real Commanded Position (mm)
Real Motor Tuning Params
Ixx02
Comms (Macro Ring)
Amp
Motor
M
Position Loop
Actual Position
Ixx03, Ixx04
Real Motor Encoder Feedback
ECT Source Address
E
Linear Encoder
Ixx03, Ixx04
Load Cell Signal Feedback
ECT Source Address
S
Load Cell

FIG. 23A

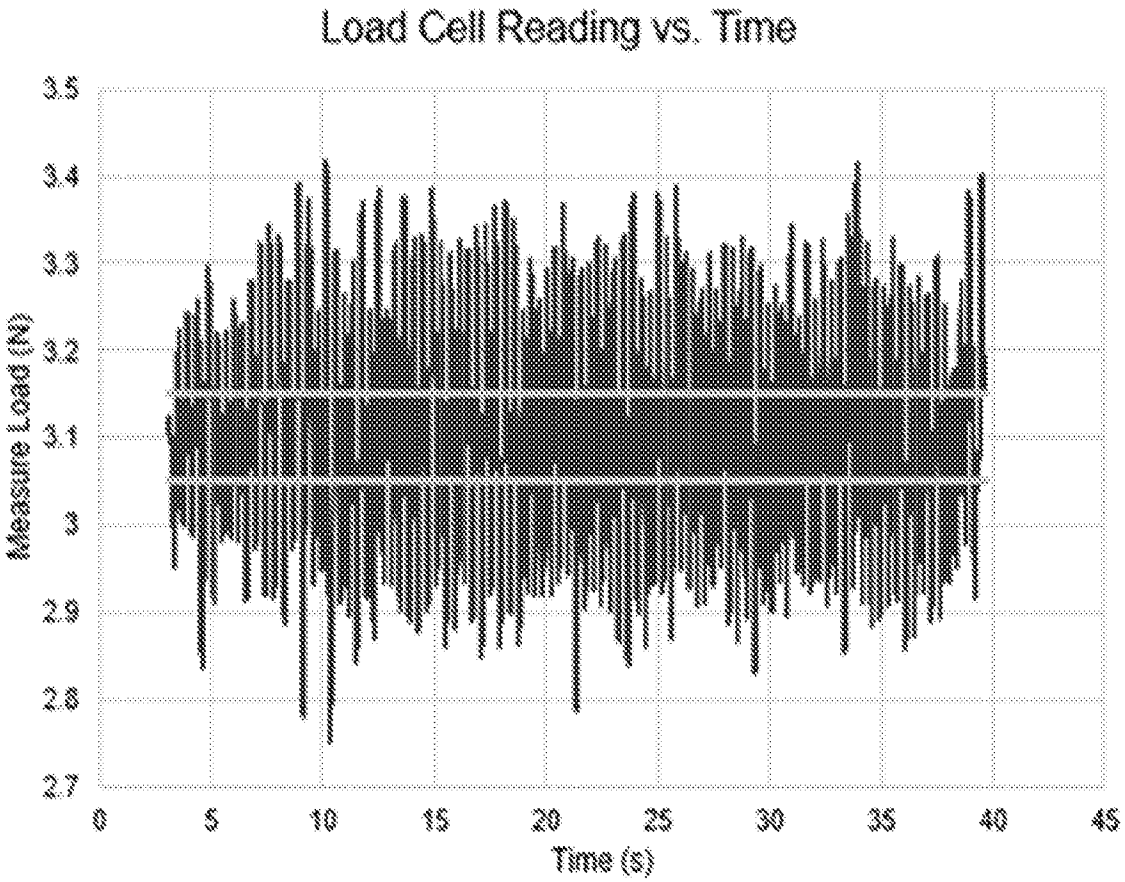

Load Cell Reading vs. Time
Measure Load (N)
3.5
3.4
3.3
3.2
3.1
3
2.9
2.8
2.7
0
5
10
15
20
25
30
35
40
45
Time (s)

FIG. 23B

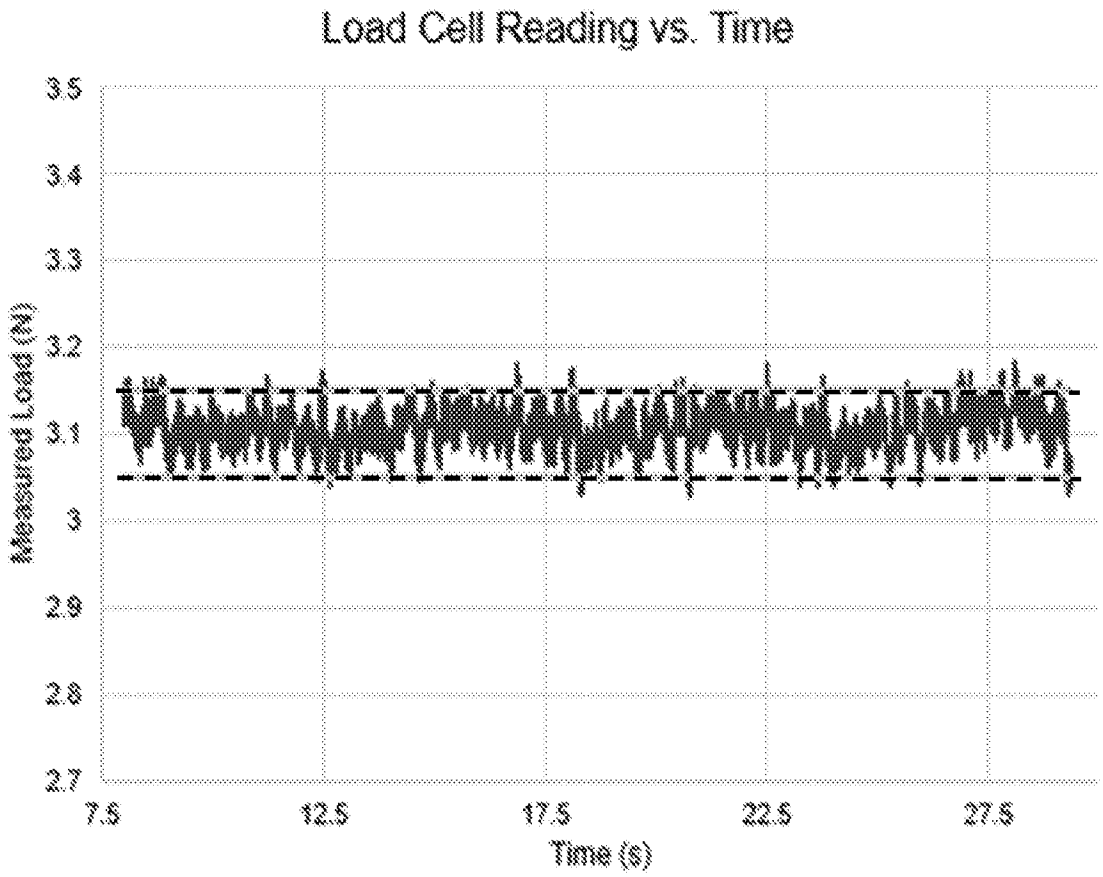

Load Cell Reading vs. Time
Measured Load (N)
3.5
3.4
3.3
3.2
3.1
3
2.9
2.8
2.7
7.5
12.5
17.5
22.5
27.5
Time (s)

FIG. 23C

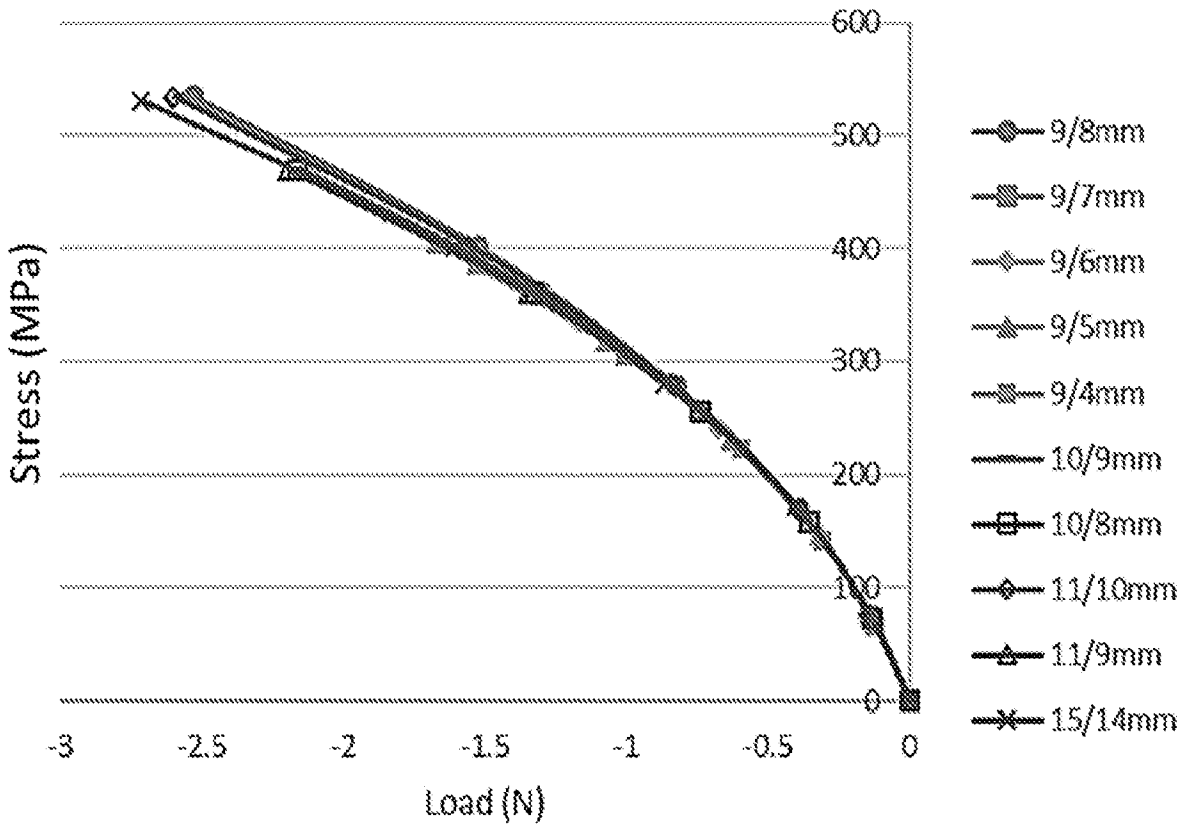

600
500
400
300
200
100
0
Stress (MPa)
-3
-2.5
-2
-1.5
-1
-0.5
0
Load (N)
9/8mm
9/7mm
9/6mm
9/5mm
9/4mm
10/9mm
10/8mm
11/10mm
11/9mm
15/14mm

FIG. 24

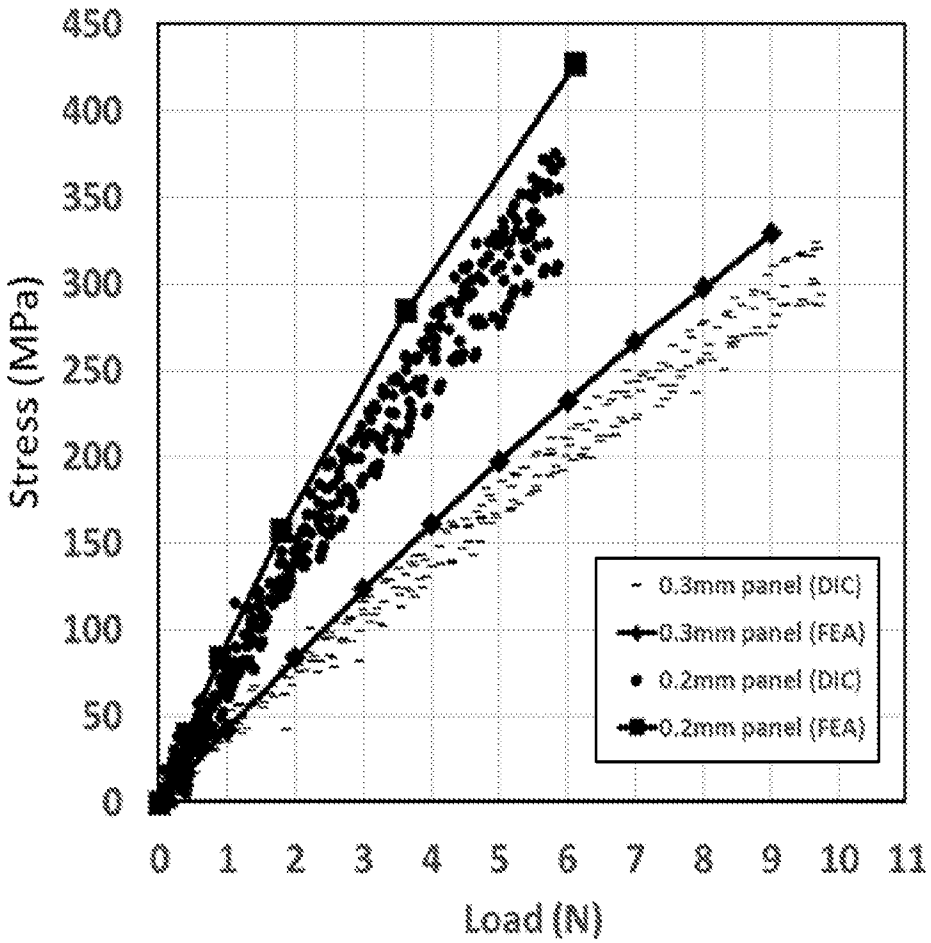

Stress (MPa)
450
400
350
300
250
200
150
100
50
0
0 1 2 3 4 5 6 7 8 9 10 11
Load (N)
0.3mm panel (DIC)
0.3mm panel (FEA)
0.2mm panel (DIC)
0.2mm panel (FEA)

FIG. 25

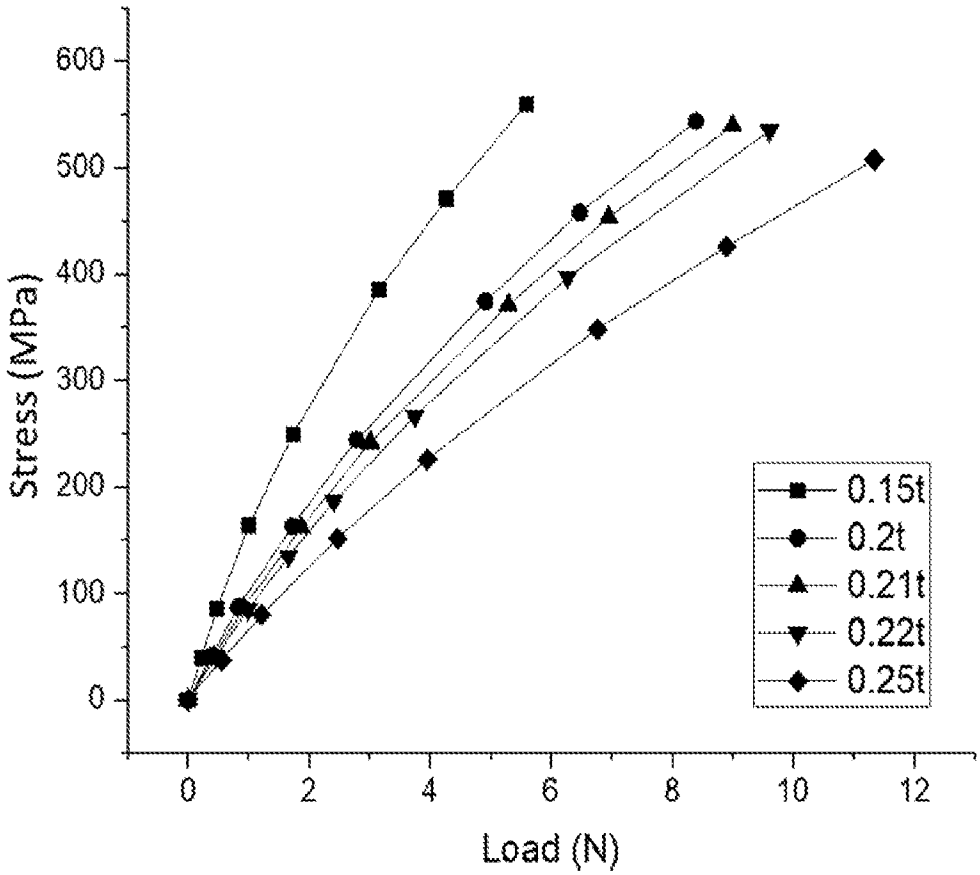

Stress (MPa)
600
500
400
300
200
100
0
0
2
4
6
8
10
12
Load (N)
0.15t
0.2t
0.21t
0.22t
0.25t

FIG. 26A

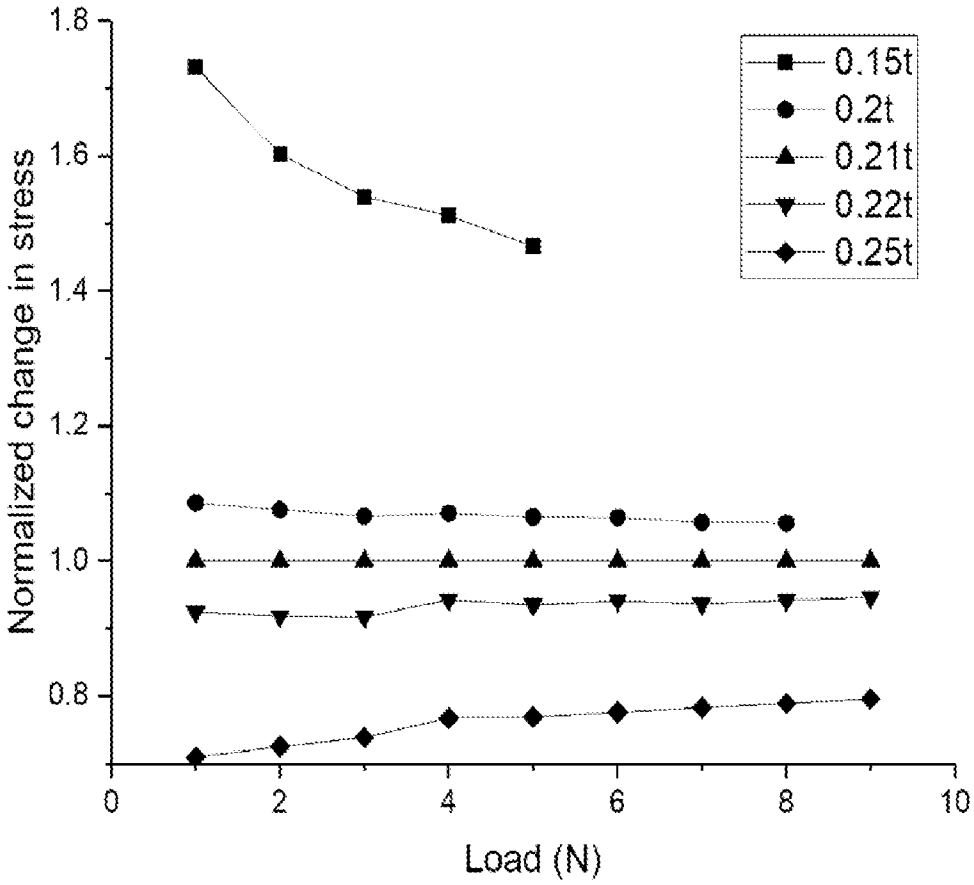

Normalized change in stress
Load (N)
0.15t
0.2t
0.21t
0.22t
0.25t
1.8
1.6
1.4
1.2
1.0
0.8
0
2
4
6
8
10

FIG. 26B

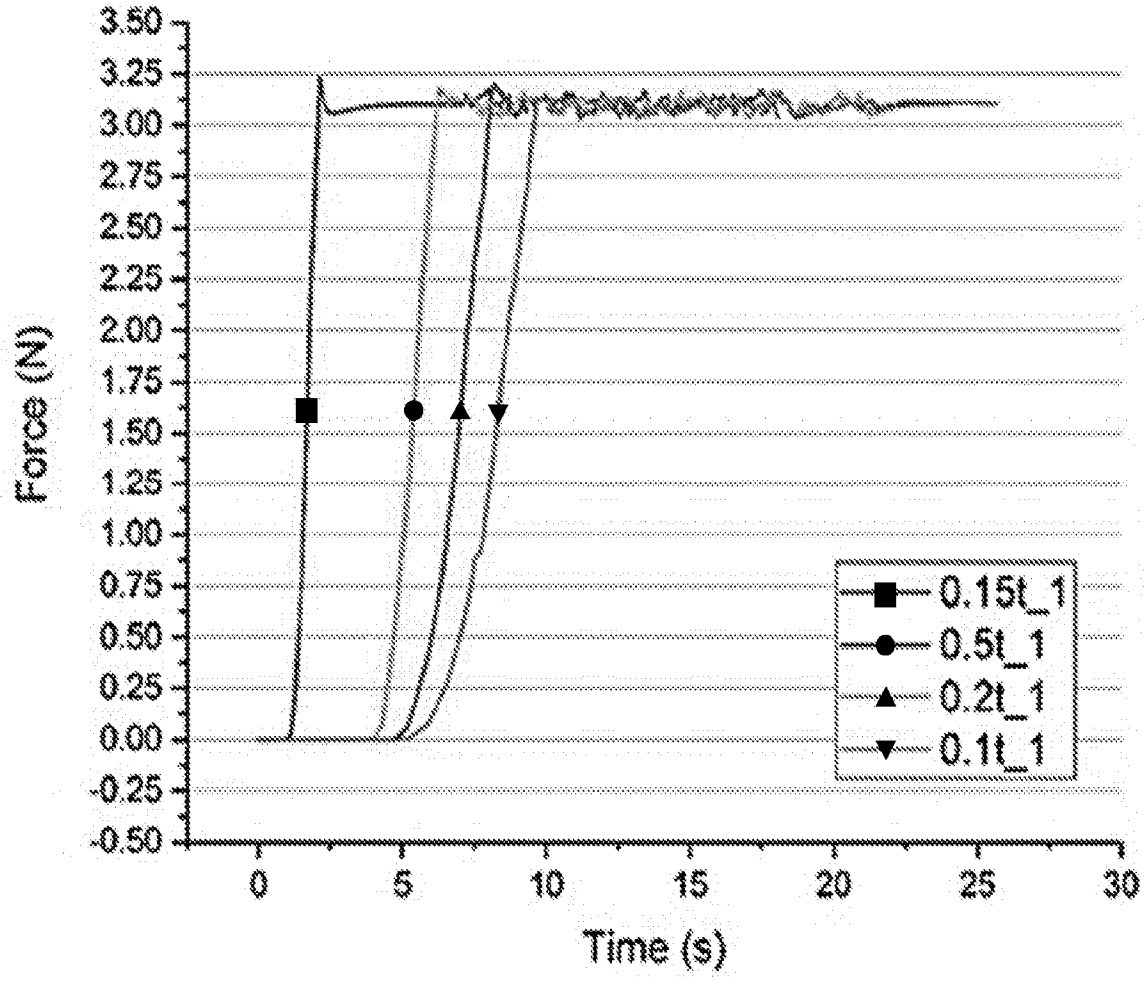

Force (N)
3.50
3.25
3.00
2.75
2.50
2.25
2.00
1.75
1.50
1.25
1.00
0.75
0.50
0.25
0.00
-0.25
-0.50
0
5
10
15
20
25
30
Time (s)
0.15t_1
0.5t_1
0.2t_1
0.1t_1

FIG. 27A

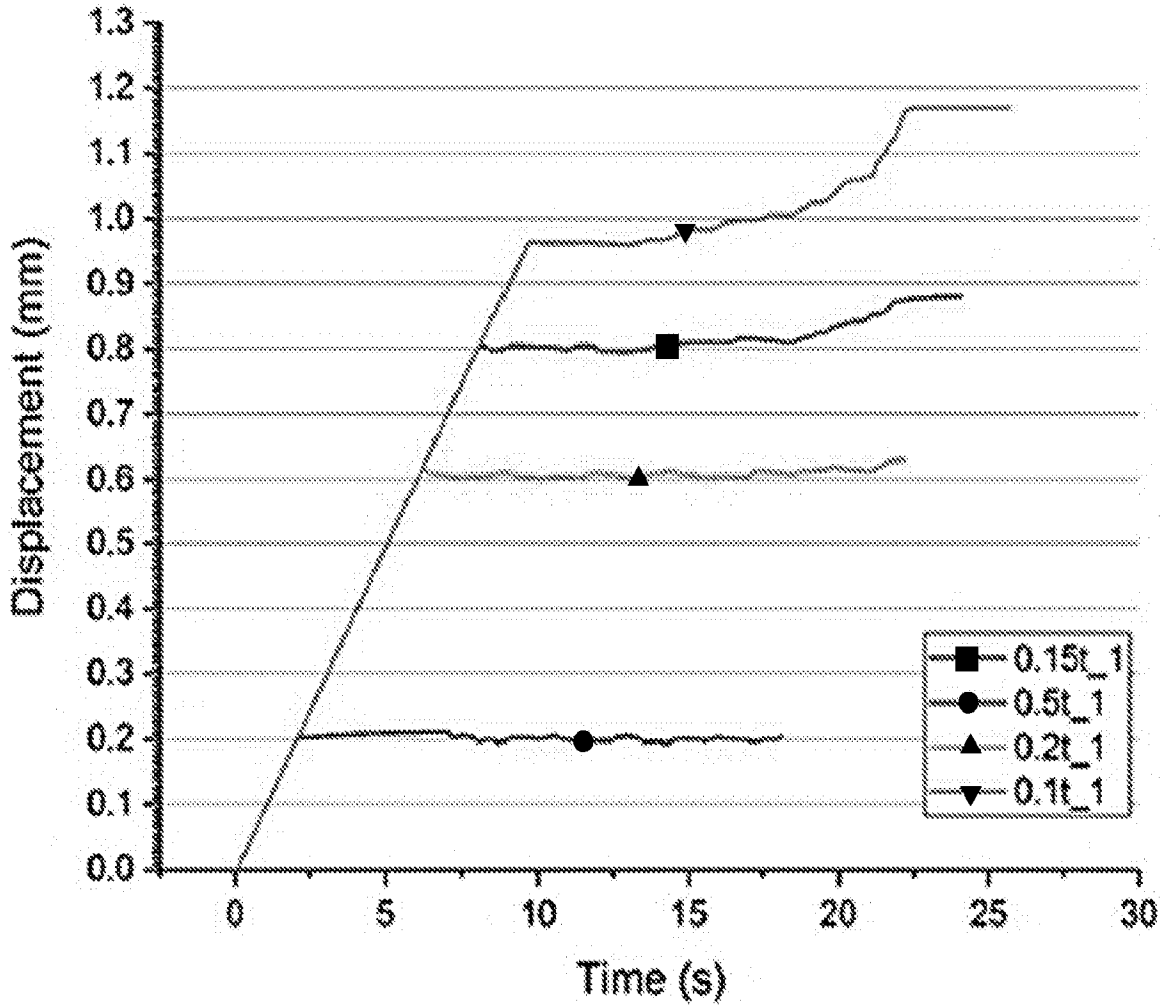

Displacement (mm)
1.3
1.2
1.1
1.0
0.9
0.8
0.7
0.6
0.5
0.4
0.3
0.2
0.1
0.0
0
5
10
15
20
25
30
Time (s)
0.15t_1
0.5t_1
0.2t_1
0.1t_1

FIG. 27B

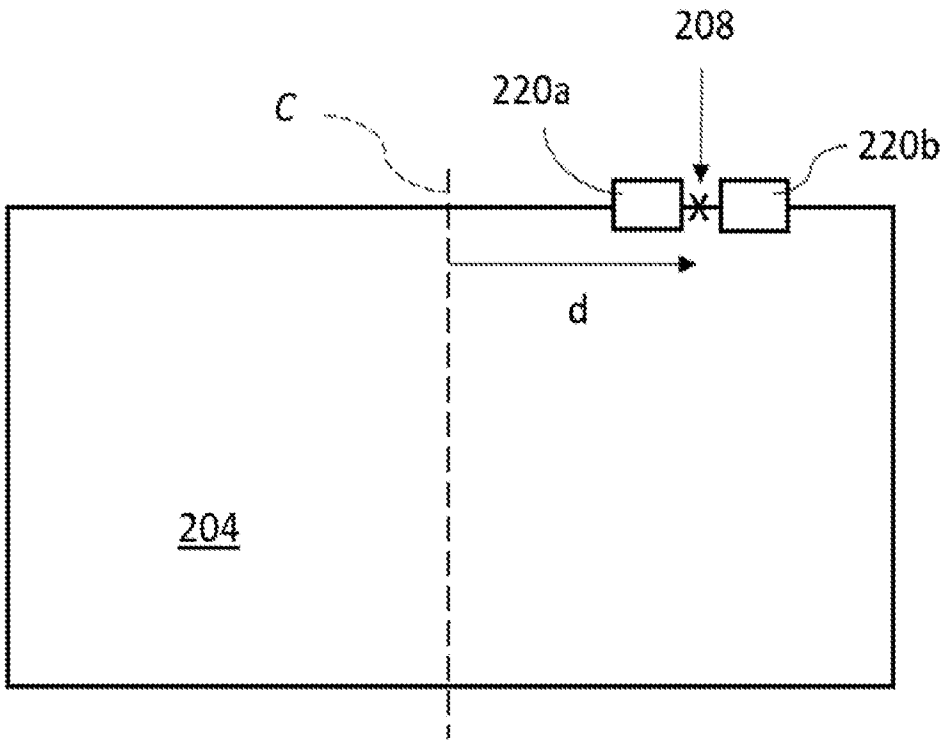


FIG. 28

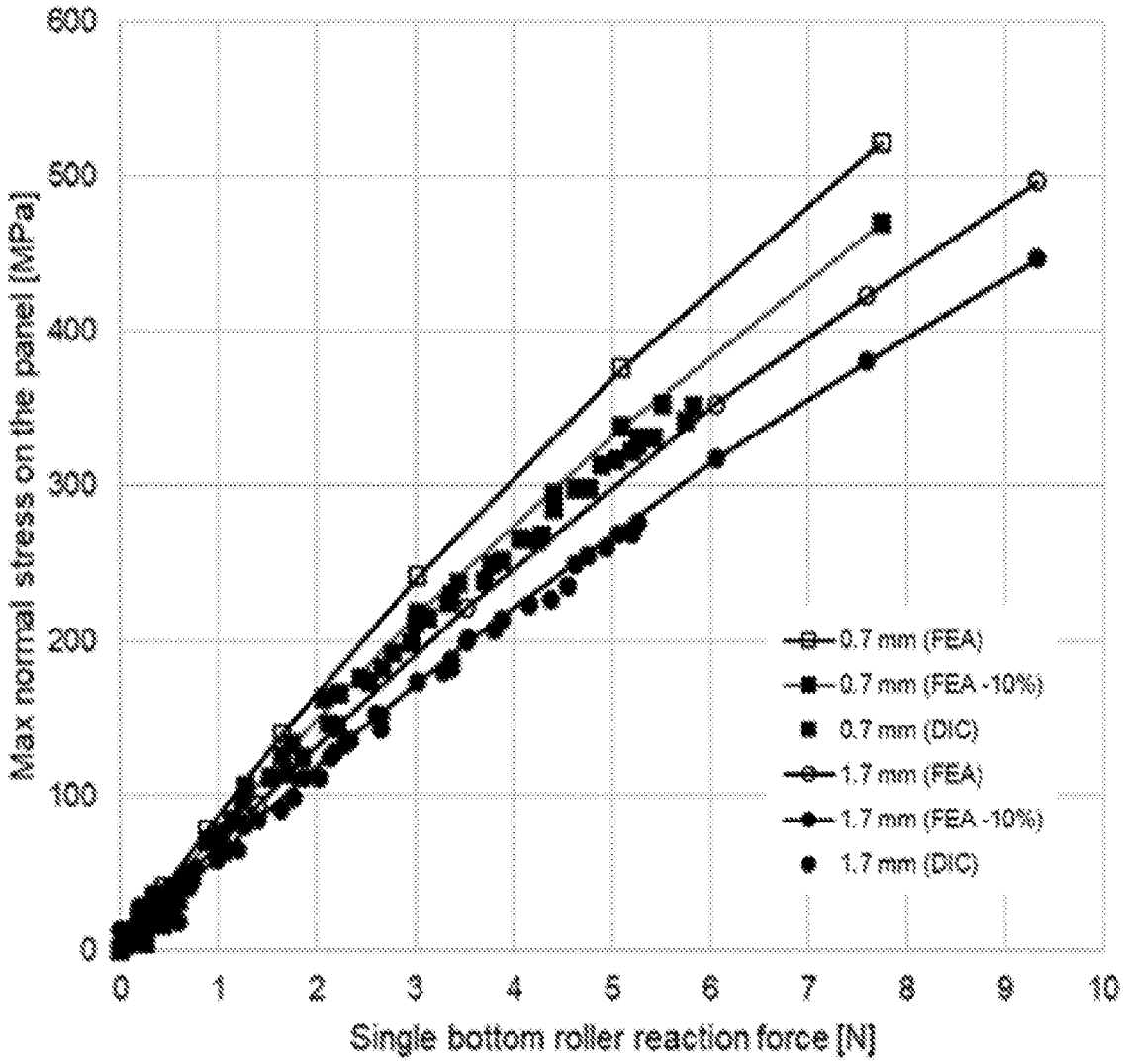

Max normal stress on the panel [MPa]
600
500
400
300
200
100
0
0
1
2
3
4
5
6
7
8
9
10
Single bottom roller reaction force [N]
0.7 mm (FEA)
0.7 mm (FEA -10%)
0.7 mm (DIC)
1.7 mm (FEA)
1.7 mm (FEA -10%)
1.7 mm (DIC)

FIG. 29

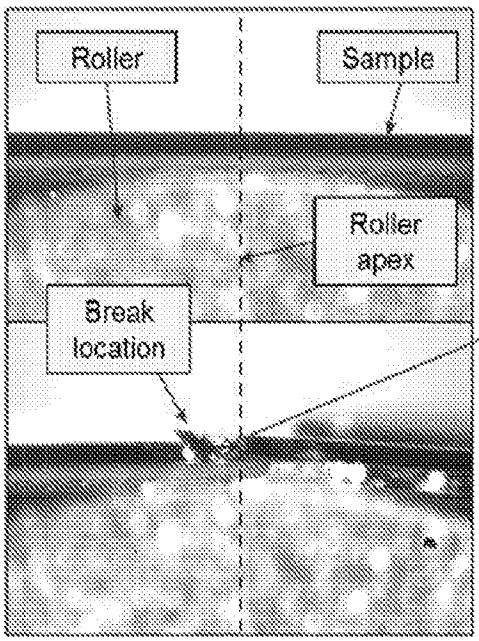


FIG. 30A

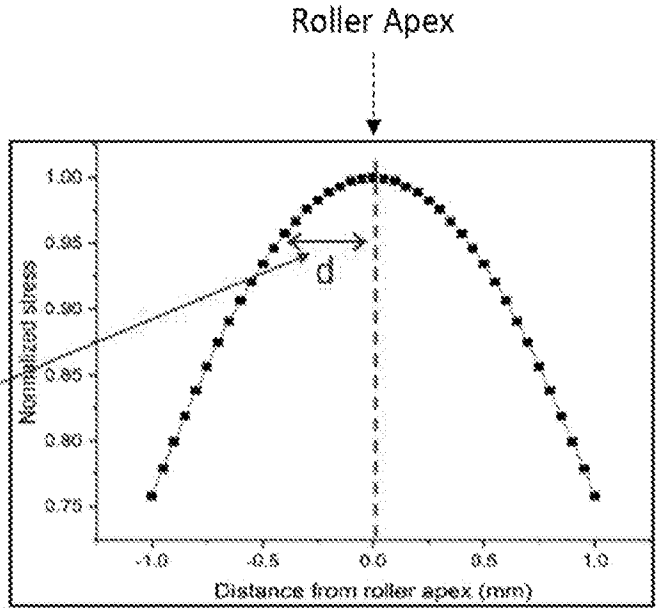


FIG. 30B

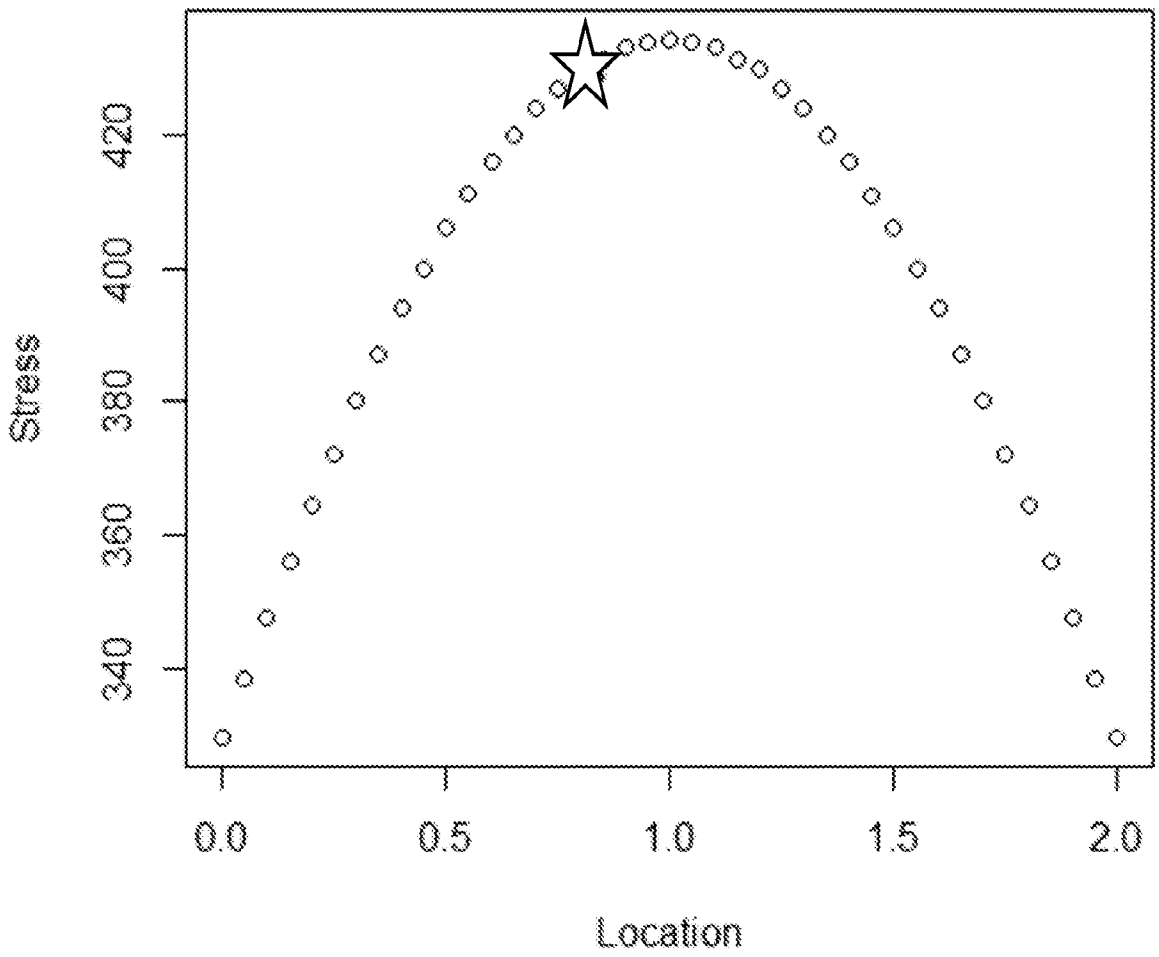


FIG. 31

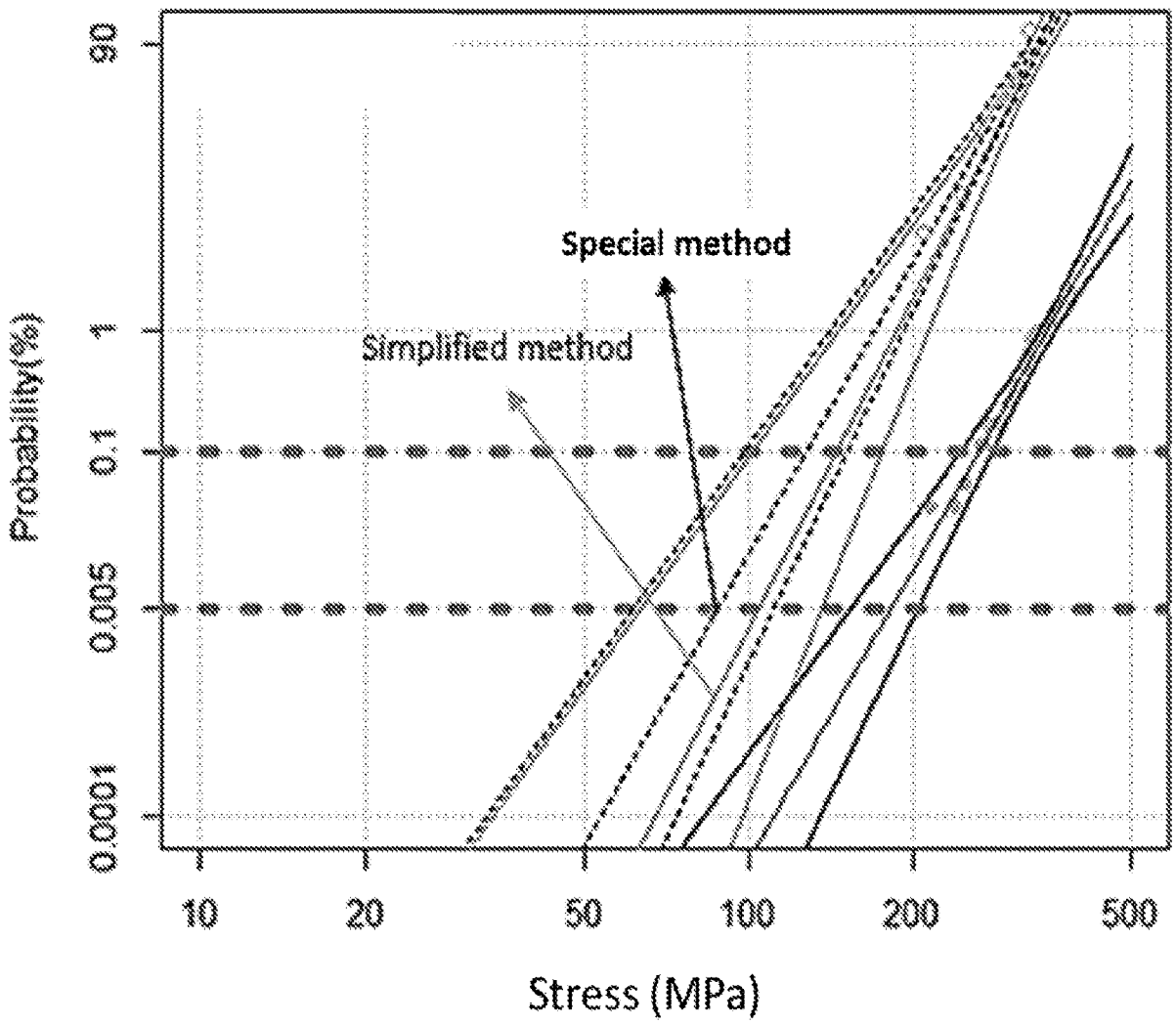

Probability(%)
90
1
0.1
0.005
0.0001
Special method
Simplified method
10
20
50
100
200
500
Stress (MPa)

FIG. 32

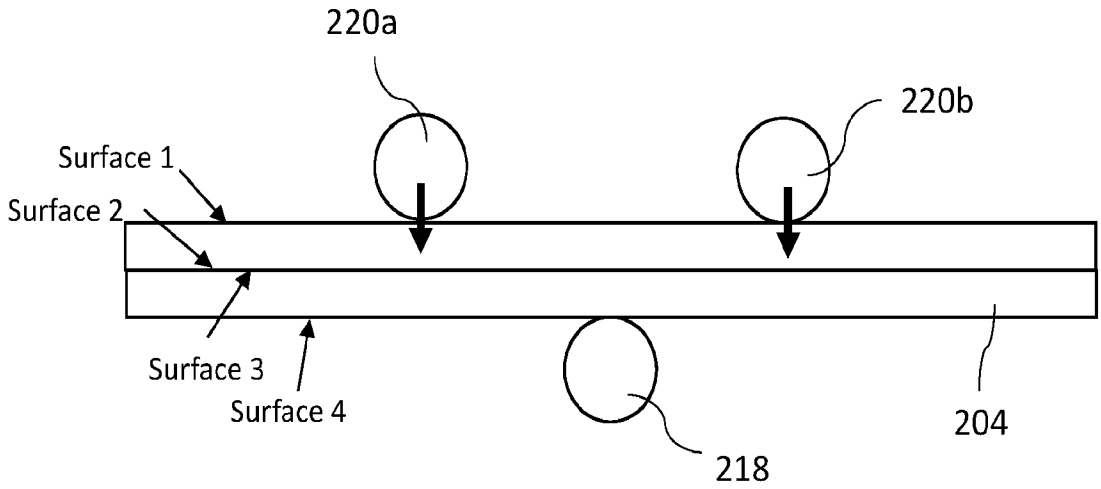


FIG. 33

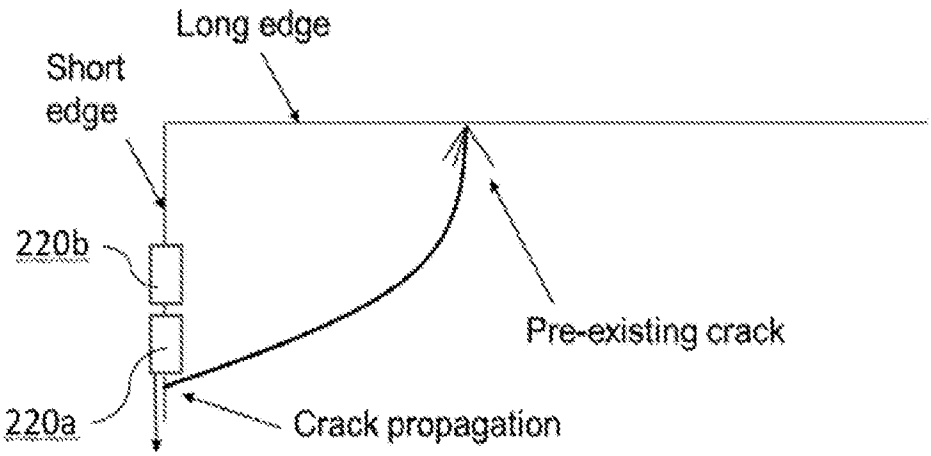

Long edge
Short edge
220b
Pre-existing crack
220a
Crack propagation

FIG. 34

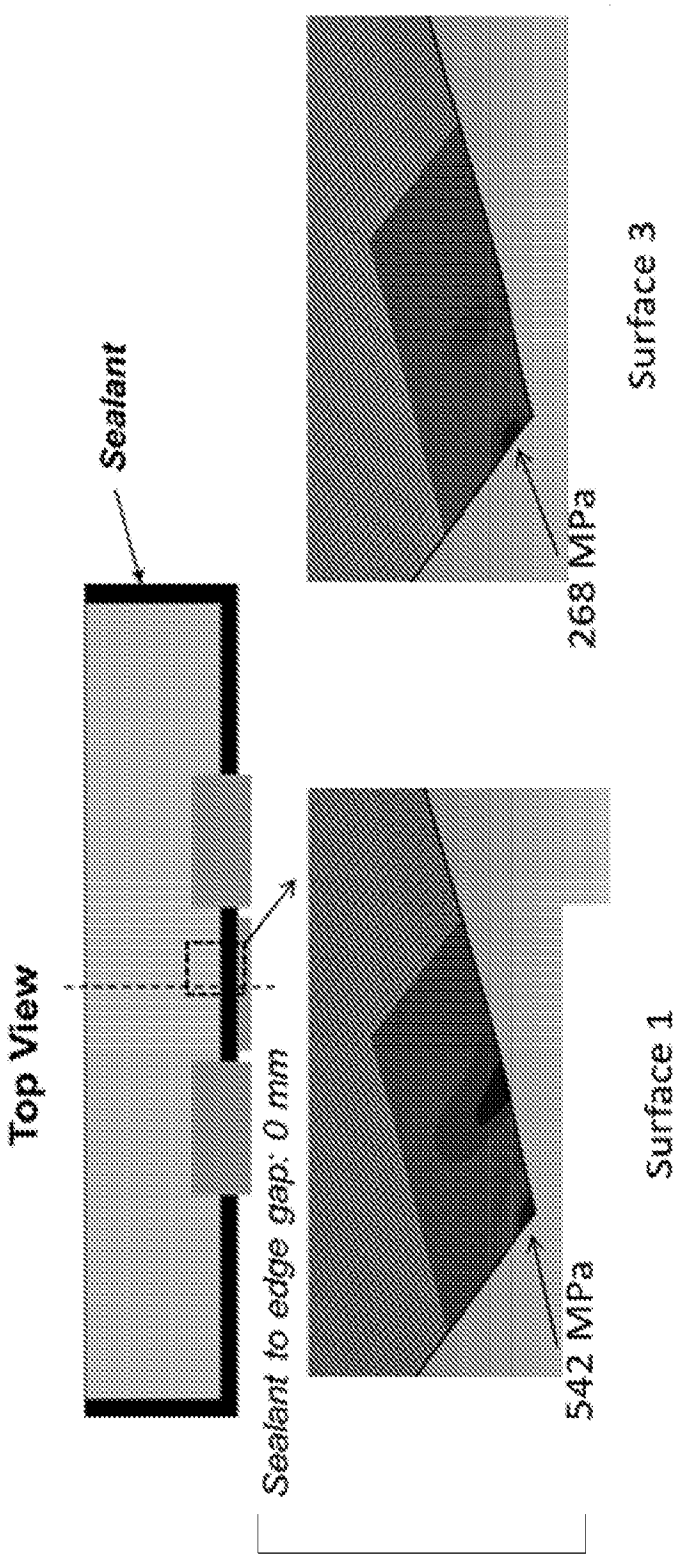

Top View
Sealant
Sealant to edge gap: 0 mm
Surface 1
542 MPa
Surface 3
268 MPa

FIG. 35

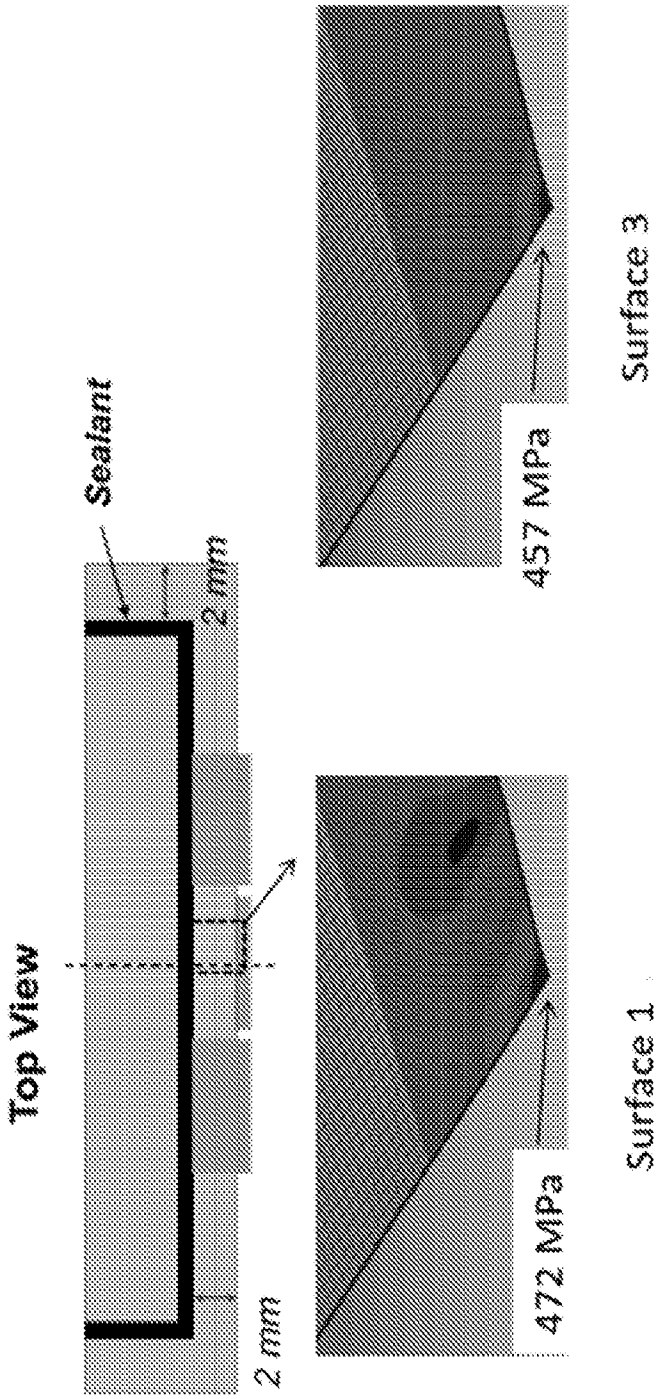


FIG. 36

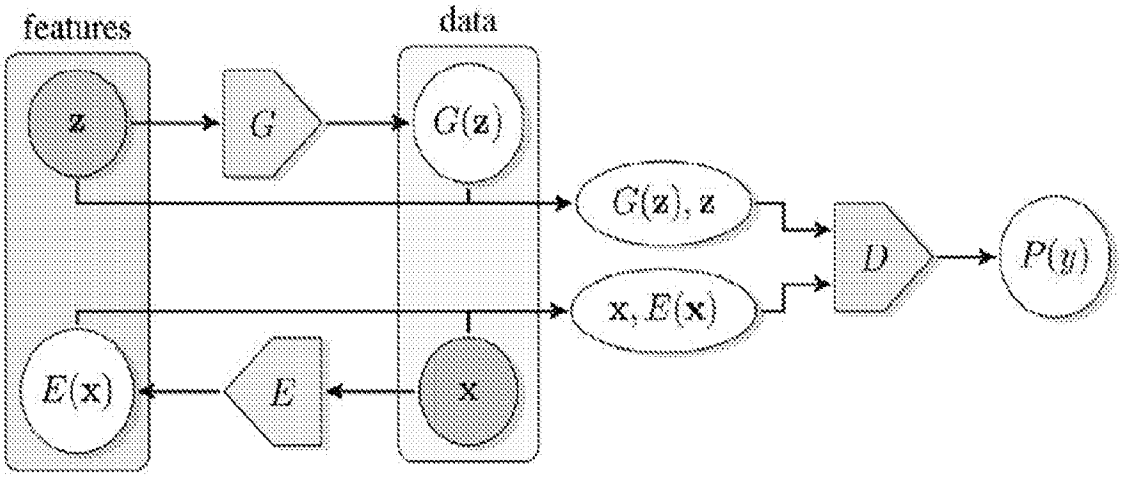


FIG. 37

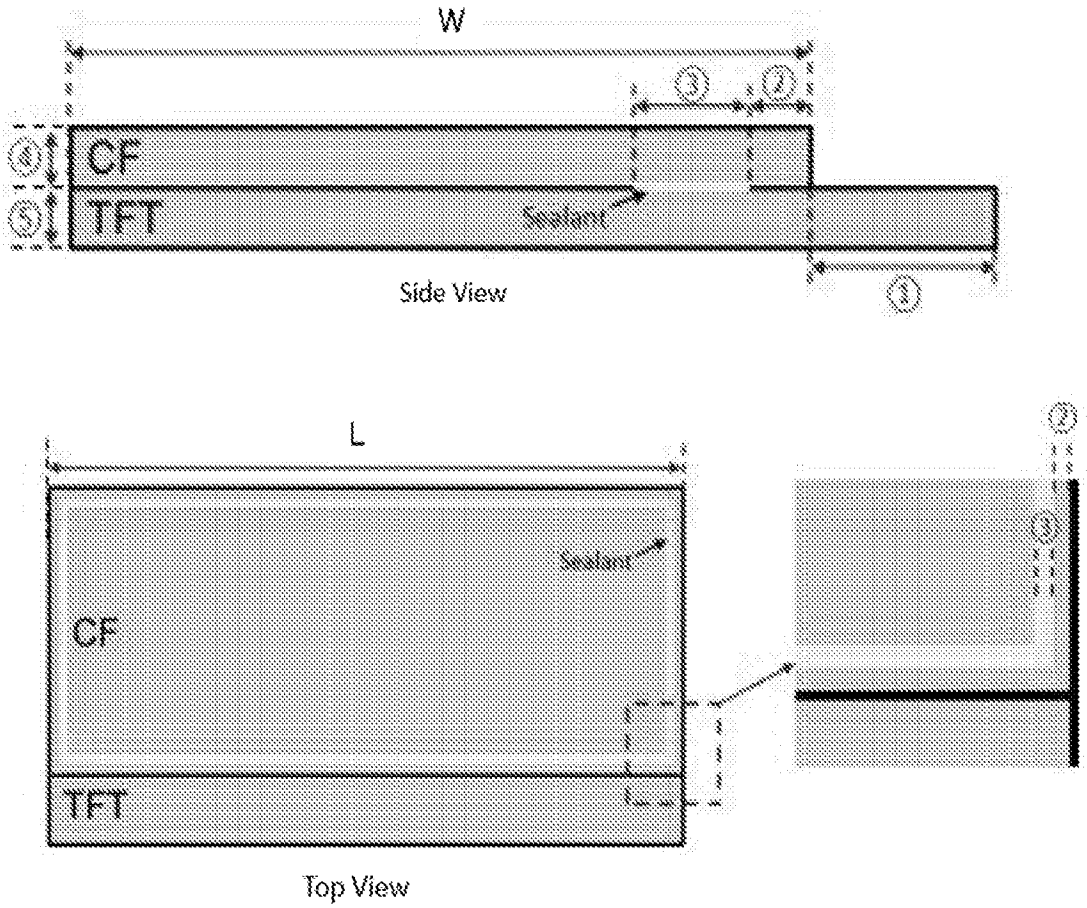


FIG. 38

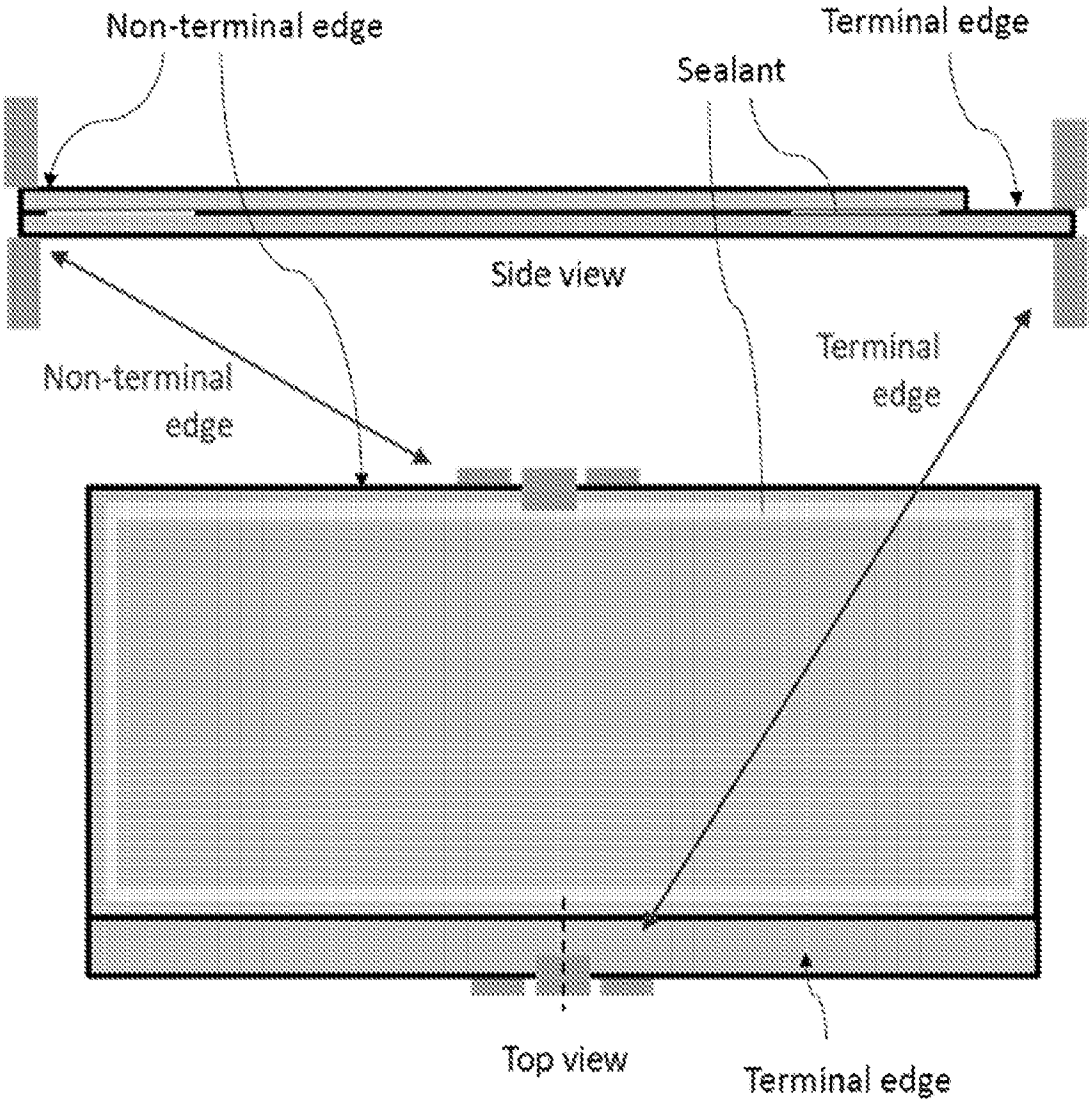

Non-terminal edge
Terminal edge
Sealant
Side view
Non-terminal edge
Terminal edge
Top view
Terminal edge

FIG. 39

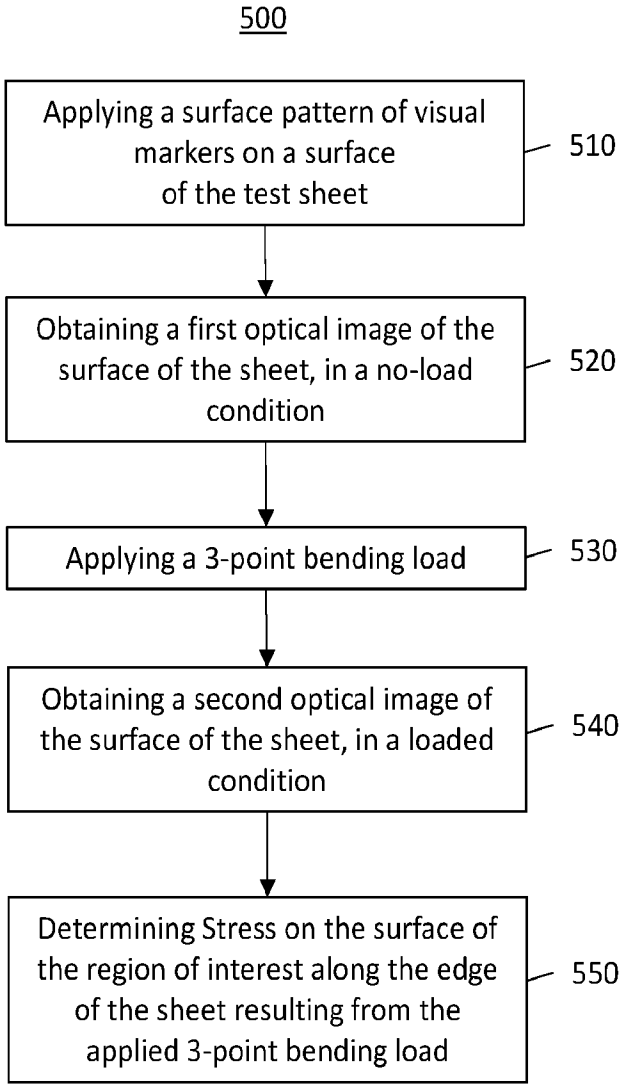

500
Applying a surface pattern of visual markers on a surface of the test sheet
510
Obtaining a first optical image of the surface of the sheet, in a no-load condition
520
Applying a 3-point bending load
530
Obtaining a second optical image of the surface of the sheet, in a loaded condition
540
Determining Stress on the surface of the region of interest along the edge of the sheet resulting from the applied 3-point bending load
550

FIG. 40

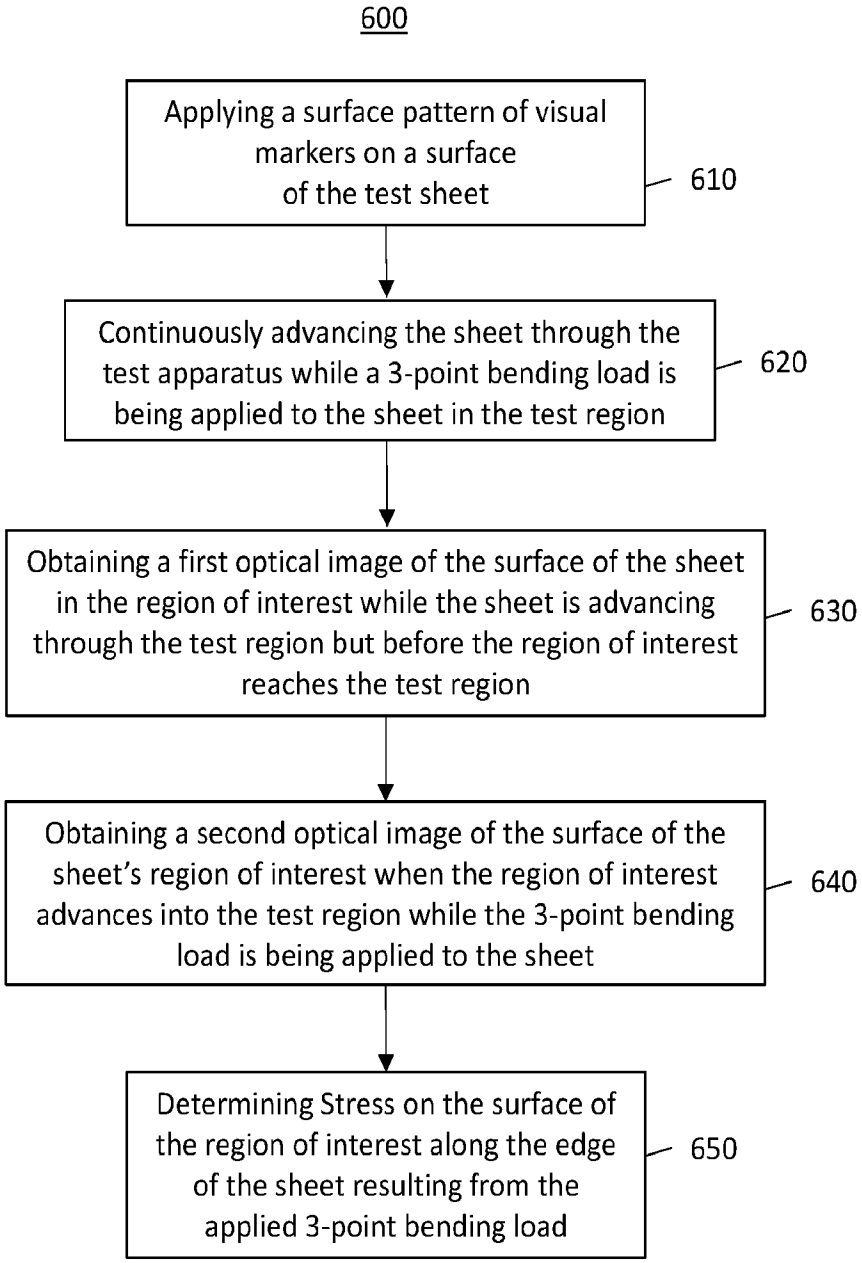

600
Applying a surface pattern of visual markers on a surface of the test sheet
610
Continuously advancing the sheet through the test apparatus while a 3-point bending load is being applied to the sheet in the test region
620
Obtaining a first optical image of the surface of the sheet in the region of interest while the sheet is advancing through the test region but before the region of interest reaches the test region
630
Obtaining a second optical image of the surface of the sheet's region of interest when the region of interest advances into the test region while the 3-point bending load is being applied to the sheet
640
Determining Stress on the surface of the region of interest along the edge of the sheet resulting from the applied 3-point bending load
650

FIG. 41

INTERNATIONAL SEARCH REPORT

International application No.
PCT/US2020/031553

A. CLASSIFICATION OF SUBJECT MATTER

G01N 3/20(2006.01)i

According to International Patent Classification (IPC) or to both national classification and IPC

B. FIELDS SEARCHED

Minimum documentation searched (classification system followed by classification symbols)
G01N 3/20; G01N 19/08; G01N 21/89; G01N 3/08; G09F 9/00; H05B 33/10

Documentation searched other than minimum documentation to the extent that such documents are included in the fields searched
Korean utility models and applications for utility models
Japanese utility models and applications for utility models

Electronic data base consulted during the international search (name of data base and, where practicable, search terms used)
eKOMPASS(KIPO internal) & Keywords:
sheet, detection mechanism, no load condition, loaded condition, 3-point bending load

C. DOCUMENTS CONSIDERED TO BE RELEVANT

Category*	Citation of document, with indication, where appropriate, of the relevant passages	Relevant to claim No.
Y	KR 10-2015-0024081 A (LG CHEM. LTD.) 06 March 2015 paragraphs [0014], [0039]-[0095], claim 1 and figures 3-6, 10, 14	1-21
Y	US 2018-0073967 A1 (CORNING INCORPORATED) 15 March 2018 paragraph [0039] and figures 6A-6B	1-21
A	US 2013-0215419 A1 (KUO et al.) 22 August 2013 paragraphs [0017]-[0028] and figures 2-3	1-21
A	US 4346601 A (FRANCE, PAUL W.) 31 August 1982 claims 1-12 and figures 3-7	1-21
A	KR 10-2014-0122932 A (SAMSUNG DISPLAY CO., LTD.) 21 October 2014 paragraphs [0022]-[0055] and figures 3-6	1-21

☐ Further documents are listed in the continuation of Box C.

☒ See patent family annex.

* Special categories of cited documents:
"A" document defining the general state of the art which is not considered to be of particular relevance
"D" document cited by the applicant in the international application
"E" earlier application or patent but published on or after the international filing date
"L" document which may throw doubts on priority claim(s) or which is cited to establish the publication date of another citation or other special reason (as specified)
"O" document referring to an oral disclosure, use, exhibition or other means
"P" document published prior to the international filing date but later than the priority date claimed
"T" later document published after the international filing date or priority date and not in conflict with the application but cited to understand the principle or theory underlying the invention
"X" document of particular relevance; the claimed invention cannot be considered novel or cannot be considered to involve an inventive step when the document is taken alone
"Y" document of particular relevance; the claimed invention cannot be considered to involve an inventive step when the document is combined with one or more other such documents,such combination being obvious to a person skilled in the art
"&" document member of the same patent family

Date of the actual completion of the international search	Date of mailing of the international search report
28 August 2020 (28.08.2020)	**28 August 2020 (28.08.2020)**

Name and mailing address of the ISA/KR
International Application Division
Korean Intellectual Property Office
189 Cheongsa-ro, Seo-gu, Daejeon, 35208, Republic of Korea
Facsimile No. +82-42-481-8578

Authorized officer
BAHNG SEUNG HOON
Telephone No. +82-42-481-5560

INTERNATIONAL SEARCH REPORT

Information on patent family members

International application No.

PCT/US2020/031553

Patent document cited in search report	Publication date	Patent family member(s)	Publication date
KR 10-2015-0024081 A	06/03/2015	KR 10-1703954 B1	07/02/2017
US 2018-0073967 A1	15/03/2018	CN 107636442 A	26/01/2018
		EP 3268718 A1	17/01/2018
		EP 3268718 A4	07/11/2018
		JP 2018-511795 A	26/04/2018
		KR 10-2017-0126486 A	17/11/2017
		TW 201640089 A	16/11/2016
		US 10613007 B2	07/04/2020
		WO 2016-149016 A1	22/09/2016
US 2013-0215419 A1	22/08/2013	CN 103293160 A	11/09/2013
		EP 2631634 A1	28/08/2013
		JP 2013-171034 A	02/09/2013
		KR 10-2013-0096620 A	30/08/2013
		TW 201335607 A	01/09/2013
		TW I443352 B	01/07/2014
US 4346601 A	31/08/1982	None	
KR 10-2014-0122932 A	21/10/2014	CN 104101544 A	15/10/2014
		CN 104101544 B	12/04/2019
		KR 10-2090560 B1	19/03/2020
		TW 201438830 A	16/10/2014
		TW I664036 B	01/07/2019
		US 2014-0305180 A1	16/10/2014
		US 9616478 B2	11/04/2017